Chemical Modification of Polybutene-1 Resins

by

Xiaorong Zhang

A thesis

presented to the University of Waterloo

in fulfillment of the

thesis requirement for the degree of

Master of Applied Science

in

Chemical Engineering

Waterloo, Ontario, Canada, 2019

© Xiaorong Zhang 2019

AUTHOR'S DECLARATION:

I hereby declare that I am the sole author of this thesis. This is a true copy of the thesis, including any required final revisions, as accepted by my examiners.

I understand that my thesis may be made electronically available to the public.

ABSTRACT

Controlled rheology polybutene (CRPB) resins have been produced by peroxide induced degradation during reactive processing in a batch mixing operation. Two grades of commodity polybutene-1 (PB-1) resins were selected for this study. Experiments were carried out at various peroxide concentrations and the resulting materials were characterized in terms of their molecular weight distribution (MWD) by high temperature size exclusion chromatography (SEC), linear viscoelastic properties by oscillatory shear measurements and melting/crystallization behavior by differential scanning calorimetry (DSC). Similar trends were observed for materials resulting from both commodity resins in the sense that increasing peroxide concentrations resulted in reduced molecular weight (MW) and rheological properties. The melt flow rate (MFR) was measured using a melt flow indexer and it was found to increase with peroxide concentration for both resins. Linear viscoelastic properties (complex viscosity and moduli) were also found to decrease with peroxide concentration, however the flow activation energy remained approximately constant for all materials. The melting temperature decreased with peroxide concentration, however, no significant effects were found on crystallization temperature. Finally, correlations were developed between zero-shear viscosity and weight-average molecular weight (M_W), as well as between polydispersity index (PDI) and cross-over frequency and modulus for all samples produced.

ACKNOWLEDGEMENTS

I would like to express my deep and sincere gratitude to my supervisor, Professor Costas Tzoganakis, whose guidance, encouragement; patient and knowledgeable make me succeed the course of my work. He has done so much for my work that I could have not done by myself. I learned a lot from him and will benefit from his influence in the future.

I would like to thank Professors Alexander Penlidis and Tizazu Mekonnen for patiently reading, correcting the manuscript of the thesis to ensure accurate expression of concepts in it. In addition, as the oral defense examiners, their comments and critique were very valuable and inspiring for me.

I would like to express my gratitude to the dear members of the Polymer Processing Lab, Dr. Prashant Mutyala, Ankita Sakia, Umar Farooq and Julia Durocher for their generous assistance in the lab. Also, I would like to thank Dr. Shuihan Zhu for his patient training on experimental techniques and sharing of his solid research knowledge. In addition, I would like to thank Bert Habicher and Ravindra Singh of the Department of Chemical Engineering for their help with equipment repairs. Finally, I would like to thank Professor Zatloukal from the Tomas Bata University in the Czech Republic for assistance with rheological measurements.

Finally, I thank my whole family for their unconditional support, encouragement, trust and love.

TABLE OF CONTENTS

AUTHOR'S DECLARATION: ii

ABSTRACT iii

ACKNOWLEDGEMENTS iv

LIST OF FIGURES vii

LIST OF TABLES ix

NOMENCLATURE x

THESIS OUTLINE 1

1.1 Background 1

1.2 Objectives 2

1.3 Thesis Outline 2

LITERATURE REVIEW 4

2.1 Controlled Rheology Polypropylene (CRPP) 4

2.2 Linear viscoelastic behavior of PB-1 7

2.3 Polybutene-1 as a packaging material 8

2.4 Structure-property-processing relationships of polypropylene-polybutene blends 9

EXPERIMENTAL 11

3.1 Production of CRPBs 12

3.1.1 Materials 12

3.1.2 Equipment 14

3.1.3 Experimental Procedures 14

3.2 Rheological Characterization 16

RESULTS AND DISCUSSION 21

4.1 Introduction 21

4.2 Torque profiles 22

4.3 Melt Flow Rate (MFR) 26

4.4 Molecular Weight Distribution (MWD) 28
4.5 Thermal Properties 32
4.6 Linear viscoelastic properties 34
CONCLUSIONS AND RECOMMENDATIONS 56
5.1 Conclusions 56
5.2 Recommendations for Future Work 57
REFERENCES 59
Appendix A: 63
Appendix B: 76

LIST OF FIGURES

Figure 2. 1 Reaction scheme for CRPP production [7]. 5

Figure 3. 1 Chemical structure of the 2,5-bis(tert-butylperoxy)-2,5-dimethyl hexane (DHBP). .. 13

Figure 3. 2 Haake Rheocord 90 batch mixer with rotors..... 17

Figure 3. 3 Laboratory grinder. 17

Figure 3. 4 Hot press. 17

Figure 3. 5 TAI AR2000 rotational rheometer. 20

Figure 3. 6 Dynisco D4002 melt flow indexer. 20

Figure 4. 1 Torque profiles for controlled rheology PB samples produced from resin 1. 24

Figure 4. 2 Torque profiles for controlled rheology PB samples produced from resin 2. 24

Figure 4. 3 Steady state torque values as a function of peroxide concentration. 25

Figure 4. 4 Relationship between MFR and torque with peroxide concentration for resin 1 (top) and resin 2 (bottom). 27

Figure 4. 5 MWDs of CRPBs produced from resin 1 using various amounts of peroxide. 29

Figure 4. 6 MWDs of CRPBs produced from resin 2 using various amounts of peroxide. 29

Figure 4. 7 Relationship between Mw and PDI with peroxide concentration for resin 1. 31

Figure 4. 8 Relationship between Mw and PDI with peroxide concentration for resin 2. 31

Figure 4. 9 Strain sweep test for resin 2 at 170 ^{o}C at a frequency of 628 rad/s. 35

Figure 4. 10 Complex viscosity as function of angular frequency with temperatures for resin 1 at (a) 0 wt%, (b) 0.01 wt%, (c) 0.02 wt%, (d) 0.04 wt%, (e) 0.06wt% and (f) 0.08 wt% peroxide concentration respectively. 36

Figure 4. 11 Complex viscosity as function of angular frequency with temperatures for resin 2 at (a) 0 wt%, (b) 0.01 wt%, (c) 0.02 wt%, (d) 0.04 wt%, (e) 0.06wt% and (f) 0.08 wt% peroxide concentration respectively. 38

Figure 4. 12 Complex viscosity as function of angular frequency for resin 1 at (a) 150 °C (top), (b) 170 °C (middle) and (c) 190 °C (bottom)..... 39
Figure 4. 13 Complex viscosity as function of angular frequency for resin 2 at (a) 150 °C (top), (b) 170 °C (middle) and (c) 190 °C (bottom)..... 40
Figure 4. 14 Correlation between zero-shear viscosity and temperature for resin 1. 44
Figure 4. 15 Correlation between zero-shear viscosity and temperature for resin 2. 44
Figure 4. 16 Correlation between zero-shear viscosity and Mw with different temperatures for resin 1. 46
Figure 4. 17 Correlation between zero-shear viscosity and Mw with different temperatures for resin 2. 46
Figure 4. 18 Storage modulus G' and loss modulus G" as function of angular frequency. 47
Figure 4. 19 G' and G" as function of angular frequency with peroxide concentration for resin 1 at temperature of (a) 150 °C (top), (b) 170 °C (middle) and (c) 190 °C (bottom). 48
Figure 4. 20 G' and G" as function of angular frequency with peroxide concentration for resin 2 at temperature of (a) 150 °C (top), (b) 170 °C (middle) and (c) 190 °C (bottom). 49
Figure 4. 21 Storage modulus G' as function Loss modulus G" for resin 1 at (a) 150 °C (top), (b) 170 °C (middle) and (c) 190 °C (bottom). 52
Figure 4. 22 Storage modulus G' as function Loss modulus G" for resin 2 at (a) 150 °C (top), (b) 170 °C (middle) and (c) 190 °C (bottom). 53
Figure 4. 23 PDI of resin 2 CRPBs as function of Wc at different temperatures. 55
Figure 4. 24 PDI of resin 2 CRPBs as function of inverse G_c at different temperatures. 55

LIST OF TABLES

Table 2. 1 Industrial peroxides used for CRPP production [38]..... 6

Table 2. 2 Structure parameters of polybutene-1 samples [34]..... 7

Table 3. 1 Properties of LyondellBasell polybutene-1 resins..... 12

Table 3. 2 Properties of the Luperox® 101 (L101) peroxide..... 13

Table 3. 3 Properties of acetone..... 14

Table 4. 1 Evolution of final torques and percentage torque drop with peroxide concentration for all samples..... 23

Table 4. 2 Effect of peroxide concentration of molecular weight averages and PDI..... 28

Table 4. 3 Thermal properties of CRPBs produced from resin 1..... 32

Table 4. 4 Thermal properties of CRPBs produced from resin 2..... 32

Table 4. 5 Summary of power-law index values for all CRPBs..... 41

Table 4. 6 Zero-shear viscosity and time constant calculated from Carreau-Yasuda model for resin 1 at different temperatures..... 42

Table 4. 7 Zero-shear viscosity and time constant calculated from Carreau-Yasuda model for resin 2 at different temperatures..... 42

Table 4. 8 Activation energy of all CRPB samples..... 43

Table 4. 9 Summary of cross-over modulus G_c and frequency W_c for all samples..... 50

NOMENCLATURE

A	frequency term depending on entropy of activation
a	power factor in equation 4, dimensionless
E	activation energy in equation 3, J/mol
G’	storage modulus, Pa
G”	loss modulus, Pa
G_c	cross-over modulus, Pa
ΔH_c	heat of crystallization, J/g
ΔH_m	heat of melting, J/g
k	consistency coefficient in equation 1, dimensionless
k_t	temperature dependent coefficient in equation 4, dimensionless
M_n	number average molecular weight, g/mol
M_w	weight average molecular weight, g/mol
M_z	z-average molecular weight, g/mol
n	power law index in equation 1, dimensionless
R	gas constant in equation 3, J/(mol·K)
T	temperature, K or ^oC
T_c	crystallization temperature, ^oC
$T_{c,onset}$	crystallization onset temperature, ^oC
T_m	melting temperature, ^oC
w (wt)	weight, g

Greek letters:

$\dot{\gamma}$	shear rate, s^{-1}
η	shear viscosity, Pa·s
η^*	complex viscosity, Pa·s
η_0	zero-shear viscosity, Pa·s
η_∞	infinite shear viscosity, Pa·s
λ	relaxation time constant, s

Chapter 1

THESIS OUTLINE

1.1 Background

The production of peroxide-induced controlled rheology polypropylene (CRPP) has been well studied and used successfully in industry for a few decades. Polybutene-1 (PB-1), a member of the polyolefins family which is similar to PP, traditionally has been used on its own for specific extrusion application or it has been mixed with other polyolefins to expand their application properties. In terms of reactive processing and modification of PB-1, there is no previous work published in the open literature. However, due to it similarity with PP, it is expected that when treated with a peroxide, similar observations should be expected in terms of molecular weight distribution (MWD) modification for the purpose of producing controlled-rheology polybutene-1 (CRPB). The goal of this work was to study the production of such CRPB and the effect of peroxide concentration on molecular weight characteristics, thermal and rheological properties. For that purpose, CRPBs were produced from two commodity polybutene-1 resins under various peroxide concentrations and their properties were evaluated.

1.2 Objectives

The main objective of this work was to study the production of CRPB through reactive processing and characterize the properties of these materials. This was achieved by:

1) Produce CRPBs from two commercial virgin resins through reactive processing experiments using varying amounts of a peroxide

2) Study the molecular weight (MW) and MWD of all samples produced as well as their linear viscoelastic and thermal properties.

3) Attempt to develop correlations between peroxide concentration and molecular weight characteristics and rheological properties.

1.3 Thesis Outline

Chapter 1:

The background and the initial objectives of this work are overviewed. A brief outline of different chapters is introduced for the reader.

Chapter 2:

A literature review of previous studies related to this work is provided with emphasis on CRPP technology, characteristics of PB-1 and recent studies on PB-1.

Chapter 3:

The experimental methods and equipment used for this study are introduced and the experimental procedures are discussed.

Chapter 4:

Production of CRPB in a batch mixer with various peroxide concentrations is discussed and the experimental results on the properties of all samples produced are presented. In addition, correlations between different molecular and rheological properties and peroxide concentration are developed.

Chapter 5:

Concluding remarks are made on the findings of this work and recommendations are presented for future work.

Chapter 2

LITERATURE REVIEW

2.1 Controlled Rheology Polypropylene (CRPP)

Polypropylene (PP), a typical thermoplastic material, is a popular commodity resin used in various extrusion and molding applications due to its diverse properties. In all applications, MWD and rheological properties greatly determine the performance of PP products [1]. Thus, these properties need to be controlled during production of various resin grades for different applications. Controlling MWD during polymerization of various PP grades requires frequent change of polymerization reactor conditions which is rather uneconomical. Therefore, the CRPP technique was introduced to economically produce various PP resins of controlled-rheology via reactive extrusion during a post-reactor stage [2-5].

Peroxide-promoted degradation of polymer chains is the key step in the production of CRPP resins. Specifically, the generation of free radicals from peroxides that are added into PP leads to several reactions such as β-scission, transfer, degradation and termination. The reaction mechanism for this free radical promoted CRPP process has been studied and discussed widely previously [4-10] and it is presented in Figure 2.1.

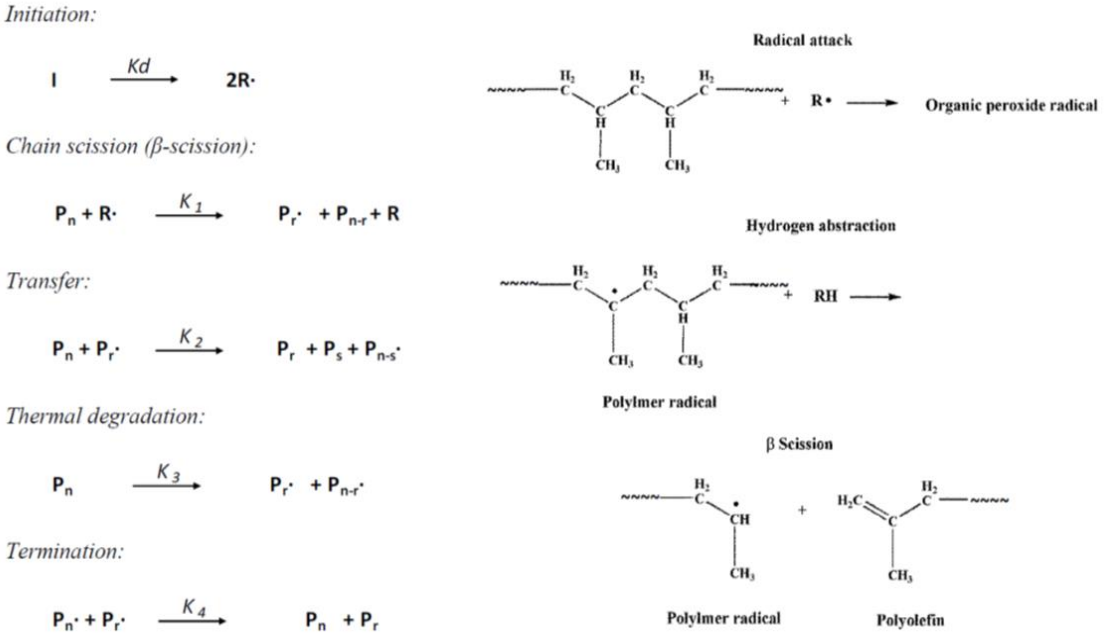

Figure 2. 1 Reaction scheme for CRPP production [7].

When added into a PP melt during reactive extrusion or reactive processing in general, the peroxide decomposes into primary radicals that randomly attack and abstract the tertiary hydrogen atoms on the backbone of PP chains. Due to the steric hindrance effect of methyl group, the formed polymer radical is unstable and further decomposes through a scission reaction. This type of reaction is called β-scission and leads to production of shorter polymer chains thus a lower MW PP is produced. Production of CRPPs using this technique has been studied extensively in terms of kinetic and flow model development, rheological properties as well as crystallization and mechanical properties of resulting resins [11-33]. Regardless of the type of extrusion equipment used (single versus twin-screw extruders), increasing peroxide concentration leads to progressively reduced MW and reduced PDI of the MWD which results in reduced melt elasticity and reduced

viscosity. DSC tests have shown that the melting point (T_m) of CRPPs is not affected by the reduction of MW, however, the crystallization point (T_c) is increasing slightly with peroxide concentration [29]. In terms of mechanical properties, tensile test results have shown that CRPPs exhibit relatively constant tensile properties at low peroxide concentrations. At high peroxide concentrations, the failure mechanism changed from ductile to brittle and elongation at break decreased. Furthermore, the impact strength decreased with increasing peroxide concentration because it depends on molecular weight directly [25].

The decomposition characteristics of the peroxide are critical. Selection of peroxide has to take into account the half-life time of the peroxide at the processing temperature and the relatively short residence in an extruder. Also, the method of addition has to be optimized to ensure that the peroxide is completely mixed into the molten PP prior to decomposition [4-5]. The most commonly used organic peroxides in industrial CRPP production processes are listed in Table 2.1.

Table 2. 1 Industrial peroxides used for CRPP production [38].

Chemical Name	Abbreviation
2,5-Dimethyl-2,5-Di-t-butyperoxyhexane	DHBP
2,5-Dimethyl-3-hexin-2,5-di-t-butylperoxide	DYBP
Di-t-butyl peroxide	DTBP
Dicumyl peroxide	DCUP

2.2 Linear viscoelastic behavior of PB-1

The linear viscoelastic properties of PB-1 resins have been studied to a limited extent [34-35]. In these studies [34-35], six different types of PB-1 samples were used for rheological measurements. The isotacticity and molecular weights of these samples as shown in Table 2.2. Dynamic rheological tests were applied on each sample, including strain sweep, frequency sweep, temperature sweep, and stress relaxation. The data were collected from a stress-controlled rheometer with a parallel-plate configuration with 1 mm gap at 180 ^{o}C. Different frequencies and percentage strains were also applied in the experiments that were used to compare the performances of PB-1 under various testing conditions.

From strain sweep tests, the linear viscoelastic region was determined and the moduli were found to increase with increasing M_w or increased polydispersity of the MWD due to more entanglements in PB-1 with higher M_w. In addition, it was found that the linear viscoelastic region is getting narrower at higher frequencies. Furthermore, the non-linear region was observed at strains above 30%. Frequency sweep tests showed that these materials exhibited shear thinning behavior and that viscosity versus frequency followed a

Table 2. 2 Structure parameters of polybutene-1 samples [34].

Samples No.	Isotacticity [c] (%)	M_w [d]	M_w/M_n [d]
PB1 [a]	95.43	1220000	6.76
PB2 [a]	98.35	627000	6.25
PB3 [a]	93.27	124000	5.82
PB4 [b]	90.75	552000	7.10
PB5 [a]	95.37	561000	11.97
PB6 [a]	91.25	543000	17.30

[a] Polymer supplied by Dongfang Hongye Chemical Co., Ltd;
[b] Polymer synthesized in our own laboratory;
[c] Measured in diethyl ether in a Soxhlet extraction system for 48 h;
[d] M_w, M_w/M_n values were determined by GPC with monodisperse polystyrene as the standard sample.

power-law dependence at high frequencies. It was also found that zero-shear viscosity, relaxation time, transition zone from Newtonian plateau to power-law and reduction of viscosity were increased with higher Mw. Other than Mw, isotacticity and loss angle are also involved in leading the differences of viscosity among samples. Specifically, viscosity increases with increasing degree of isotacticity. Storage modulus (G') increased faster than loss modulus (G'') as a function of frequency and the cross-over modulus G_c was found to increase with decreasing polydispersity. Finally, temperature seemed to affect more the elastic than the viscous behavior.

2.3 Polybutene-1 as a packaging material

One of the major applications of PB-1 is in packaging. Work at Mobil Chemical Company has investigated the properties of PB-1 using as a packaging material [36]. In this study, morphology, tensile properties, creep behavior, high temperature properties, stress crack resistance, chemical resistance and permeability are discussed. Moreover, the performance of PB-1 is generally compared with that of polyethylene (PE) and polypropylene (PP) to demonstrate the advantages of PB-1 in packaging applications.

Crystallization of PB-1 is relatively slower and a stable hexagonal structure is formed during cooling from melt which improves the physical properties of PB-1 such as density, hardness, rigidity and strength. This morphological behavior results in a more flexible and elastic structure of PB-1, which means the chance of failure due to stress relief of molded parts is decreased. From tensile tests, a behavior different from PE and PP was discovered. No distinct necking down was observed, instead, a continuous region of increasing stress with strain was found. This region was found in a wide range of strains

compared to PE and PP behavior. Due to this, it was inferred that PB-1 films strongly resist impact and tearing. Below the tensile yield point, PB-1 shows very high resistance to cold flow but this creep behavior was not fully explained. Temperature tests indicated that tensile yield of PB-1 was four times higher than that of LDPE at high temperature (75^{o}C). In addition, the creep of PB-1 under elevated temperatures was low. Stress crack resistance was also tested and the results showed that PB-1 never failed the test at 50^{o}C in over 2000 hours as a resulted of its morphology. In addition, PB-1 exhibited chemical resistance to dilute inorganic acids, bases, salts and most organic aliphatic solvents at room temperature. Compared to PE and PP, PB-1 showed less swelling effects in the presence of ether, iso-octane, gasoline, benzene, toluene, and tetrahydronaphthalene at 23^{o}C and 60^{o}C. In terms of permeability, PB-1 behaved similarly to PE of the same crystallinity. PB-1 showed good moisture and oxygen barrier properties but increased permeability to carbon dioxide. In general, the advantages of using PB-1 as packaging material are toughness, stress crack resistance, low creep and high temperature resistance.

2.4 Structure-property-processing relationships of polypropylene-polybutene blends

In order to improve properties of PB-1, mixing with other polymers is used industrially. An extensive study of PP/PB-1 blends has investigated the morphology, properties and crystallization of blends prepared by different methods [37]. The resins used in this study were two commercial one, polypropylene, (Alco 8526 with MFR=3.0) and polybutene (Shell, Mn=74,000, Mw=730,000, Mz=3,600,000). Air-quenched compression-molded samples (AQCM), ultra-quenched compression-molded samples

(UQCM), and ultra-quenched solution cast samples (UQSC) were used to process three different blends. Those blends were examined by DSC, torsional pendulum, optical microscopy, transmission electron microscopy, X-ray diffraction, and small-angle light scattering. Additional tensile tests were performed on the AQCM blend.

In AQCM blends tensile tests, plots of both tensile modulus and yield strength versus blend composition showed a linear trend. It was demonstrated that PP and PB-1 are very compatible and the elongation at break varied significantly with composition, the highest elongation at break being over 400%. In addition, the failure mechanism varied from a brittle one to a ductile one depending on composition. DSC and X-ray scattering demonstrated that PP and PB-1 crystallized individually during crystallization of the blends. It was determined from DSC measurements that the melting point of PB-1 did not change but that of PP decreased up to 8 ^{o}C. During the melt crystallization for AQCM samples, the second component will affect the crystallization behavior. For instant, the presence of PP during crystallization will result in a crystallization temperature increase for PB-1. It was implied that this may be related to the degree of homogeneity of the blends. On the other hand, in UQCM samples a reduction of PB-1 crystallization in PP rich samples was observed. In the UQCM samples, the presence of PB-1 molecules delays the PP crystallization.

Chapter 3

EXPERIMENTAL

In this chapter, the experimental aspects of the production of controlled-rheology polybutene-1 (CRPB) from commodity PB-1 resins are presented. The methodology used is described and the materials, equipment, procedures, and characterization techniques are highlighted.

CRPB samples were produced in a batch mixer. The commodity PB-1 resins were molten and were reacted with an organic peroxide at various concentrations. The peroxide was dissolved in acetone and the solution was added into the polymer melt. The purpose of using an acetone solution was to minimize the amount of peroxide loss by evaporation when adding to the batch mixer and to ensure mixing into the polymer before peroxide decomposition.

Rheological properties, including complex viscosity, storage and loss moduli, and melt flow rate (MFR) were evaluated for both the virgin PB-1 and CRPB samples. The molecular weight distributions (MWD) of all samples were measured with high temperature size exclusion chromatography (SEC) and an attempt was made to derive correlations between molecular weight characteristics and rheological properties.

3.1 Production of CRPBs

3.1.1 Materials

Polybutene-1

Two commodity homopolymer polybutene-1 resins were used in this study. They were supplied by LyondellBasell and their main properties (as provided by LyondellBasell) are listed in Table 3.1.

Table 3. 1 Properties of LyondellBasell polybutene-1 resins.

Typical properties	**Resin 1**	**Resin 2**
Physical		
Melt Flow Rate (g/10min)		
(190 ^{o}C/ 2.16 kg) (190 ^{o}C/ 10.0 kg)	4 70	0.4 12
Density (g/cm^{3})	0.915	0.914
Mechanical		
Flexural Modulus (MPa)	450	450
Tensile Strength at Break (MPa)	35	35
Tensile Elongation at Break (%)	300	300
Thermal		
Melting Temperature (^{o}C)		
T_m1 T_m2	127 116	128 117

Organic peroxide

The peroxide used in this study was 2, 5-bis(tert-butylperoxy)-2, 5-dimethyl hexane (DHBP) and was purchased from SIGMA-ALDRICH with the trade name of Luperox® 101 (L101). Its structure and properties are shown in Figure 3.1 and Table 3.2.

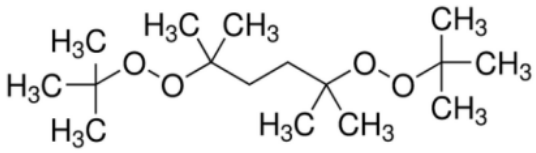

Figure 3. 1 Chemical structure of the 2,5-bis(tert-butylperoxy)-2,5-dimethyl hexane (DHBP).

Table 3. 2 Properties of the Luperox® 101 (L101) peroxide.

Properties	**Value**
Chemical formula	$C_{16}H_{34}O_4$
Molecular weight	290.44 g/mol
Boiling point	55-57 ^oC @ 7 mmHg
Density	0.877 g/cm^3 @ 25 ^oC
Flash point	65 ^oC

This peroxide has selected because it has been previously used in the production of CRPP extensively [33, 38].

Acetone

The acetone used in this work was wash-grade from the Chemical Stores at the University of Waterloo supplied by Sigma Aldrich. The properties of acetone are shown in Table 3.3.

Table 3. 3 Properties of acetone.

Property	**Value**
Boiling point	56 – 57 ^{o}C
Density	0.791 g/cm^{3} @ 25 ^{o}C
Flash point	-17 ^{o}C

3.1.2 Equipment

A Haake Rheocord 90 batch mixer equipped with a Rheomix 3000 chamber and a set of roller-blade rotors was used in these experiments for the production of CRPB materials (Figure 3.2). Experiments were carried out at a constant rotational speed and temperature. The data of torque were collected through the RC 9000 software.

3.1.3 Experimental Procedures

The following processing factors were used in these experiments.

Rotor speed

A rotor speed of 80 rpm was used for melting the PB-1 resins and mixing the peroxide for producing CRPB samples. A value of 80 rpm was selected in order to minimize shear degradation [33, 38].

Operating temperature

The operating temperature is another important factor that needs to be discussed. The batch mixer chamber temperature (200 ^{o}C) was selected by considering the recommended resin processing temperature in the technical data sheet from the supplier and the decomposition kinetics of the peroxide.

Mixing time

The process for production of CRPB in the batch mixer involved two steps. In the first step, the PB-1 resin were loaded into the mixer and melted at certain temperature and rotational speed. In the second step, once the torque was stabilized after melting, peroxide was added dropwise into the batch mixer and started to react with the PB-1 melt. The time required for completing the reaction between peroxide and PB-1 melt was selected based on a similar previous study on controlled rheology polypropylene (CRPP) by Nie [33, 38] using the same peroxide. Based on the decomposition kinetics of L101, current experiments were carried out at 200 ^{o}C and the duration of the second step was at least 3 minutes to ensure completed decomposition of the peroxide. The end of the reaction was indicated by a second torque stabilization.

Peroxide Addition Protocol

The peroxide was added into the PB-1 melt in the form of a solution. A solution of 20 wt% of L101 in acetone was prepared for that purpose. Experiments were carried out at 0 – 0.08 wt% peroxide concentrations based on PB-1 weight. In each experiment, the

required amount of solution was added into the molten PB-1 once the torque was stabilized. After adding the peroxide solution, the torque dropped indicating a reduction of viscosity and molecular weight due to β-scission reactions initiated by the peroxide radicals.

3.2 Rheological Characterization

The rheological properties of the virgin PB-1 as well as those of the CRPB samples were characterized. Oscillatory shear measurements were carried out on a parallel-plate rheometer to assess the linear viscoelastic properties and melt flow indexer was used to measure the melt flow rate (MFR) of all samples.

Sample preparation

Molten samples collected from the batch mixer were spread into a thin sheet and cooled down to room temperature. The solidified sample sheets were then ground using a laboratory scale Wiley Will grinder (see Figure 3.3).

The ground material sample was either used as is for MFR measurements or pressed for oscillatory shear measurements. In the latter case, the ground sample was placed into a steel mold cavity (dimensions of 15x15x0.05 cm) and pressed into a sheet using a hot-press machine (PHI Press, see Figure 3.4.) at 180 ^{o}C and 20,000 lb_fs pressure for 5 minutes. The pressed sample was cooled down to room temperature under the same pressure to avoid warping of the sheet. Subsequently, a round sharp-edged cutting die (ODC Tooling and Molds Inc.) was used to punch out several 25mm diameter disks that were used for oscillatory shear rheological measurements.

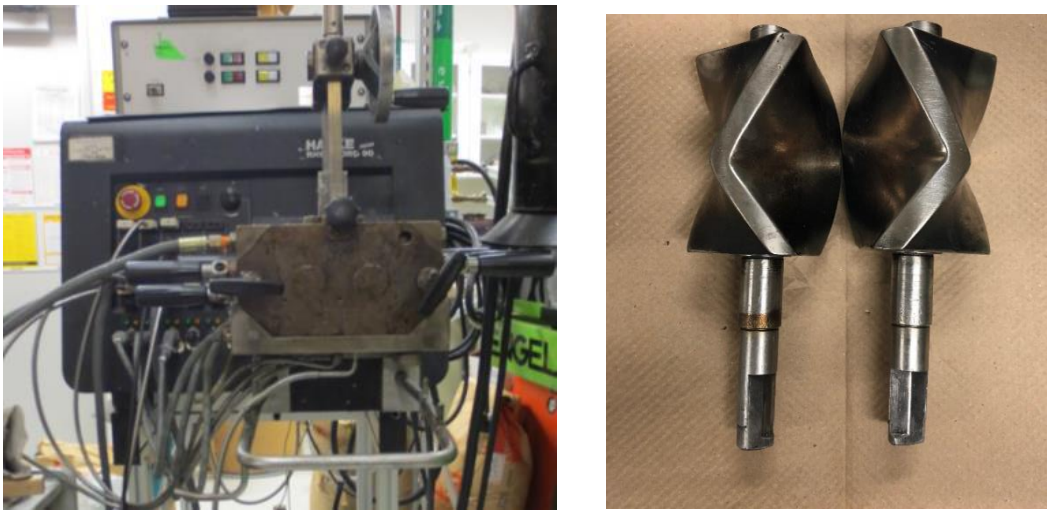

Figure 3. 2 Haake Rheocord 90 batch mixer with rotors.

Figure 3. 3 Laboratory grinder.

Figure 3. 4 Hot press.

Rheological Measurements

A controlled-stress rotational rheometer (AR2000, TA Instruments, New Castle, DE, USA), was used for rheological characterization. As illustrated in Figure 3.5, the sample (blue area) is pressed between two circular plates. The upper plate is connected to a low friction rotational motor with a sensor to measure the strain and the lower plate is a static one that is used for loading the sample and recording the value of normal force. In order to run a test, the chamber was preheated to the target temperature. Once the chamber reached the target temperature, the sample disk was placed on the bottom static plate and allowed to melt for 3 minutes. Then, the upper plate was lowered to a position 5% larger than the target gap and a waiting period was allowed for the normal force to relax to zero. The sample disk was then trimmed and the gap was adjusted to the target gap to insure that the sample was properly filled. When the normal force relaxed close to zero again, the experiment was ready to start. During the experiments, pure nitrogen gas was pumped into the chamber to avoid sample oxidation at high temperatures. Strain sweeps (0.01 to 20%) were run at 100 Hz on all samples to determine the linear viscoelastic region and subsequently, frequency sweeps were carried out at a fixed frequency within the linear viscoelastic region (LVR) of the strain sweep test.

MFR measurements were carried out using a Dynisco D4002 Melt Flow Indexer (Figure 3.6) at 190 ^{o}C using a 2.16 kg weight. The standard die was set at the bottom of the barrel and preheated to 190 ^{o}C. The sample was then loaded into the barrel and allowed a 6-minute period to fully melt. Once the test was ready to run, the weight was added to the

piston and the amount of molten polymer emerging from the die was collected and weighed to determine the MFR in g/10 min.

Measurement of molecular weight distribution (MWD)

The MWD for each sample was measured by a high temperature size exclusion chromatography (SEC) (HT-PGC, Polymer CHAR, Spain), using 1,2,4 tri-chlorobenzene as the eluent solvent with 50 mg/L Irganox 1010 at 145 ^{o}C.

Thermal properties

A differential scanning calorimeter (DSC) (Q-2000, TA Instruments) was used to measure the thermal properties of all samples. To prepare the sample for testing, a small amount of sample was encapsulated in a Tzero® aluminum pan and lid using the Tzero® DSC Sample Encapsulation Press. The encapsulated sample pan was then placed in the auto-sampler. An empty pan was placed as reference. TA Platinum™ Software was used to operate the machine and collect data. A heat-cool-heat procedure was used to run the test for each sample. To be specific, the sample was heated up from 35^{o}C to 150 ^{o}C in a ramp of 20 ^{o}C per minute to remove the thermal history of the sample. The sample was then held isothermal at 150 ^{o}C for 5 minutes and then cooled down to -30 ^{o}C in the same ramp for the cooling cycle. Subsequently, the sample was kept isothermally for another 5 minutes and then heated up to 150 ^{o}C again in the same ramp. In this process, the first cooling and second heating cycles were used for analyzing the thermal crystallization and melting properties.

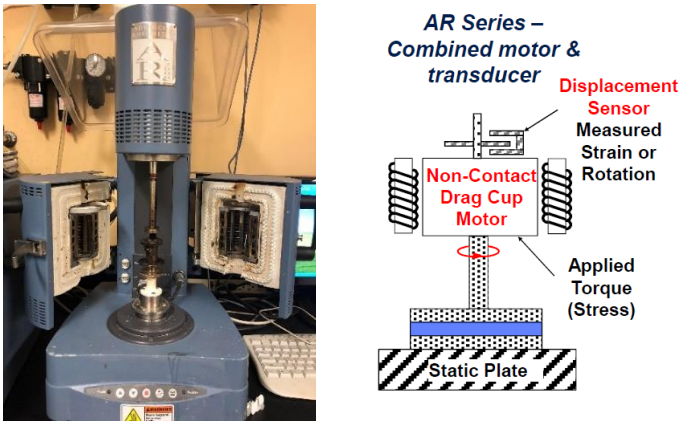

Figure 3. 5 TAI AR2000 rotational rheometer.

Figure 3. 6 Dynisco D4002 melt flow indexer.

Chapter 4

RESULTS AND DISCUSSION

4.1 Introduction

This chapter summarizes and discusses all experimental results for the samples produced according to the experimental plan discussed in chapter 3. According to that plan, CRPB samples were produced from both commodity PB-1 resins using various peroxide concentrations. Samples from both resins have been characterized in terms of their molecular weight, rheological properties and thermal properties and an attempt is made to highlight relationships between them.

Because of the similarity between PP and PB-1, the plausible reaction scheme for the production of CRPB is expected to be similar to that for the production of CRPP. This scheme is shown below and it involves hydrogen abstraction and beta-scission reactions.

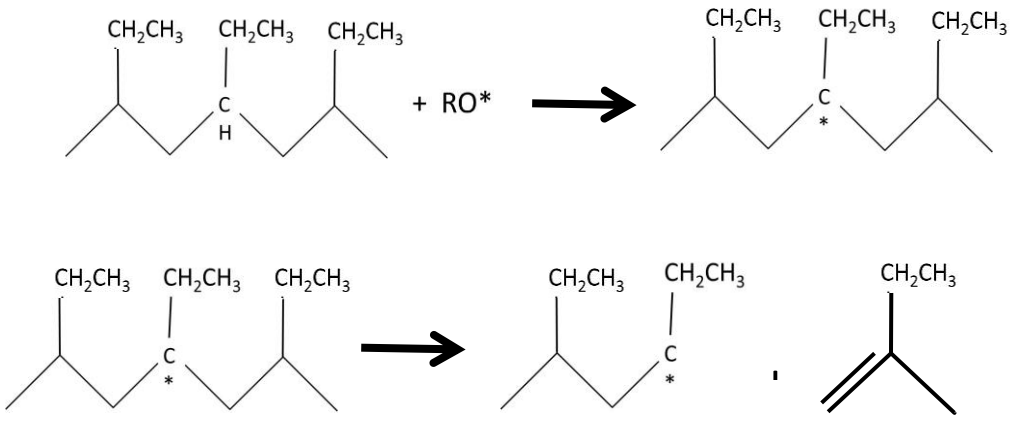

4.2 Torque profiles

During processing in the batch mixer, torque initially increases as the resin pellets are fed into the batch mixer. As the material melts, the torque starts to drop until a plateau is reached when the resin is fully molten. When the peroxide is added into the molten resin, the torque starts to drop again due to chain scission reactions until all peroxide has been consumed and a new steady state torque value is reached.

Figures 4.1 and 4.2 show the torque profiles obtained in the batch mixer during the modification experiments. In both cases, it can be observed that addition of peroxide leads to a reduction of the final steady state torque compared to the virgin PB-1 resin. Furthermore, the torque reduction compared to that of the virgin resin, appears to be proportional to the peroxide concentration. The torque reduction reflects the reduction of viscosity caused by molecular weight reduction due to chain scission reactions.

Table 4.1 summarizes all the steady-state torque values for CRPBs produced from both resins. These values are plotted against peroxide concentration in Figure 4.3.

Table 4. 1 Evolution of final torques and percentage torque drop with peroxide concentration for all samples.

RESIN 1				RESIN 2			
Sample	Peroxide Concentration (wt%)	Torque (g-m)	% torque drop	Sample	Peroxide Concentration (wt%)	Torque (g-m)	% torque drop
1-1	0	1969	0	2-1	0	3692	0
1-2	0.01	1765	21	2-2	0.01	2352	34
1-3	0.02	1297	34	2-3	0.02	2217	38
1-4	0.04	800	55	2-4	0.04	1555	58
1-5	0.06	715	60	2-5	0.06	1296	63
1-6	0.08	586	68	2-6	0.08	812	77

It can be seen that the largest drop in torque is observed within the 0-0.4% peroxide concentration range and the effect of peroxide concentration on torque is more pronounced for resin 2 which is a higher molecular weight one.

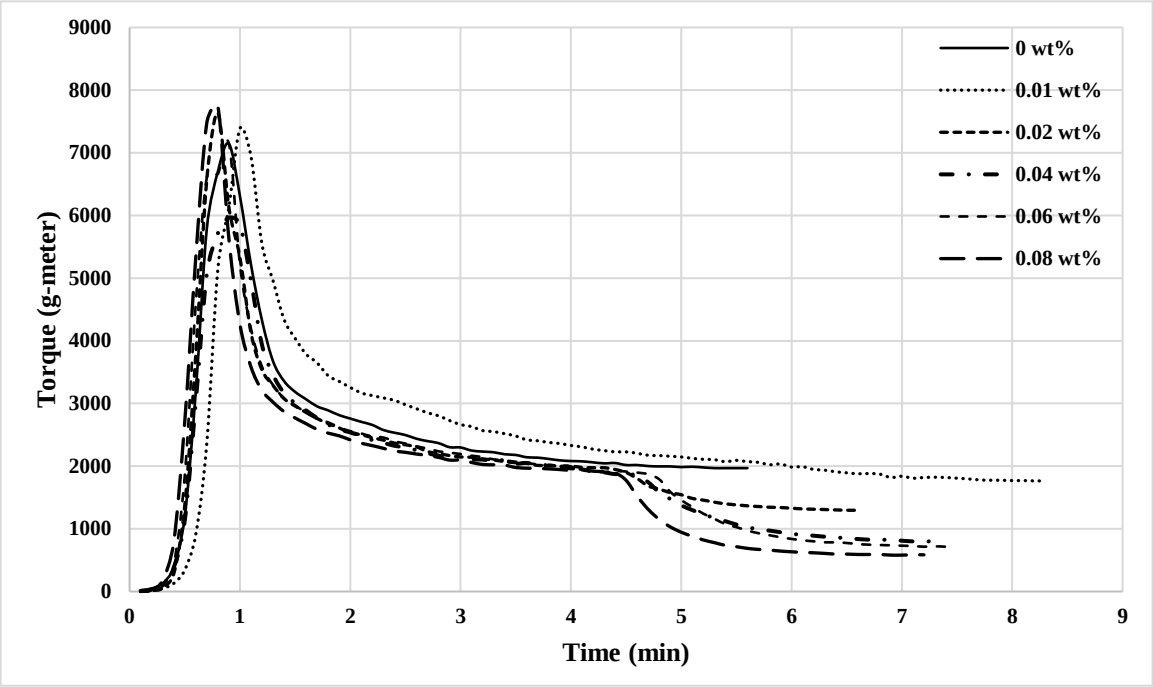

Figure 4. 1 Torque profiles for controlled rheology PB samples produced from resin 1.

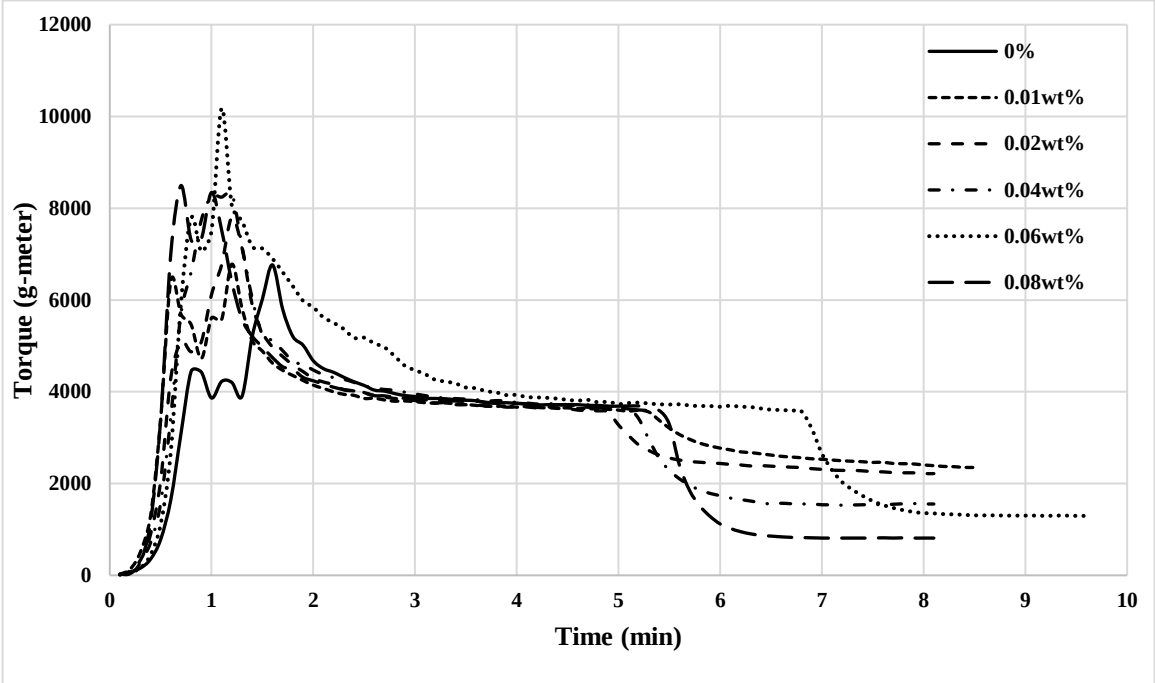

Figure 4. 2 Torque profiles for controlled rheology PB samples produced from resin 2.

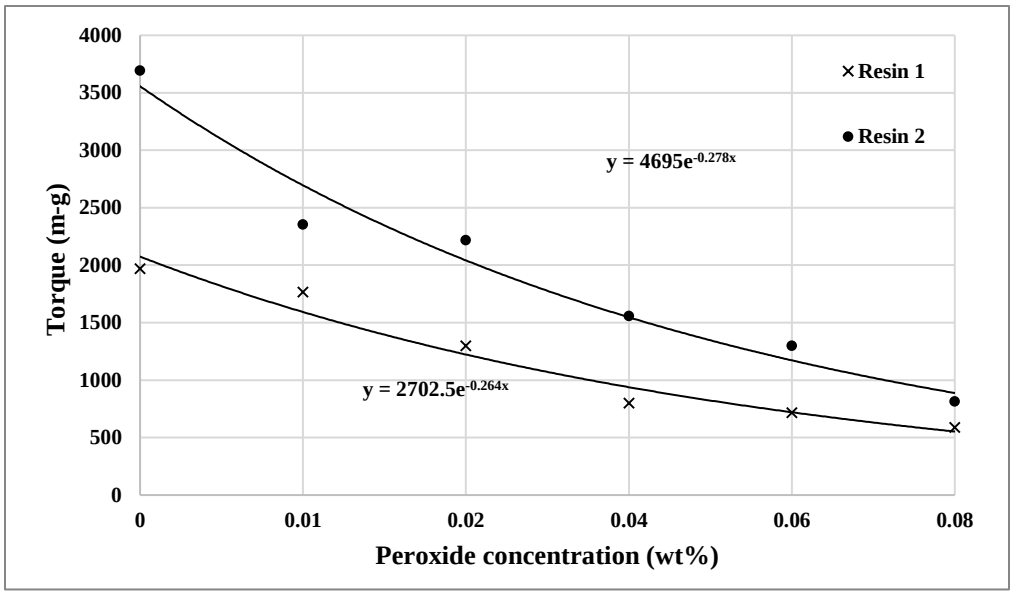

Figure 4. 3 Steady state torque values as a function of peroxide concentration.

4.3 Melt Flow Rate (MFR)

Figure 4.4 shows the MFR results as a function of peroxide concentrations for both resins. It can be seen that MFR increases and torque decreases as peroxide concentration increases. Both trends reflect the effect of reduced molecular weight on resin viscosity. The results show that the torque drops exponentially while the MFR is increasing linearly with peroxide concentration for both resins.

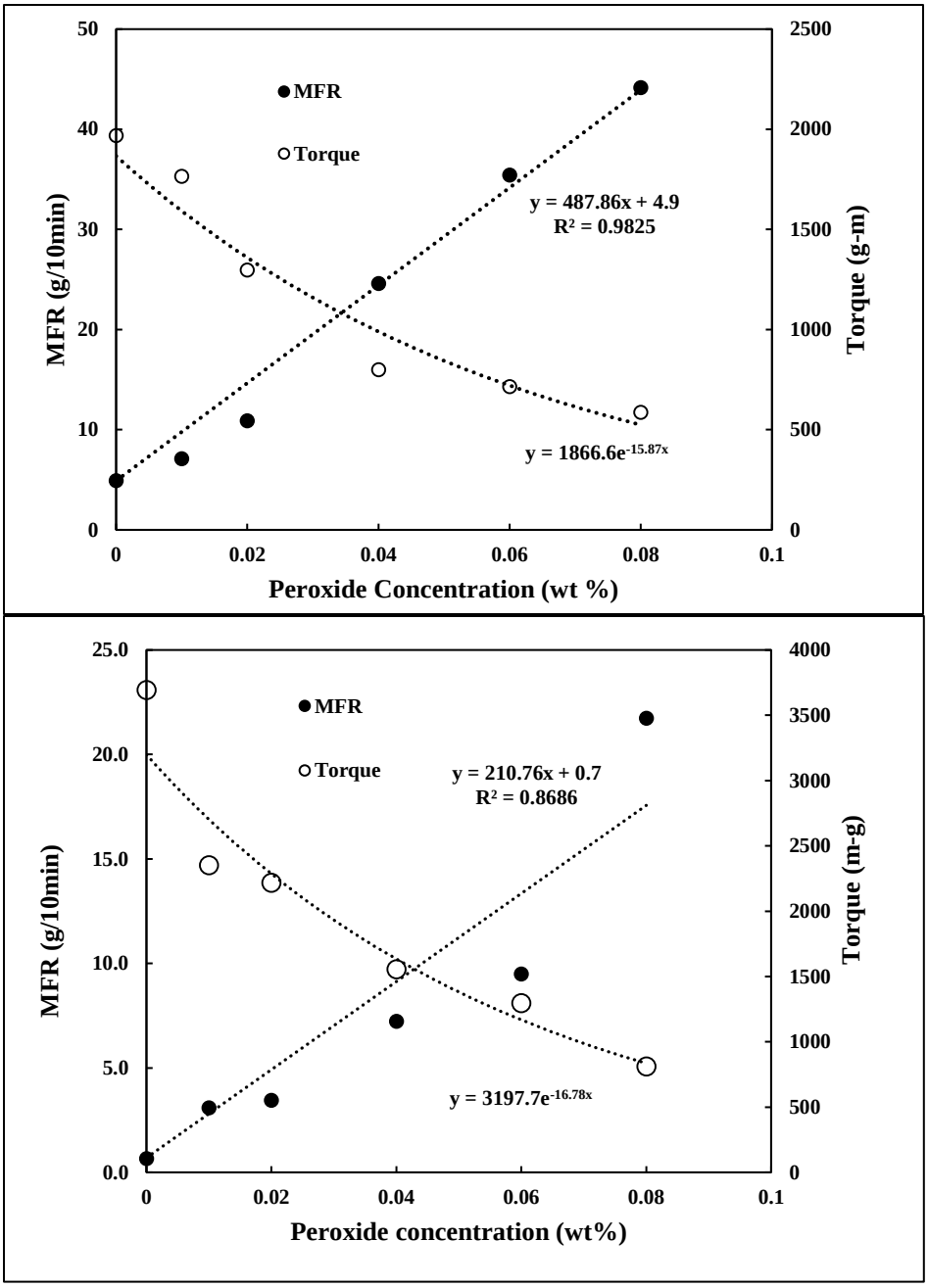

Figure 4. 4 Relationship between MFR and torque with peroxide concentration for resin 1 (top) and resin 2 (bottom).

4.4 Molecular Weight Distribution (MWD)

The changes in torque and MFR discussed above reflect changes in molecular weight (MW) and molecular weight distribution (MWD) of the starting resins. Figure 4.5 shows the MWDs of commodity resin 1 and the CRPBs produced from it using different peroxide concentrations. It can be seen that the breadth of the MWDs does not change significantly, however, the MWD shifts more to lower molecular weight as peroxide concentration increases. Similarly, the MWDs for resin 2 and the corresponding CRPBs are shown in Figure 4.6. It can be observed that the starting resin has a broader MWD than resin 1. Also, as in Figure 4.5, it may be seen that as peroxide concentration increases the MWD shifts to lower molecular weights without dramatic change in polydispersity (PDI).

Table 4.2 summarizes the effect of peroxide concentration on the average molecular weights and PDI of both resins and the modified CRPBs.

Table 4. 2 Effect of peroxide concentration of molecular weight averages and PDI.

Peroxide Conc. (%wt)	Sample	Mw (g/mol)	Mw/Mn	Mz (g/mol)	Sample	Mw (g/mol)	Mw/Mn	Mz (g/mol)
virgin	1-0	231339	3.74	496731	2-0	399069	4.27	854675
0	1-1	226693	3.70	467502	2-1	358405	4.05	740443
0.01	1-2	202085	3.26	390849	2-2	251924	3.37	497358
0.02	1-3	179259	3.11	342502	2-3	244384	3.47	495665
0.04	1-4	157233	3.18	299983	2-4	207443	3.18	414755
0.06	1-5	141962	3.19	272738	2-5	200129	3.13	410023
0.08	1-6	128581	3.20	242178	2-6	157940	2.97	323608

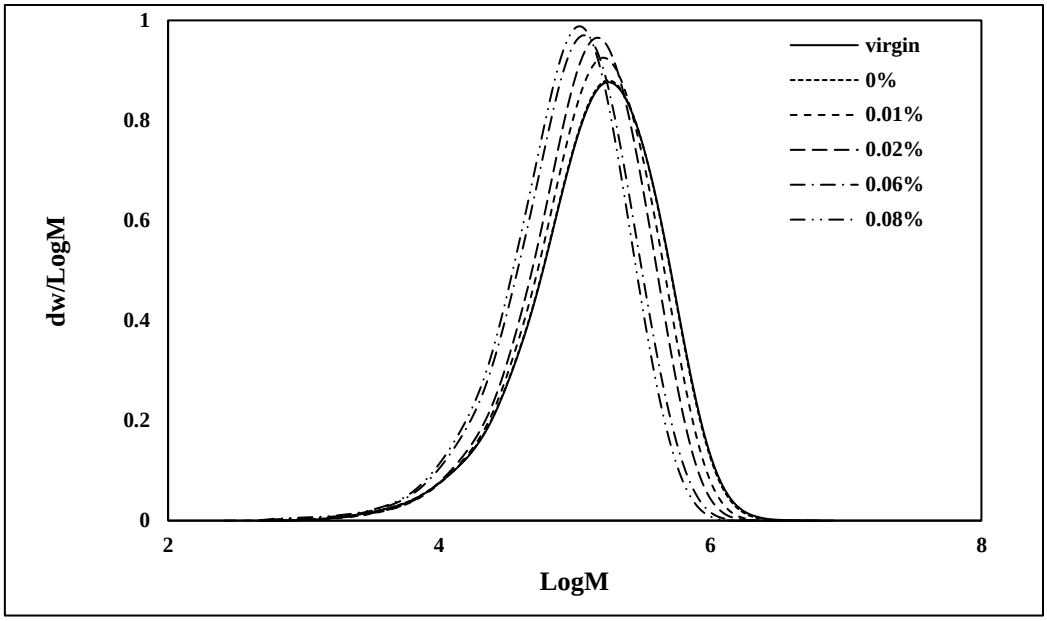

Figure 4. 5 MWDs of CRPBs produced from resin 1 using various amounts of peroxide.

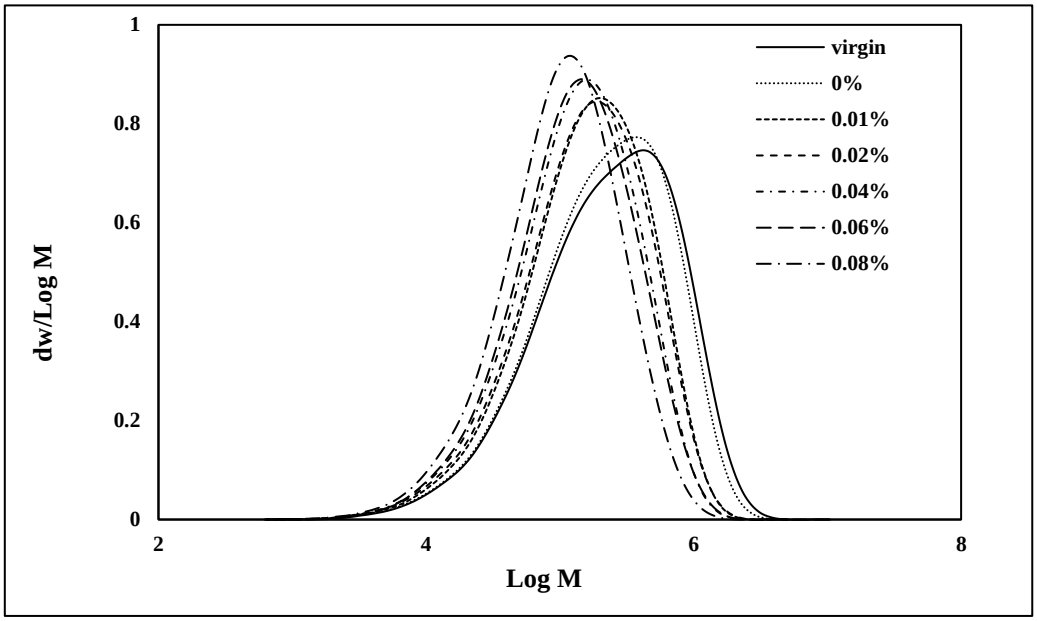

Figure 4. 6 MWDs of CRPBs produced from resin 2 using various amounts of peroxide.

Figures 4.7 and 4.8 show the effect of peroxide concentration on weight-average molecular weight (M_w) and PDI for samples based on resin 1 and resin 2, respectively. For resin 1, it can be seen (Figure 4.7) that PDI remains almost constant after the initial reduction at low peroxide concentration. For resin 2 (Figure 4.8), PDI keeps decreasing slightly with peroxide concentration. For both resins, PDI appears to approach a value of 3 asymptotically.

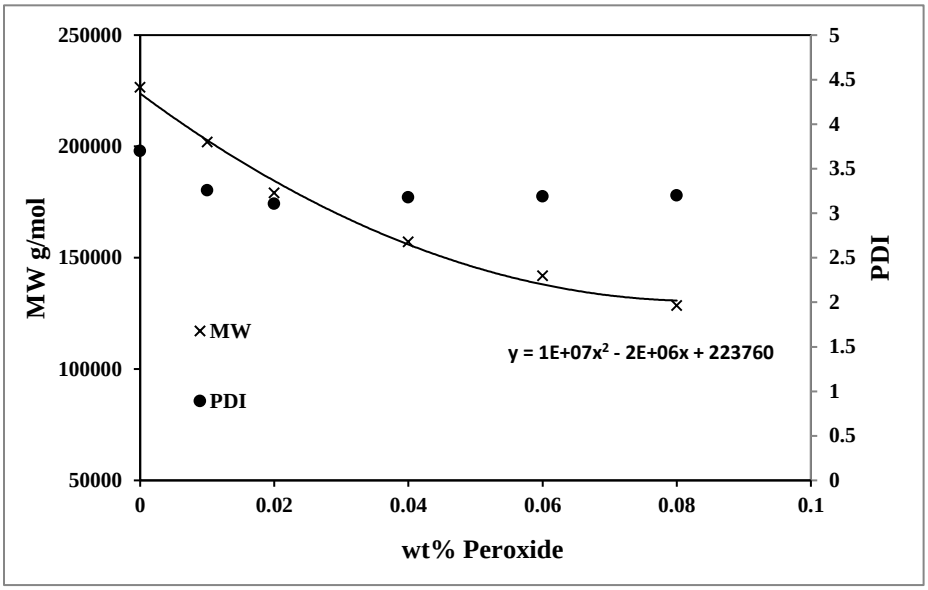

Figure 4. 7 Relationship between Mw and PDI with peroxide concentration for resin 1.

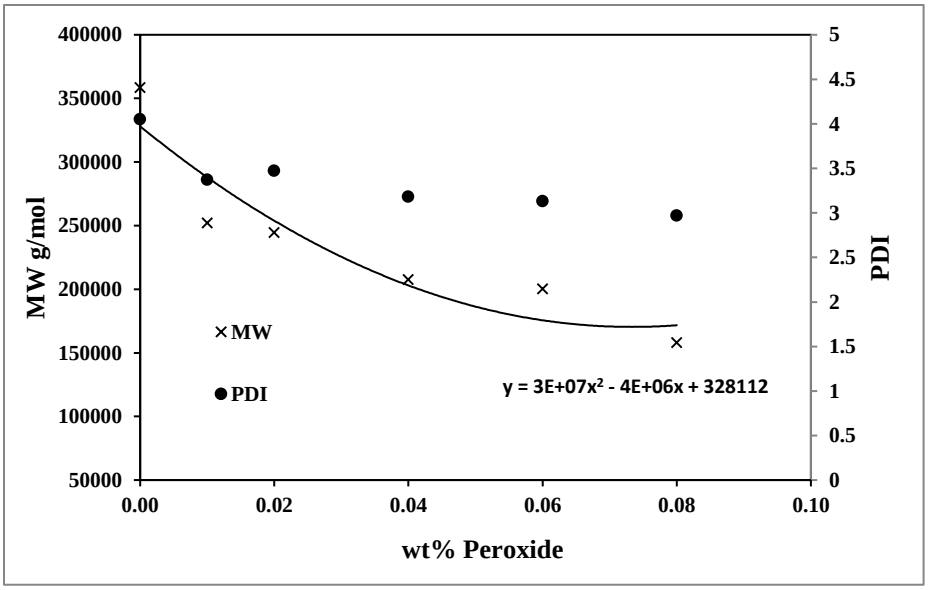

Figure 4. 8 Relationship between Mw and PDI with peroxide concentration for resin 2.

4.5 Thermal Properties

As molecular weight and PDI is decreasing with peroxide concentration, the melting and crystallization properties may be affected. These properties were measured by differential scanning calorimetry (DSC) for all samples. DSC scans are listed in Appendix A for all samples and results are summarized in Table 4.3 and Table 4.4.

Table 4. 3 Thermal properties of CRPBs produced from resin 1.

Sample	Peroxide Conc. (%wt)	Melting Temperature T_m (°C)	Heat of melting ΔH_m (J/g)	Crystallization temperature T_c (°C)	Crystallization onset temperature $T_{c,onset}$	Heat of crystallization ΔH_c (J/g)
1-1	0	117.3	35.3	72.2	85.4	39.9
1-2	0.01	116.3	33.2	72.0	85.6	37.8
1-3	0.02	115.2	31.7	72.1	85.3	37.6
1-4	0.04	112.9	33.8	72.3	87.6	38.2
1-5	0.06	112.2	33.6	71.6	84.8	37.6
1-6	0.08	111.8	34.5	71.6	85.2	37.9

Table 4. 4 Thermal properties of CRPBs produced from resin 2.

Sample	Peroxide Conc. (%wt)	Melting temperature T_m (°C)	Heat of melting ΔH_m (J/g)	Crystallization temperature T_c (°C)	Crystallization onset temperature $T_{c,onset}$	Heat of crystallization ΔH_c (J/g)
2-1	0	117.7	34.4	70.5	85.4	36.2
2-2	0.01	114.0	40.6	70.1	86.1	36.8
2-3	0.02	114.1	35.8	72.2	87.1	38.2
2-4	0.04	113.0	30.3	71.6	88.2	34.6
2-5	0.06	112.9	35.7	71.2	84.5	37.2
2-6	0.08	111.9	34.8	72.5	84.6	35.0

It can be seen that the melting temperature of both resins decreases slightly with peroxide concentration. This is expected because of the reduction of MW as shorter chains require less energy for phase change transitions [39]. In terms of crystallization temperature, it appears that peroxide concentration does not have a significant effect and we can only observe a slight increase of the crystallization temperature for resin 2 at high peroxide concentrations. No trends can be seen in terms of the effect of peroxide concentration on the heats of melting and crystallization. These results are in general agreement with previous general studies, in which polymer crystallization temperature was not found to change with molecular weights [39]. Overall, the data presented in Tables 4.3 and 4.4 suggest that not significant changes in crystallization should be expected due to the chain scission reaction initiated by the peroxide radicals. In the future, additional experiments at higher levels of peroxide should be performed to see if this is still the case at much lower molecular weights.

4.6 Linear viscoelastic properties

The linear viscoelastic properties of the virgin resins as well as those of all CRPB samples were measured through oscillatory shear tests using a parallel plate rheometer as described in Chapter 3. Strain sweep experiments were first carried out to determine the linear viscoelastic region (LVR) for all samples. The LVR represents a range of strain values in which the rheological properties (complex viscosity and moduli) do not depend on the strain magnitude. Figure 4.9 shows an example of a strain sweep experiment for resin 2 at a temperature of 170 ^{o}C.

At strains lower than 2%, the moduli and viscosity are not changing with percentage strain. This defines the LVR region. Based on such strain sweep experiments, a strain of 0.1% was selected to be used in all frequency sweep experiments from 0.1 to 628 rad/s. Such frequency sweep tests provide measurements of rheological properties such as complex viscosity (η^*) and storage and loss moduli (G' and G").

In frequency sweep mode, the experiments were carried out at three different temperatures (150^{o}C, 170 ^{o}C and 190 ^{o}C). Figure 4.10 shows the results of frequency sweep tests for resin 1 CRPBs at different temperatures with various peroxide concentrations. In each graph, it can be seen that complex viscosity decreases with increasing temperature and that the spread between curves appears the same for all peroxide concentrations. Additionally, the shear thinning behavior seems to not be changing with temperature and peroxide concentration.

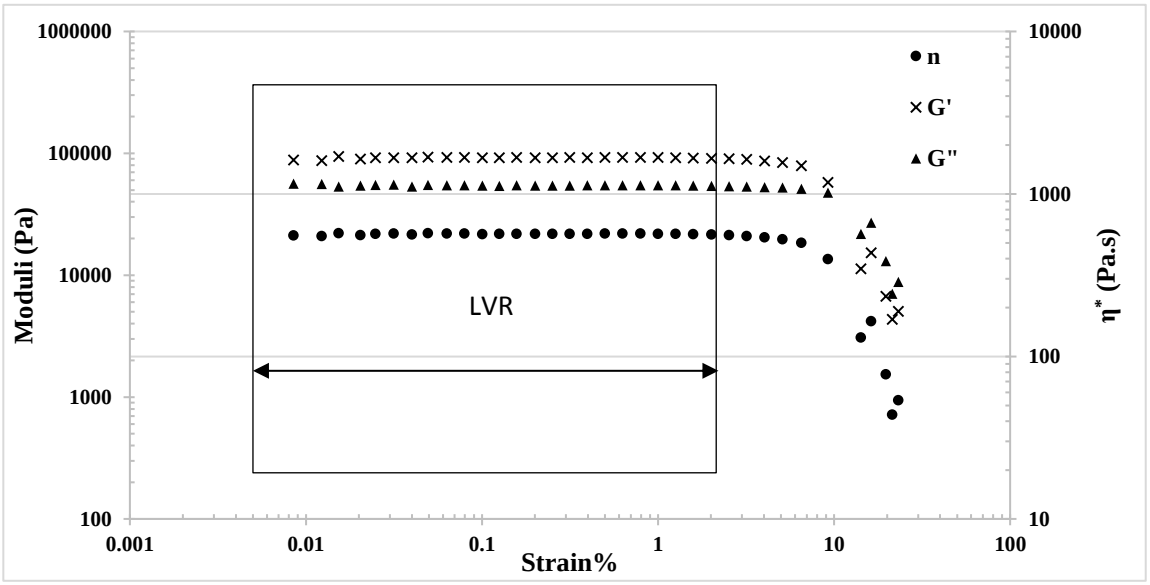

Figure 4. 9 Strain sweep test for resin 2 at 170 ºC at a frequency of 628 rad/s.

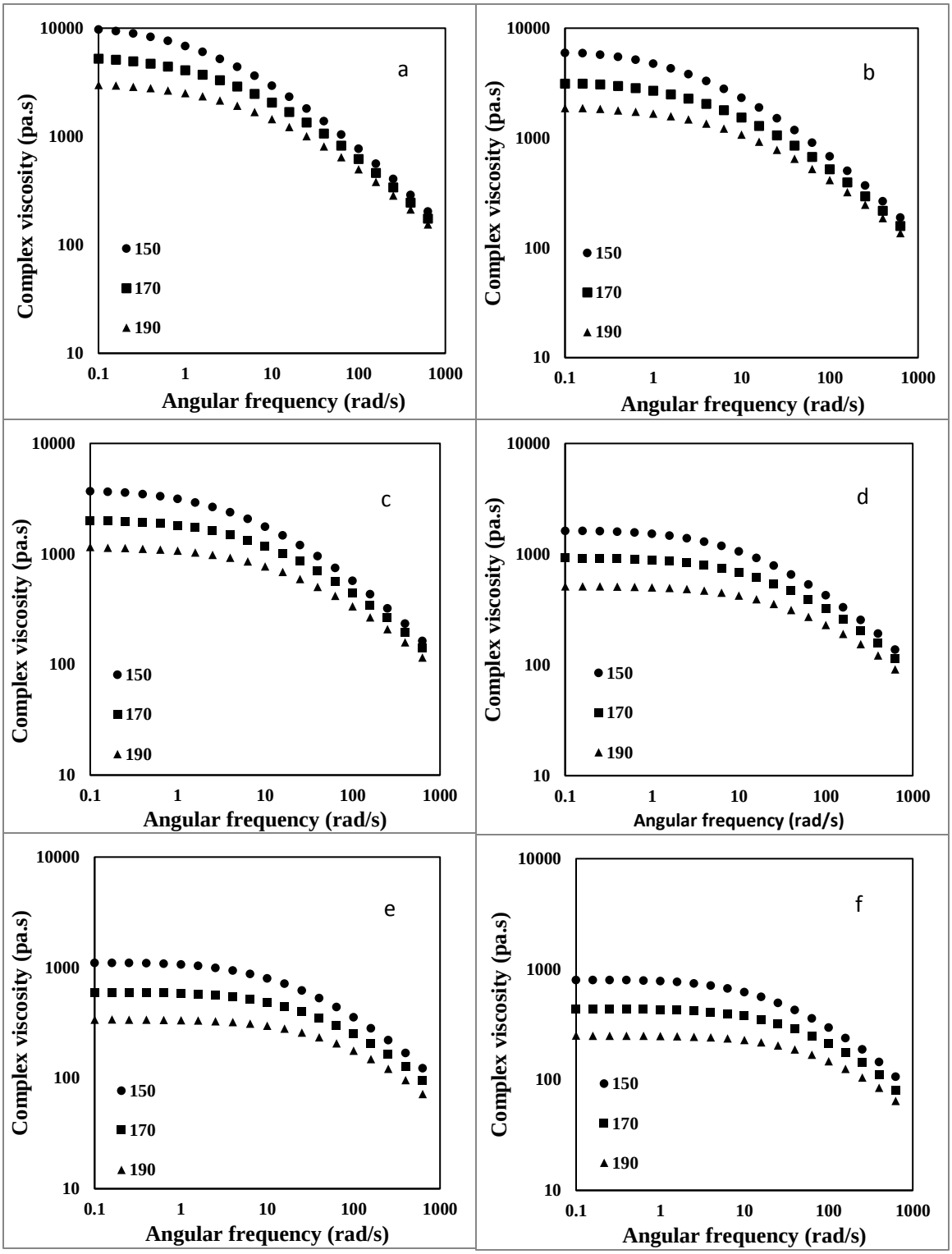

Figure 4. 10 Complex viscosity as function of angular frequency with temperatures for resin 1 at (a) 0 wt%, (b) 0.01 wt%, (c) 0.02 wt%, (d) 0.04 wt%, (e) 0.06wt% and (f) 0.08 wt% peroxide concentration respectively.

Figure 4.11 shows similar frequency test results for resin 2. Similar temperature effect is observed for resin 2 CRPBs and the effect of peroxide concentration on viscosity reduction and shear thinning behavior is more pronounced. The peroxide concentration effects on complex viscosity at different temperatures are shown in Figure 4.12 and Figure 4.13 for both resins. Increasing peroxide level leads to reduced zero-shear viscosity; however, the shear thinning behavior at high shear rates seems to remain the same. This agrees with previous observations of shear thinning properties of PB-1 [35]. Note that the lowest angular frequency used in the experiments is 0.1 rad/s so the zero-shear viscosity was estimated by fitting the Carreau-Yasuda model to these data.

In order to fit the Carreau-Yasuda model, the power-law index was estimated first from the shear thinning region by using the power-law model shown in Equation 4.1:

$$\eta = k * \dot{\gamma}^{n-1} \qquad \text{Equation 4.1}$$

where η is complex viscosity; k is the consistency index which is numerically equal to the viscosity at 1 s^{-1}; $\dot{\gamma}$ is the shear rate and n is the power-law index.

Power-law index values calculated by fitting equation 4.1 to the experimental data are listed in Table 4.5. The power-law index seems to be increasing slightly with both peroxide concentration and temperature in agreement with the observations from Figures 4.10 to Figure 4.13.

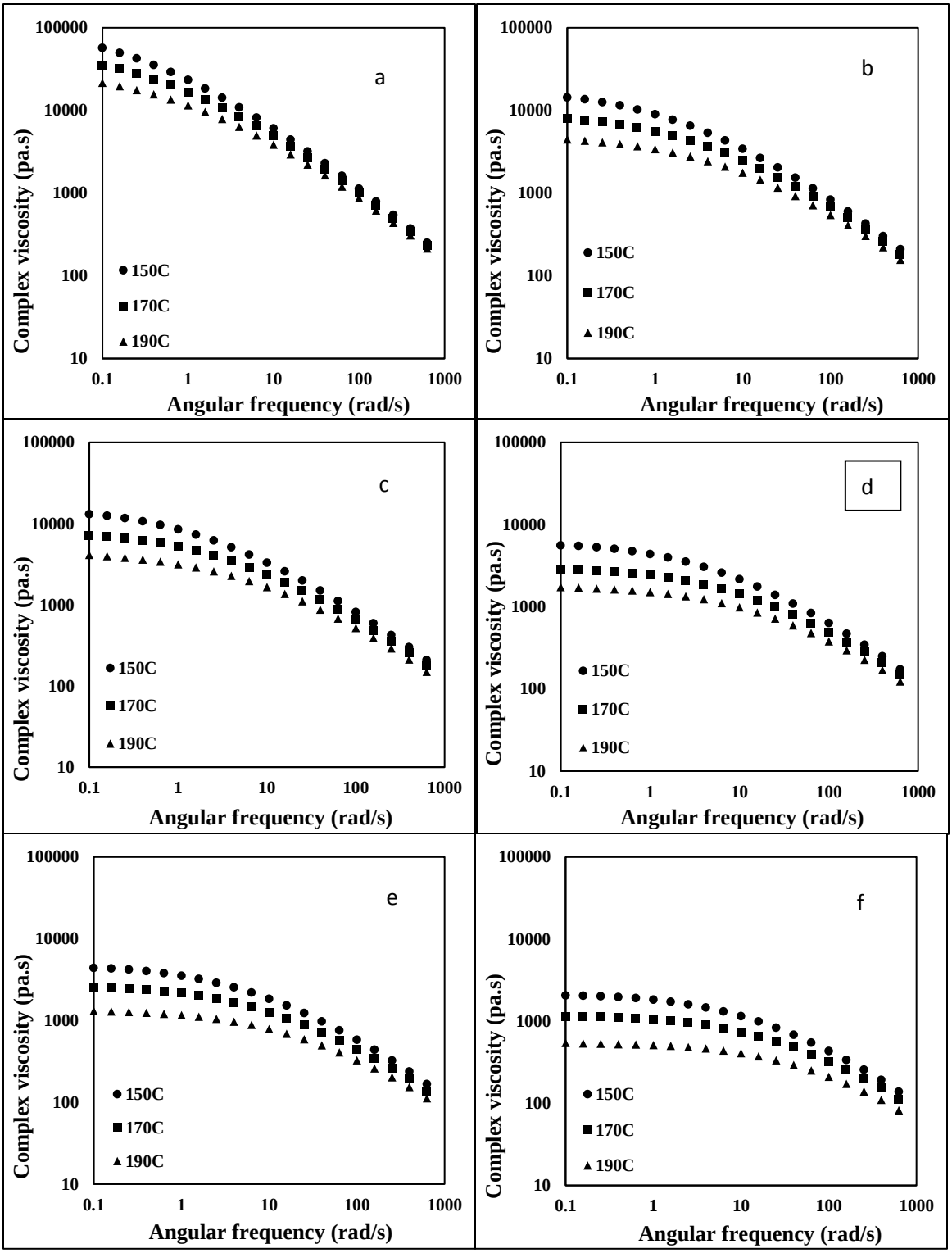

Figure 4. 11 Complex viscosity as function of angular frequency with temperatures for resin 2 at (a) 0 wt%, (b) 0.01 wt%, (c) 0.02 wt%, (d) 0.04 wt%, (e) 0.06wt% and (f) 0.08 wt% peroxide concentration respectively.

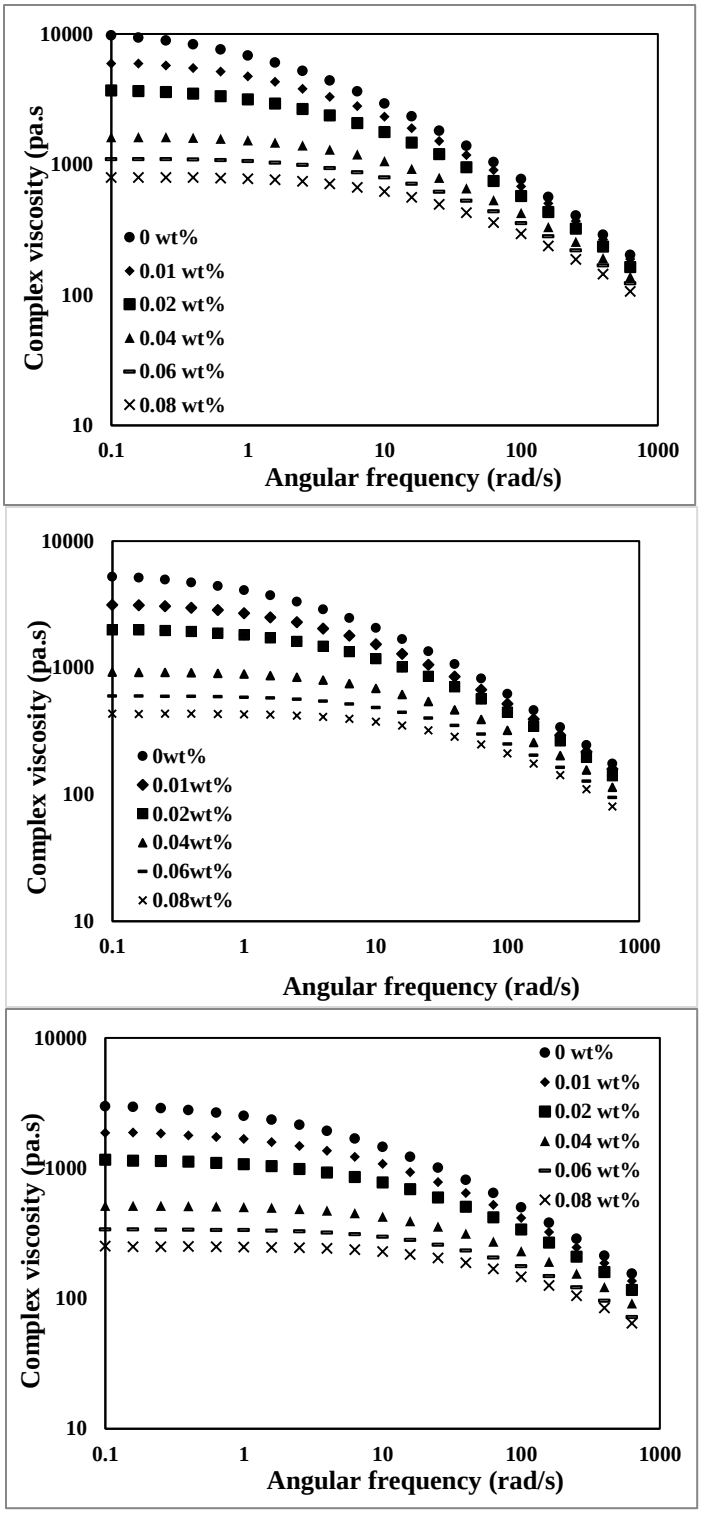

Figure 4. 12 Complex viscosity as function of angular frequency for resin 1 at (a) 150 ºC (top), (b) 170 ºC (middle) and (c) 190 ºC (bottom).

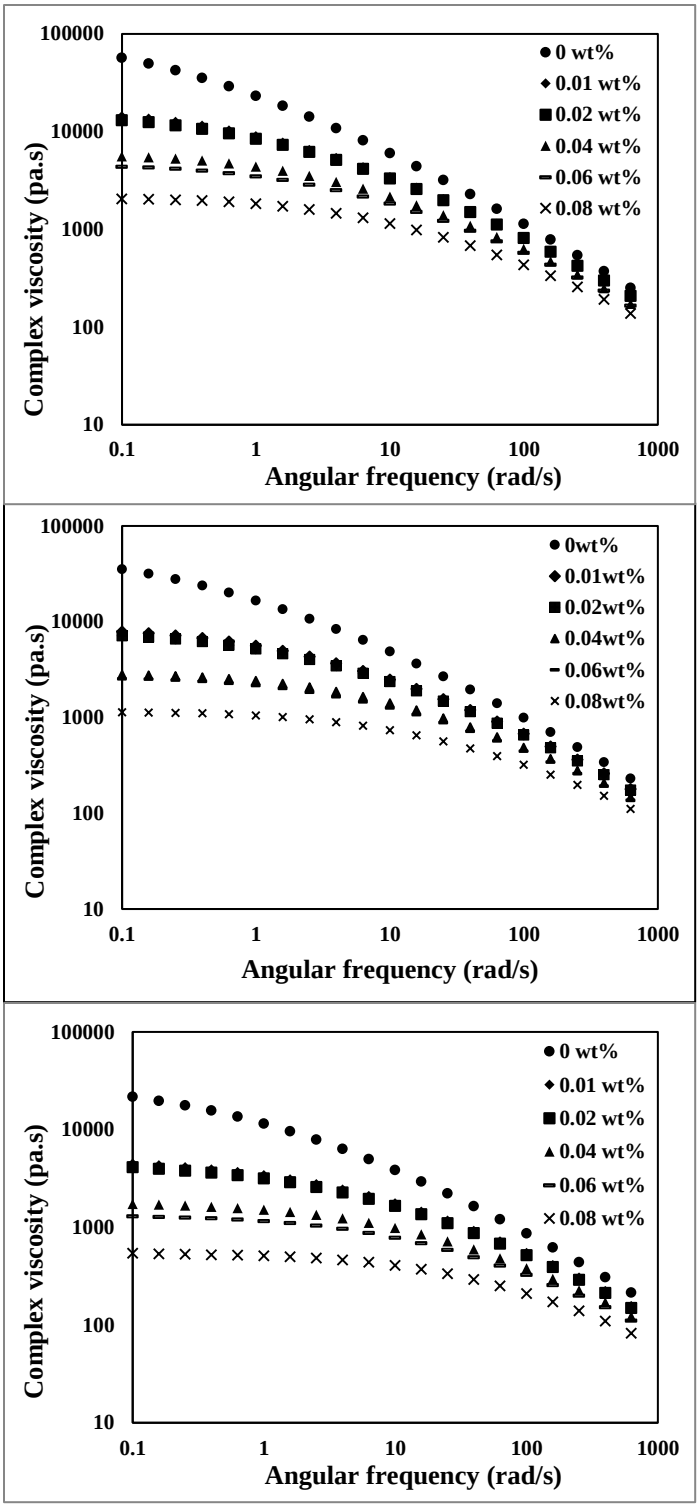

Figure 4. 13 Complex viscosity as function of angular frequency for resin 2 at (a) 150 ºC (top), (b) 170 ºC (middle) and (c) 190 ºC (bottom).

Table 4. 5 Summary of power-law index values for all CRPBs.

	Power law index n				Power law index n		
sample	150 ℃	170 ℃	190 ℃	sample	150 ℃	170 ℃	190 ℃
1-1	0.4	0.4	0.46	2-1	0.29	0.32	0.34
1-2	0.39	0.45	0.48	2-2	0.34	0.37	0.4
1-3	0.43	0.46	0.49	2-3	0.35	0.37	0.4
1-4	0.46	0.49	0.53	2-4	0.37	0.41	0.43
1-5	0.5	0.5	0.47	2-5	0.4	0.42	0.46
1-6	0.47	0.43	0.48	2-6	0.42	0.45	0.46

Once the power-law index is found, the zero-shear viscosity can be obtained by fitting the Carreau-Yasuda model shown in Equation 4.2:

$$\frac{\eta-\eta_\infty}{\eta_0-\eta_\infty} = \frac{1}{1+\lambda\dot{\gamma}^{n-1}} \qquad \text{Equation 4.2}$$

where η is the measured viscosity; η_∞ is viscosity at infinite shear rate; η_0 is viscosity at zero shear rate and λ is the relaxation time constant.

The estimated parameters in the Carreau-Yasuda model are listed in Table 4.6 and Table 4.7. Both zero-shear viscosity and relaxation time decrease with increasing peroxide concentration as expected due to the reduced molecular weight and elasticity of the materials. Also, both zero-shear viscosity and relaxation time decrease with temperature for each sample. Finally, values for resin 2 CRPBs (Table 4.7) are higher than those for resin 1 due to the higher molecular weights of these materials.

Table 4. 6 Zero-shear viscosity and time constant calculated from Carreau-Yasuda model for resin 1 at different temperatures.

	150 ℃		170 ℃		190 ℃	
sample	η_0 (Pa.s)	λ (sec)	η_0 (Pa.s)	λ (sec)	η_0 (Pa.s)	λ (sec)
1-1	9749	0.7	5220	0.5	2986	0.4
1-2	5950	0.46	3133	0.35	1868	0.25
1-3	3687	0.35	1996	0.25	1160	0.15
1-4	1623	0.15	926	0.1	514	0.07
1-5	1102	0.12	597	0.06	339	0.03
1-6	794	0.07	435	0.03	251	0.02

Table 4. 7 Zero-shear viscosity and time constant calculated from Carreau-Yasuda model for resin 2 at different temperatures.

	150 ℃		170 ℃		190 ℃	
sample	η_0 (Pa.s)	λ (sec)	η_0 (Pa.s)	λ (sec)	η_0 (Pa.s)	λ (sec)
2-1	59320	3.5	36413	3.0	21820	1.5
2-2	14417	1	7916	0.8	4470	0.5
2-3	13147	1	7171	0.6	4116	0.4
2-4	5592	0.4	2810	0.25	1739	0.2
2-5	4393	0.4	2535	0.3	1304	0.18
2-6	2053	0.2	1133	0.12	540	0.06

Using the zero-shear viscosity data at various temperatures and peroxide concentrations, the flow activation energy of all samples can be obtained by fitting the Arrhenius equation shown in equation 4.3:

$$\eta_0 = A\ exp(\frac{E}{RT}) \qquad \text{Equation 4.3}$$

where η_0 is the zero-shear viscosity, A is the frequency term and E is the flow activation energy; R is the gas constant and T is absolute temperature.

Zero-shear viscosity data are plotted against inverse temperature for all peroxide levels in Figure 4.14 and Figure 4.15 for resin 1 and resin 2, respectively. By fitting equation 4.3 to these data, the flow activation energy is estimated for each sample. The activation energy values are listed in Table 4.8. The results indicate that the flow activation energy of resin 1 series is approximately 47.5 kJ/mol for all samples. However, the flow activation energy for resin 2 series increases slightly with peroxide concentration.

Table 4. 8 Activation energy of all CRPB samples.

Sample	E (J/mol)	Sample	E (J/mol)
1-1	48171	2-1	40672
1-2	47204	2-2	47656
1-3	47085	2-3	47273
1-4	46757	2-4	47639
1-5	47985	2-5	49335
1-6	48542	2-6	54241

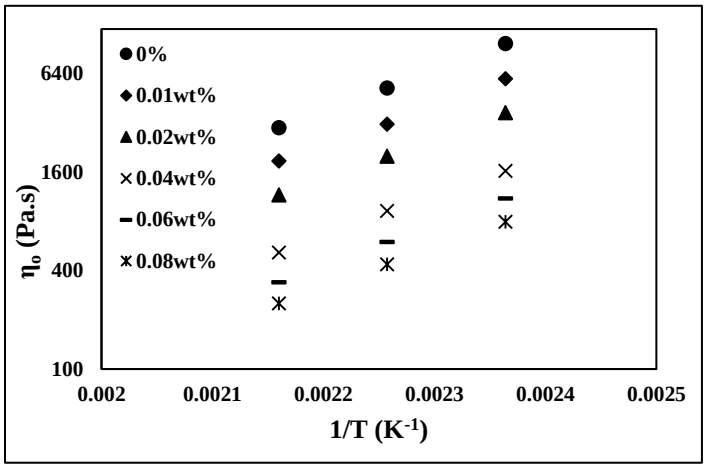

Figure 4. 14 Correlation between zero-shear viscosity and temperature for resin 1.

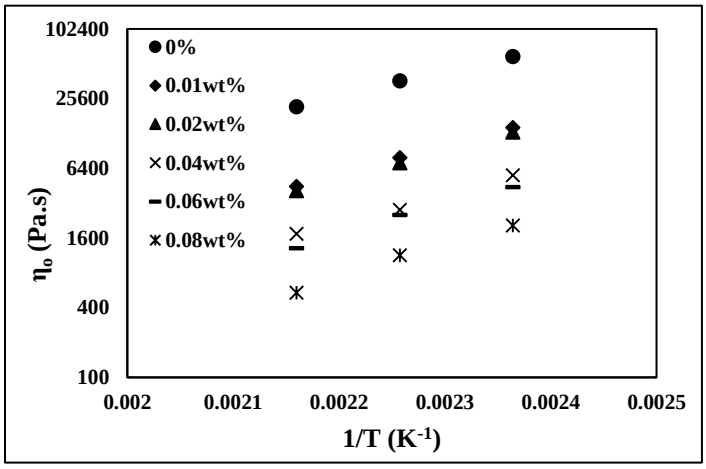

Figure 4. 15 Correlation between zero-shear viscosity and temperature for resin 2.

The zero-shear viscosity data are plotted against weight-average molecular weight in Figures 4.16 and 4.17 for resin1 and resin 2 CRPBs, respectively. It can be clearly seen that power-law dependence of equation 4.4 holds.

$$\eta_0 = K{M_w}^a \qquad \text{Equation 4.4}$$

It can be observed that the values of the exponent α are higher than the 3.4 value typically observed for linear materials. This would indicate that some branching or crosslinking may be taking place along with the peroxide induced scission reactions. No indication of branching was evident from the SEC measurements, however, the sample used in SEC is filtered so any gel present would have been removed. This needs to be further examined and any possible gel content needs to be measured by Soxhlet extraction. Also, the molecular weight measurements could be double checked for the parameters in the Mark-Houwink equation.

The storage and loss moduli data are also obtained from oscillatory shear measurements. The storage modulus G' reflects the elastic behavior of the sample while the loss modulus G" reflects the viscous one. Figure 4.18 shows a G' and G" versus frequency graph from one of the experimental results. At low frequency, G" is greater than G', which means liquid like behavior predominates; however, at high frequency, the situation is reversed to G' being greater, which means solid like behavior predominates. At the cross-over point, both moduli have the same value.

Figures 4.19 and 4.20 show the G' and G" data versus frequency for all peroxide concentrations and all test temperatures for resin 1 and resin 2, respectively. Inspection of these graphs shows that both moduli values decrease with increasing peroxide

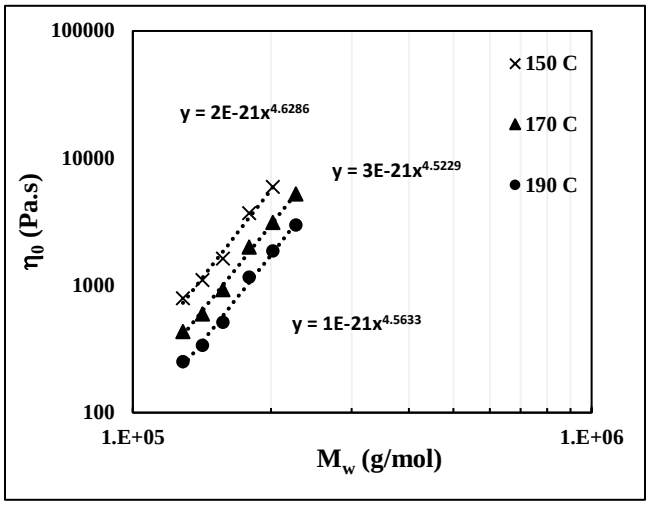

Figure 4. 16 Correlation between zero-shear viscosity and Mw with different temperatures for resin 1.

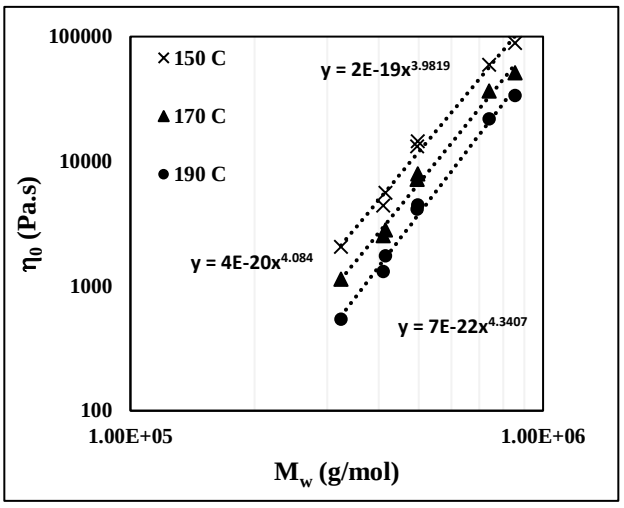

Figure 4. 17 Correlation between zero-shear viscosity and Mw with different temperatures for resin 2.

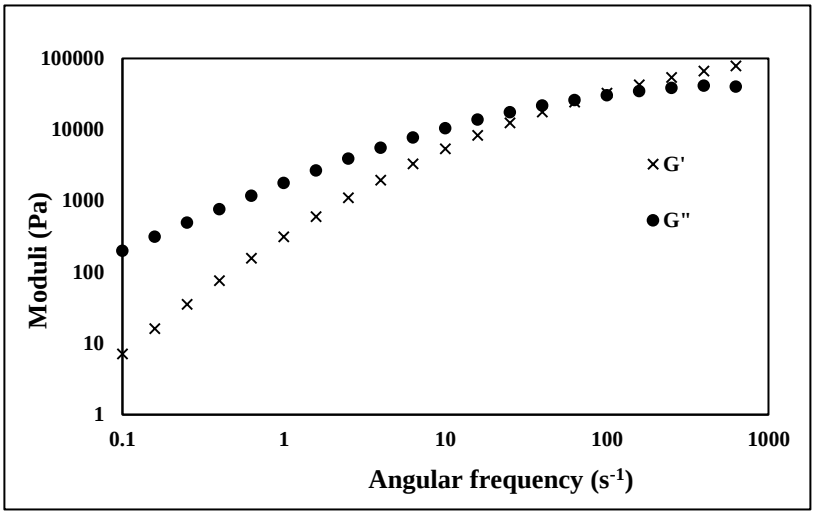

Figure 4. 18 Storage modulus G' and loss modulus G" as function of angular frequency.

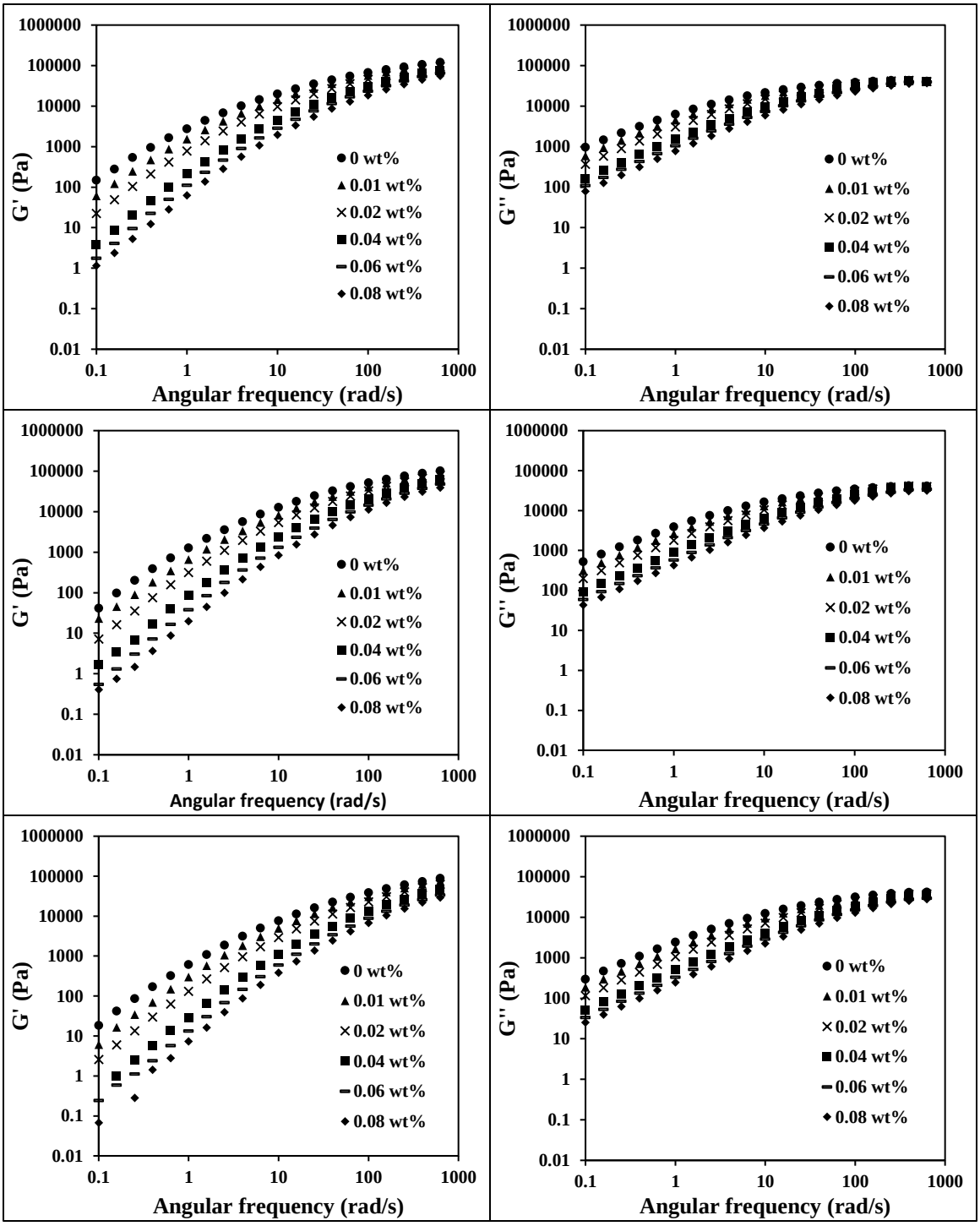

Figure 4. 19 G' and G" as function of angular frequency with peroxide concentration for resin 1 at temperature of (a) 150 °C (top), (b) 170 °C (middle) and (c) 190 °C (bottom).

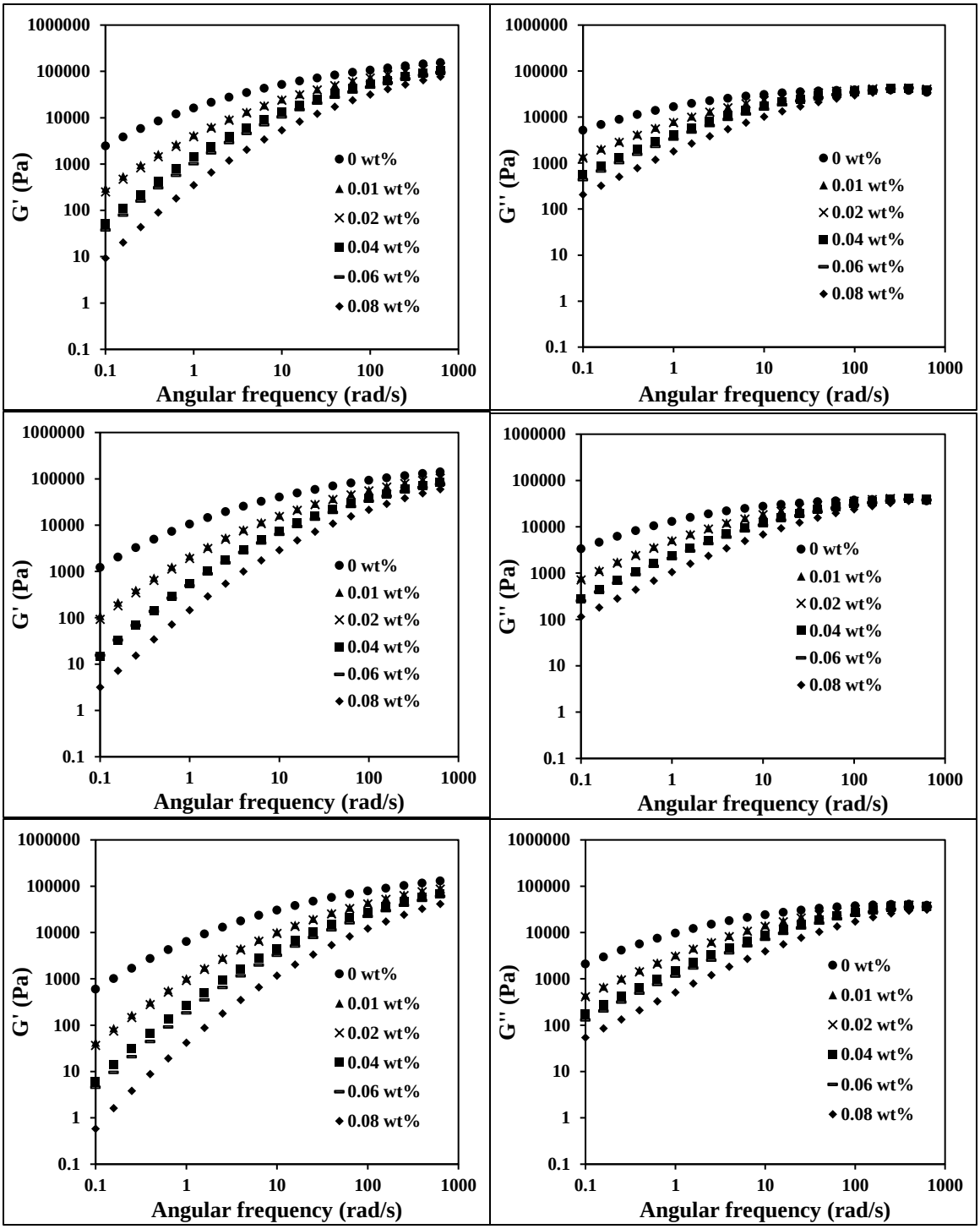

Figure 4. 20 G' and G" as function of angular frequency with peroxide concentration for resin 2 at temperature of (a) 150 ºC (top), (b) 170 ºC (middle) and (c) 190 ºC (bottom).

concentration and temperature. Also, it can be observed that the effect of peroxide concentration is more pronounced at lower frequencies. This is due to the fact scission reactions affect more the larger molecules which have larger relaxation times (probed at the lower frequencies). In addition, it can be seen that the effect of peroxide concentration is more pronounced on the storage modulus rather than the loss modulus. This is reasonable given that scission reactions affect primarily the longest molecules which dictate the elastic behavior of the material.

The cross-over modulus value is found when G' is equal to G" and is also important in characterizing a sample at this point, the elastic and viscous properties are the same. In addition, the frequency at this point is inversely proportional to relaxation time. Thus, the viscoelastic response of a sample can be predicted if the relaxation time is found. The summary of cross-over moduli and corresponding frequencies for all samples is listed in Table 4.9.

Table 4. 9 Summary of cross-over modulus G_c and frequency W_c for all samples.

		Temperature ^oC					
		150		170		190	
Peroxide conc. (%wt)	sample	G_c (Pa)	W_c (s^{-1})	G_c (Pa)	W_c (s^{-1})	G_c (Pa)	W_c (s^{-1})
0	1-1	23233	12.9	21747	21	24925	48
0.01	1-2	24717	22	24880	44	25237	75
0.02	1-3	26685	39	27746	77.6	27811	138
0.04	1-4	29361	96	29739	170	29841	303
0.06	1-5	30011	144	29893	270	28313	456
0.08	1-6	29315	196	30127	377	27072	588
0	2-1	17043	1.1	17705	2.2	18122	4.3
0.01	2-2	21108	7.8	22192	16.5	23332	21
0.02	2-3	21639	8.9	22520	18	22699	35
0.04	2-4	24260	24	25336	52	24878	89
0.06	2-5	25076	35	24251	60	25167	124
0.08	2-6	26711	78	26554	140	26630	305

These results indicate that the crossover modulus value somehow does not depend on temperature. However, the crossover frequency increases with temperature. Also, both cross-over modulus and frequency increase with peroxide concentration for both resins.

As discussed earlier in this chapter (section 4.4), the PDI for both resins decreased slightly after treated with peroxide. Figure 4.21 and Figure 4.22 show a Cole-Cole plot (G' vs G") for all samples at all temperatures. Traditionally, the slope of these lines have been related to PDI changes and they are used here to show the effect of peroxide concentration on PDI. It is evident from these graphs, that the slope of G' vs G" does not vary and it remains approximately constant. This is in agreement with PDI measurements from SEC analysis.

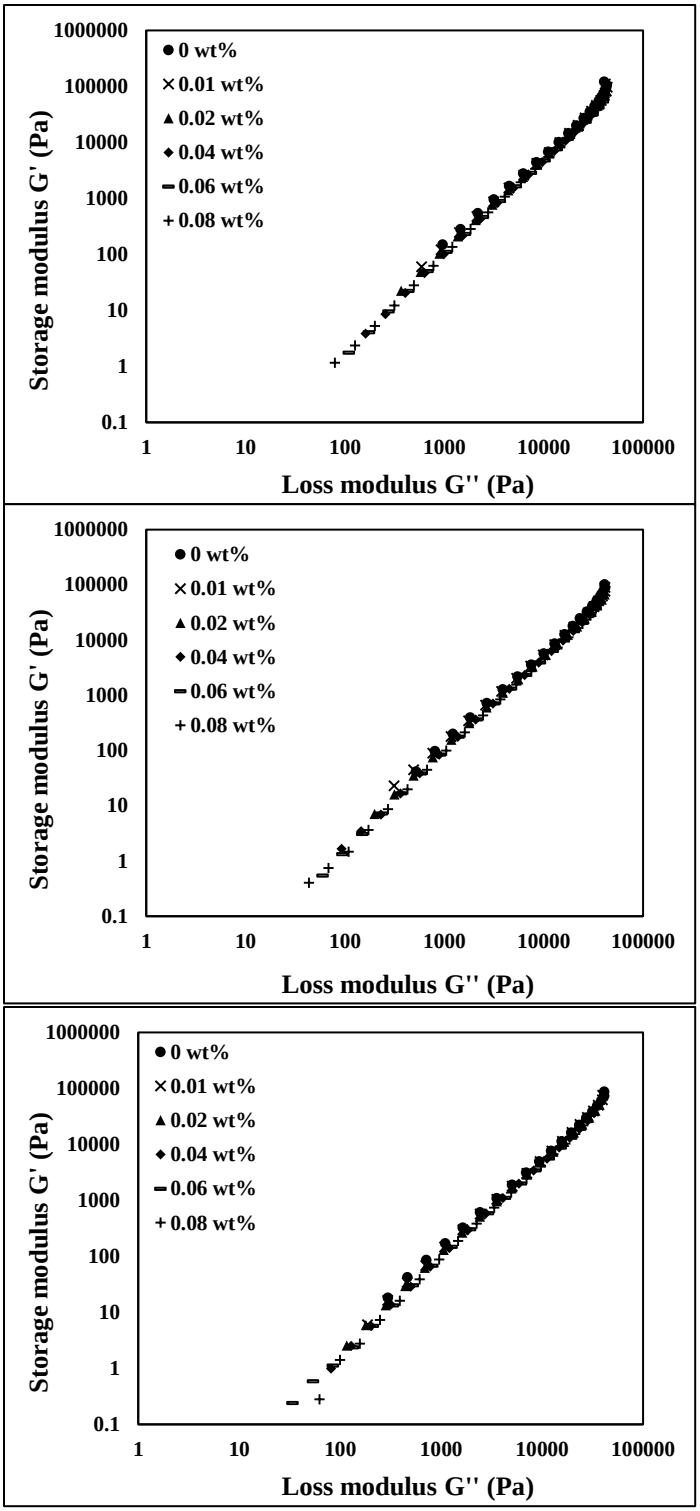

Figure 4. 21 Storage modulus G' as function Loss modulus G" for resin 1 at (a) 150 °C (top), (b) 170 °C (middle) and (c) 190 °C (bottom).

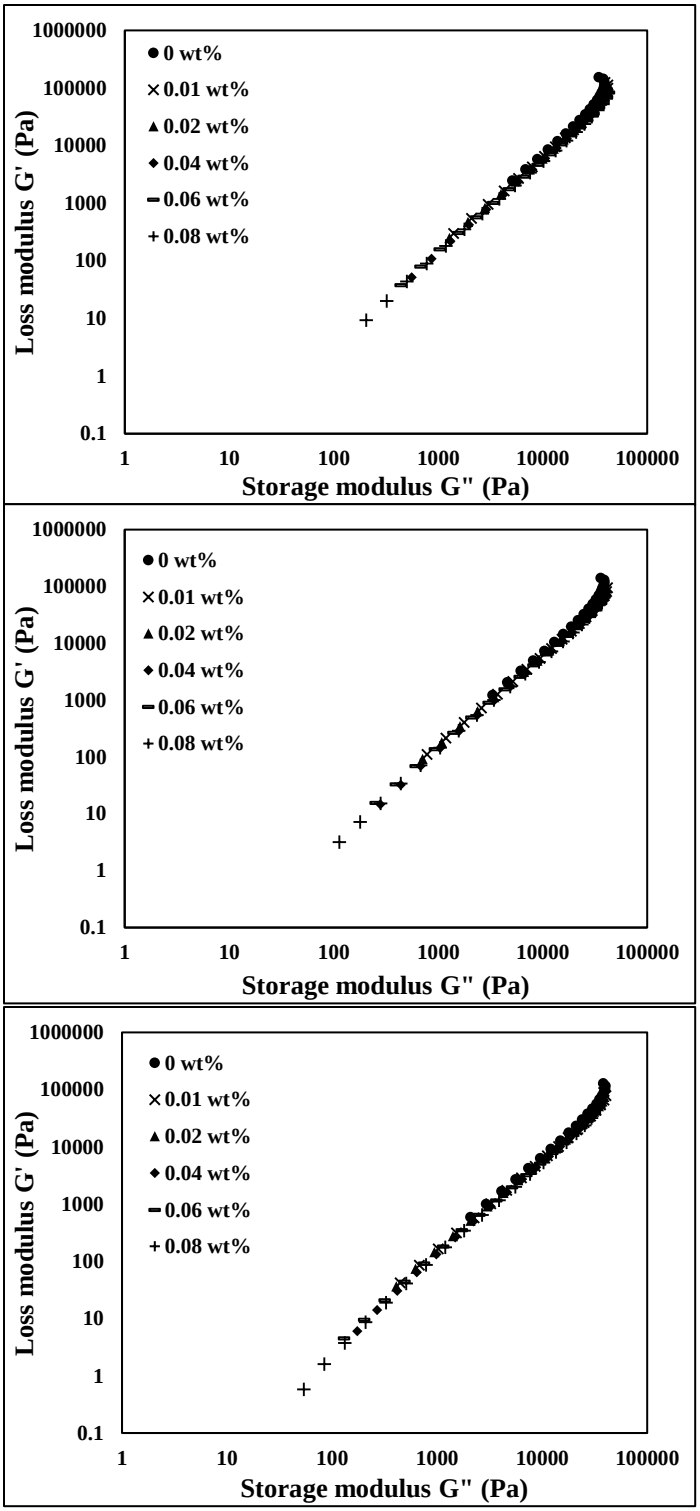

Figure 4. 22 Storage modulus G' as function Loss modulus G" for resin 2 at (a) 150 ºC (top), (b) 170 ºC (middle) and (c) 190 ºC (bottom).

Determination of PDI from SEC measurements is time consuming and not everyone has access to high temperature SEC equipment. It would be useful to be able to discern changes in PDI through rheological measurements. Therefore, it would be meaningful if correlations could be established among PDI, cross-over modulus and frequency. Such correlations for CRPBs produced from resin 2 are shown in Figure 4.23 and Figure 4.24. In Figure 4.23, the correlation between PDI and cross-over frequency seems to be following a power-law model which is temperature dependent. In addition, a linear correlation between PDI and inverse cross-over modulus is found and is shown in Figure 4.24. This correlation seems to be temperature independent at low PDI values but temperature dependent at high PDI values. Unfortunately, no similar correlations could be obtained for CRPBs produced from resin 1. This is probably due to the fact that PDI of these resins does not vary significantly.

All linear viscoelastic measurement data are provided in Appendix B.

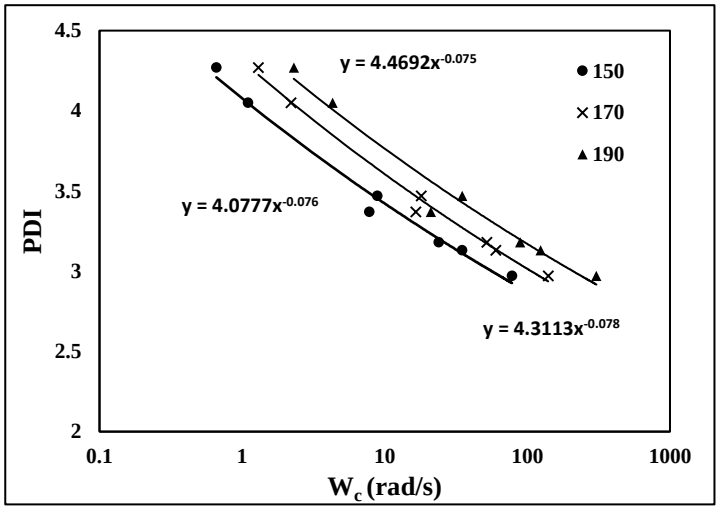

Figure 4. 23 PDI of resin 2 CRPBs as function of Wc at different temperatures.

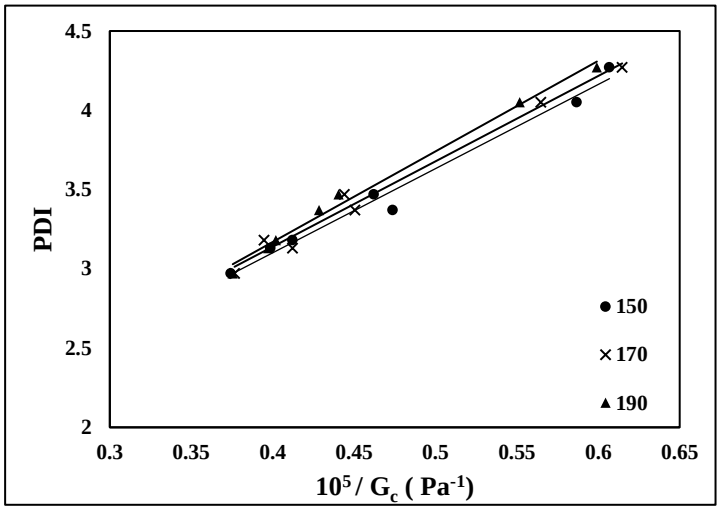

Figure 4. 24 PDI of resin 2 CRPBs as function of inverse G_c at different temperatures.

Chapter 5

CONCLUSIONS AND RECOMMENDATIONS

5.1 Conclusions

Controlled rheology polybutene-1 (CRPB) materials were produced by reactive processing in a batch mixer. This was accomplished by using two commodity PB-1 resins and various amount of an organic peroxide to induce β-scission reactions that reduce molecular weight and narrow the molecular weight distribution (MWD) of the starting polymer.

It was found that average molecular weights decrease monotonically as a function of peroxide concentration. However, it was found that the polydispersity (PDI) of the starting MWD does not change significantly. In fact, the PDI of the lower molecular weight material remains almost the same while the PDI of the higher molecular weight material is reduced slightly with increasing peroxide concentration. As a result of these molecular weight changes, the rheological properties of the resulting CRPBs are reduced. The final torque was found to decrease as a function of peroxide concentration according to a second order polynomial function while the melt flow rate (MFR) was found to increase linearly with increasing peroxide concentration. In addition, the shear thinning behavior of these materials was found to decrease as a function of peroxide. This was evident from the estimated power-law index values obtained by fitting the Carreau-Yasuda model to viscosity data. Also, the linear viscoelastic properties decreased as a function of peroxide

concentration and the zero-shear viscosity of all CRPBs produced was found to correlate well with weight-average molecular weight. In terms of storage and loss moduli of these materials, it appeared that peroxide concentration had a more pronounced effect on the storage modulus. Rheological measurements were performed at three different temperatures and the flow activation energy was found to remain approximately constant for all materials. Correlations between PDI and the cross-over modulus and cross-over frequency were developed and those can be used in future work to quickly assess changes in MWD of controlled-rheology materials. Finally, the effect of peroxide concentration on melting and crystallization temperatures was assessed. It was found that while the melting point decreased slightly as function of peroxide concentration, the crystallization temperature was not affected.

In conclusion, it was demonstrated that the well-known peroxide induced chain scission reactions, used industrially for modifying polypropylene resins, can be successfully applied in the case of polybutene-1 to produce resins of controlled-rheology.

5.2 Recommendations for Future Work

Examination of the viscosity data shows that the effect of peroxide concentration is not monotonic for CRPBs produced from resin 2. This needs to further be explored by repeating the degradation experiments at 0.01, 0.02, 0.04 and 0.06 wt% peroxide levels and re-characterizing the resulting materials.

In addition, the peroxide concentration window needs to be expanded to higher levels. The reason for that is the fact that for several applications, PB-1 materials having

lower molecular weight and larger melt flow rates are required. In addition, performing experiments at higher peroxide concentrations will allow for verification of the correlations developed in this work.

As discussed previously, the correlation between zero-shear viscosity and weight-average molecular weight indicates some deviation from what is expected for linear polymers. This needs to be further explored. Any possible gel formed during the reactive processing of these samples needs to be measured by Soxhlet extraction and the viscosity of the samples needs to be measured again. In addition, the deviation from the behavior of linear polymers could be attributed to errors in molecular weight measurements. For that reason, the SEC calibration procedure needs to be examined again. Also, the parameters in the Mark-Houwink equation for PB-1 need to be double checked.

Finally, the same technique for production of CRPBs needs to be applied to blends of polypropylene and polybutene-1 materials. Due to the high compatibility of these materials and because of their different crystallization characteristics, it will be possible to produce materials having multimodal molecular weights distributions and potentially unusual properties for typical polyolefins.

REFERENCES

1. Moore, E. P. (1996). Polypropylene handbook: Polymerization, characterization, properties, processing, applications. Munich: Hanser.

2. Harrison, J. W., Keller, J. P., Kowalski, R. C., Staton, J. C., "Controlled degradation of polypropylene in extruder-reactor" U.S. Patent No. 3,608,001. Washington, DC (1971).

3. Bartz, K. W., Steinkamp, R. A., Watson, A. T., Wilder, H. L., "Process for controlling rheology of polyolefins" U.S. Patent No. 3,898,209. Washington, DC (1975).

4. Kowalski, R.C., "Controlled Rheology of PP Resins", in *History of Polyolefins*, F.B. Seymour and T. Cheng (eds.), Springer Netherlands, p.307 (1986).

5. Xanthos, M., "Reactive Extrusion: Principles and Practice", Hanser Publishers, Oxford Univ. Press, New York (1992).

6. Hudec, P., Obdržálek, L., "The change of molecular weights at peroxide initiated degradation of polypropylene," Angew. Makrom. Che., 89(1), 41-45(1980).

7. Tzoganakis, C., Vlachopoulos, J., Hamielec, A. E., "Production of controlled-rheology polypropylene resins by peroxide promoted degradation during extrusion," Polym. Eng. Sci. 28(3), 170-180 (1988).

8. Tzoganakis, C., Vlachopoulos, J., and Hamielec, A.E., "Modelling of the Peroxide Degradation of Polypropylene", Intern. Polymer Processing, **III**, 141 (1988).

9. Suwanda, D., Lew, R., Balke, S. T., "Reactive extrusion of polypropylene I: Controlled degradation," J. Appl. Polym.Sci., *35*(4), 1019-1032(1988).

10. Suwanda, D., Lew, R., Balke, S. T., "Reactive extrusion of polypropylene II: Degradation kinetic modeling," J. Appl. Polym.Sci., *35*(4),1033-1048(1988).

11. Tzoganakis, C., Tang, Y., Vlachopoulos, J., Hamielec, A. E., "Measurements of residence time distribution for the peroxide degradation of polypropylene in a single-screw plasticating extruder," J. Appl. Polym.Sci., 37(3), 681-693(1989).

12. Tzoganakis, C., Tang, Y., Vlachopoulos, J., and Hamielec, A. E., "Controlled degradation of polypropylene: a comprehensive experimental and theoretical investigation," Polym. Plast. Tech. Eng., 28(3), 319-350(1989).

13. Tzoganakis, C., Vlachopoulos, J., Hamielec, A. E., & Shinozaki, D. M. (1989). "Effect of molecular weight distribution on the rheological and mechanical properties of polypropylene," Polymer Engineering and Science, 29(6), 390-396. doi:10.1002/pen.760290607

14. Ryu, S.H., Gogos, C.G., and Xanthos, M., "Parameters affecting process efficiency of peroxide- initiated controlled degradation of polypropylene", *Adv. Polym. Tech*., **11**, 121 (1992).

15. Tzoganakis, C., "A Rheological Evaluation of Linear and Branched Controlled-Rheology Polypropylenes", *Can. J. Chem. Eng.*, **72**, 749 (1994).

16. Krell, M.J., Brandolin, A., and Vallés, E.M., "Controlled rheology polypropylenes – an improved model with experimental validation for the single-screw extruder process," *Polym. React. Eng. J*., **2**, 389 (1994).

17. Huang, C., Tzoganakis, C., and Duever, T.A., "Monte Carlo Simulations of Peroxide Initiated Degradation of Polypropylene," *Polym. React. Eng. J.*, **3**, 43 (1995).

18. Mead, D.W., "Evolution of the molecular weight distribution and linear viscoelastic rheological properties during the reactive extrusion of polypropylene," *J. Appl. Polym. Sci.*, **57**, 151 (1995).

19. Barakos, G., Mitsoulis, E., Tzoganakis, C., Kajiwara, T., "Rheological characterization of controlled-rheology polypropylenes using integral constitutive equations," J. Appl. Polym.Sci., 59(3), 543-556(1996).

20. Carrot, C., Revenu, P., and Guillet, J., "Rheological behavior of degraded polypropylene melts: From MWD to dynamic moduli," *J. Appl. Polym. Sci.*, **61**, 1887 (1996).

21. Baik, J. J., Tzoganakis, C., "A study of extrudate distortion in controlled- rheology polypropylenes," Polym. Eng. Sci., 38(2), 274-281(1998).

22. Huang, C., Tzoganakis, C., and Duever, T.A., "Kinetic Parameter Estimation in Peroxide Initiated Degradation of Polypropylene", *Polym. React. Eng. J.*, **5**, 1 (1997).

23. Thompson, M.R., Tzoganakis, C., and Rempel, G.L., "Evaluation of Vinylidene Group Content in Degraded Polypropylene", *J. Polym. Sci.: Part A: Polym.Chem.*, **35**, 3083 (1997).

24. Dickson, S.B., Tzoganakis, C., and Budman, H., "Reactive Extrusion of Polypropylene with Pulsed Peroxide Addition: Process and Control Aspects", *Ind. Eng. Chem. Res.*, **36**, 1067 (1997).

25. Ibhadon, A.O., "Fracture mechanics of polypropylene: Effect of molecular characteristics, crystallization condition and annealing on morphology and impact performance," J. Appl Polym Sci 69 (13) (1998) 2657.

26. Iedema, P.D., Willems, C., Vliet, G.V., Bynge, W., Mutsers, S.M.P., and Hoefsloot, H.C.J., "Using molecular weight distributions to determine the kinetics of peroxide-induced degradation of polypropylene," *Chem. Eng. Sci.*, **56**, 3659 (2001).

27. Berzin, F., Vergnes, B., and Delamare, L., "Rheological behaviour of controlled-rheology polypropylenes obtained by peroxide-promoted degradation during extrusion: Comparison between homopolymer and copolymer," *J. Appl. Polym. Sci.*, **80**, 1243 (2001).

28. Asteasuain, M., Sarmoria, C., and Brandolin, A., "Controlled rheology of polypropylene: Modeling of molecular weight distributions,"*J. Appl. Polym. Sci.*, **88**, 1676 (2003).

29. Azizi, H., & Ghasemi, I. (2004). "Reactive extrusion of polypropylene: Production of controlled-rheology polypropylene (CRPP) by peroxide-promoted degradation," Polymer Testing, 23(2), 137-143. doi:10.1016/s0142-9418(03)00072-2.

30. Blancas, C., and Vargas, L., "Modeling of the industrial process of peroxide-initiated polypropylene (homopolymers) controlled degradation," *J. Macromol. Sci. Part B: Physics*, **40**, 315 (2001).

31. Scorah, M. J., Zhu, S., Psarreas, A., McManus, N. T., Dhib, R., Tzoganakis, C., Penlidis, A. "Peroxide-controlled degradation of polypropylene using a tetra-functional initiator," Polym. Eng. Sci., 49(9), 1760-1766(2009).

32. Bayu, Herlambang & Bramantika, S. (2019). Controlling polypropylene rheological properties by promoting organic peroxide during extrusion with improved properties for automotive applications. Journal of Physics: Conference Series. 1127. 012030. 10.1088/1742-6596/1127/1/012030.

33. Nie, S., and Tzoganakis, C., (2018). "Tailor-Made Controlled Rheology Polypropylenes from Metallocene and Ziegler-Natta Resins, Polym.Eng.Sci., accepted. DOI 10.1002/pen.25089

34. Shao, H-F., Wang, S-L., Dong, X., and He, A-H., " Linear viscoelastic behaviors of polybutene-1 melts with various structure parameters," Chinese J. Polym. Sci., 34, 174-184 (2016).

35. Shao, H-F., Wang, S-L., and He, A-H., "The influence of molecular weight on high shear rate macroscopic rheological properties of polybutene-1 melts through

rubber-processing analyzer", Polym. Bull. (2016) 73: 3209-3220. https://doi.org/10.1007/s00289-016-1650-2

36. Lindergren, C. R. (1970). "Polybutylene properties of a packaging material. Polymer Engineering and Science," 10(3), 163-169. doi:10.1002/pen.760100307

37. Hsu, C. and Geil, P. (1987). "Structure-property-processing relationships of polypropylene-polybutylene blends", Polym. Eng. Sci., 27(20), pp.1542-1556.

38. Nie, S., Rheological Properties of Tailor-Made Metallocene and Ziegler-Natta Based Controlled Rheology Polypropylenes, MASc Thesis, University of Waterloo (2015).

39. Mandelkern, L. (2007). "The effect of molecular weight on the crystallization, melting, and morphology of long-chain molecules. Journal of Polymer Science Part C: Polymer Symposia," 15(1), 129-162. doi:10.1002/polc.5070150112

Appendix A:
DSC raw data

Sample 1-1

Resin 1 / 0 wt% peroxide

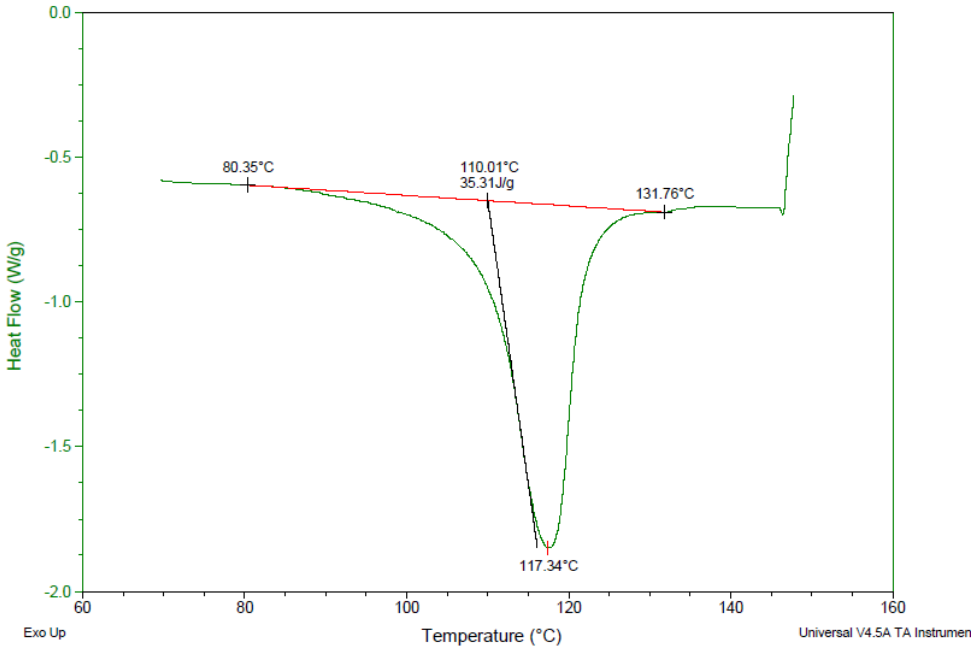

Second heating cycle

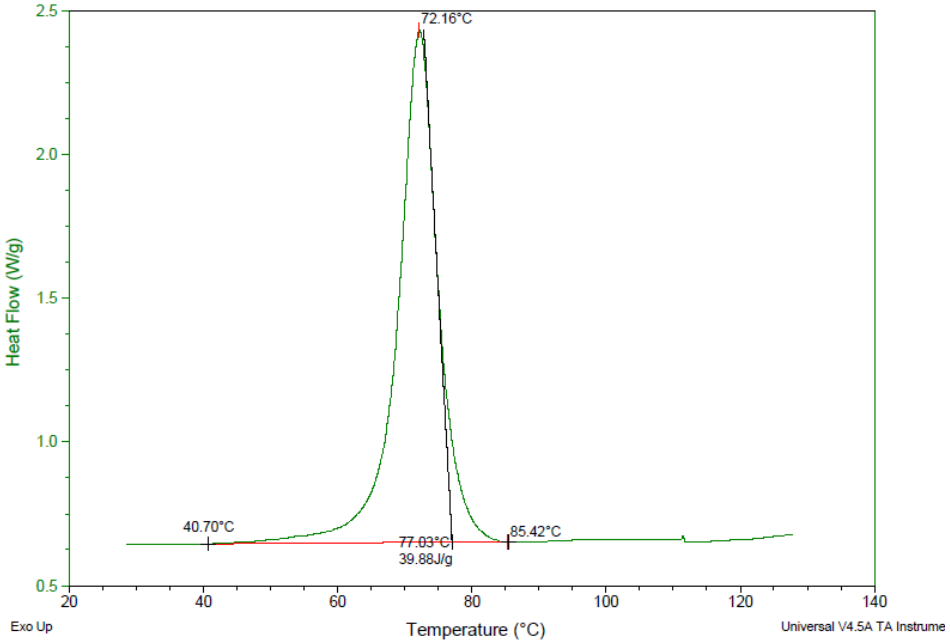

Cooling cycle

Sample 1-2

Resin 1 / 0.01 wt% peroxide

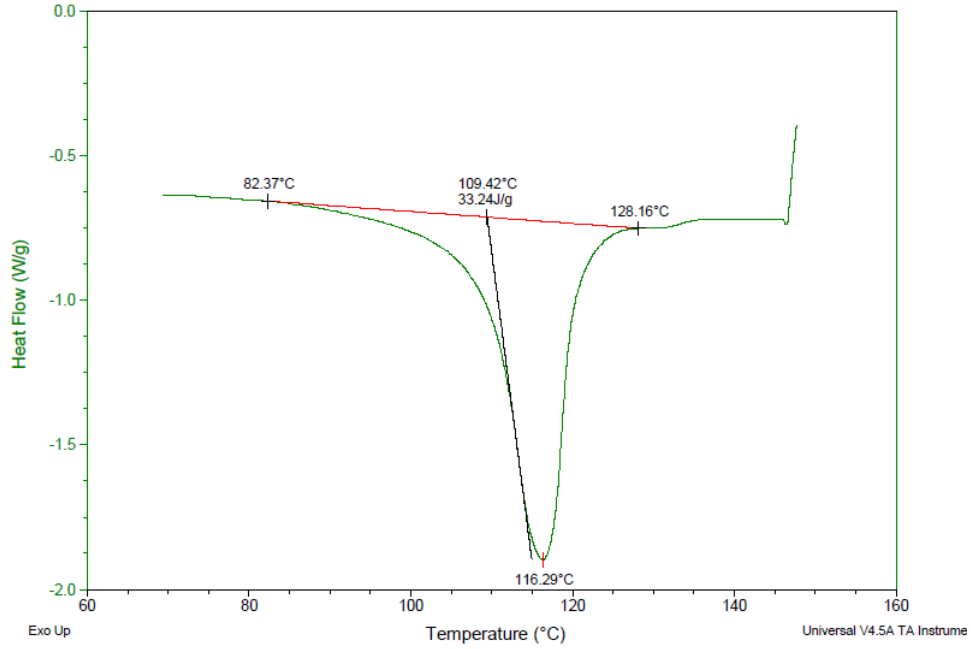

Second heating cycle

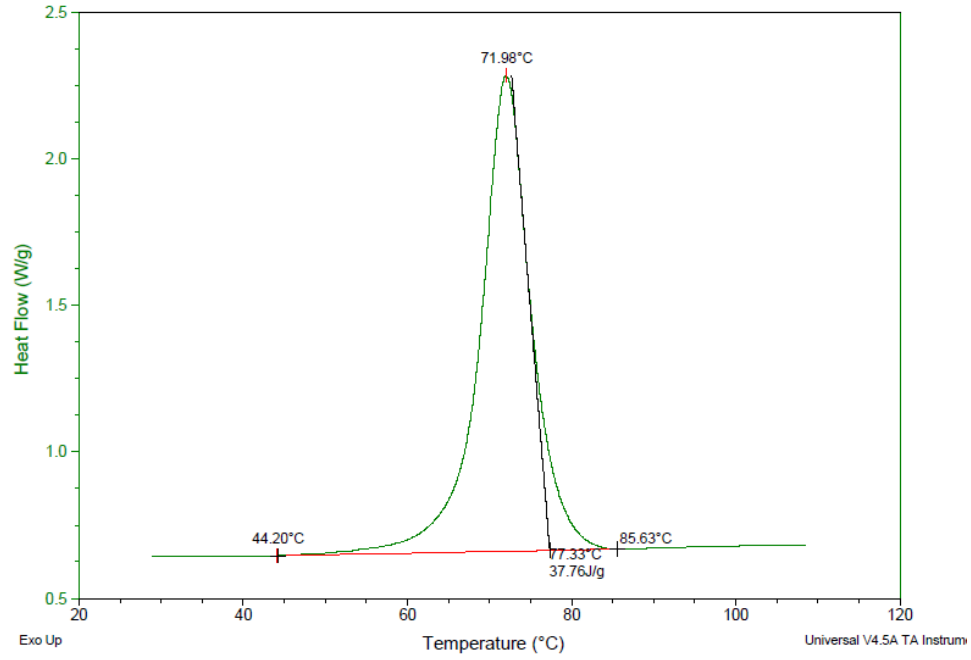

Cooling process

Sample 1-3

Resin 1 / 0.02 wt% peroxide

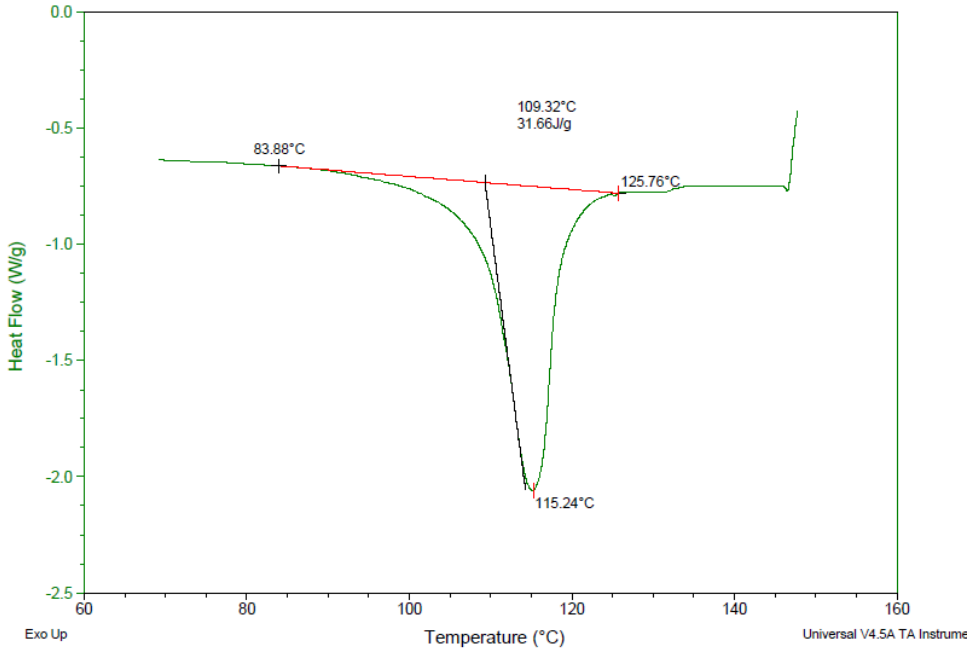

Second heating cycle

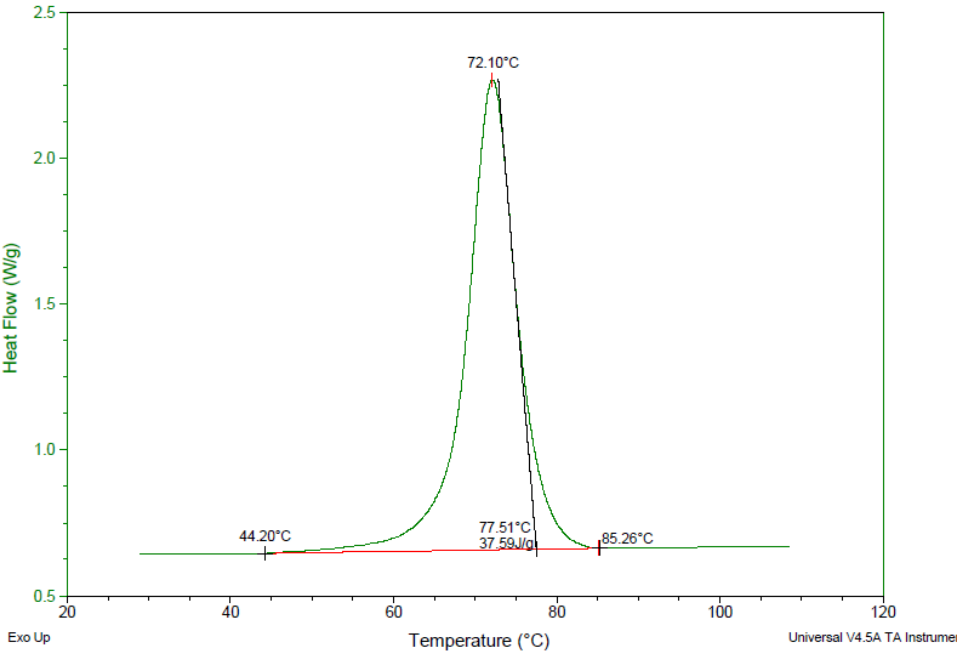

Cooling cycle

Sample 1-4

Resin 1 / 0.04 wt% peroxide

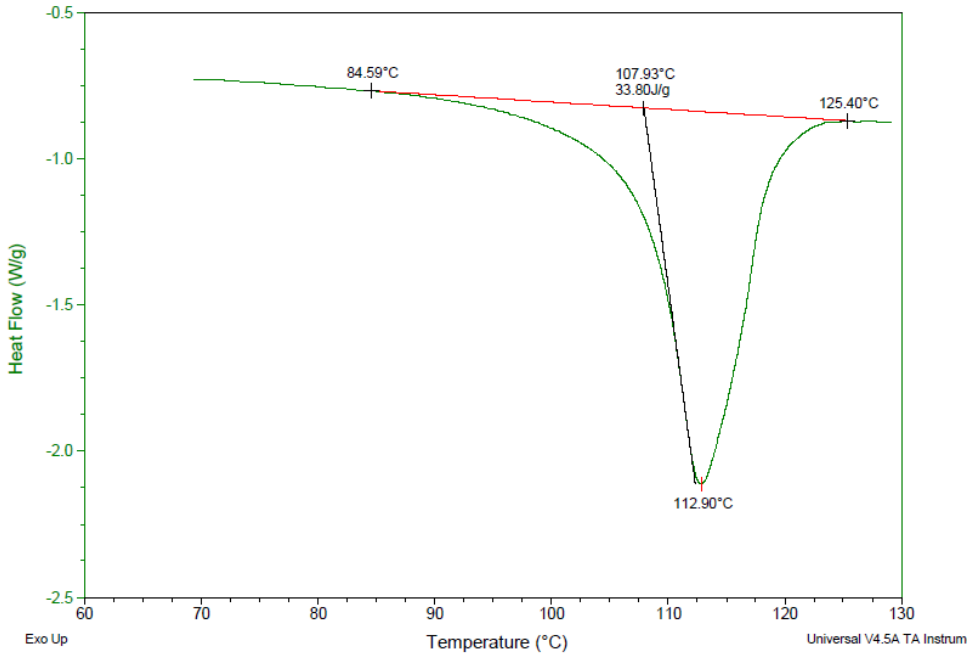

Second heating cycle

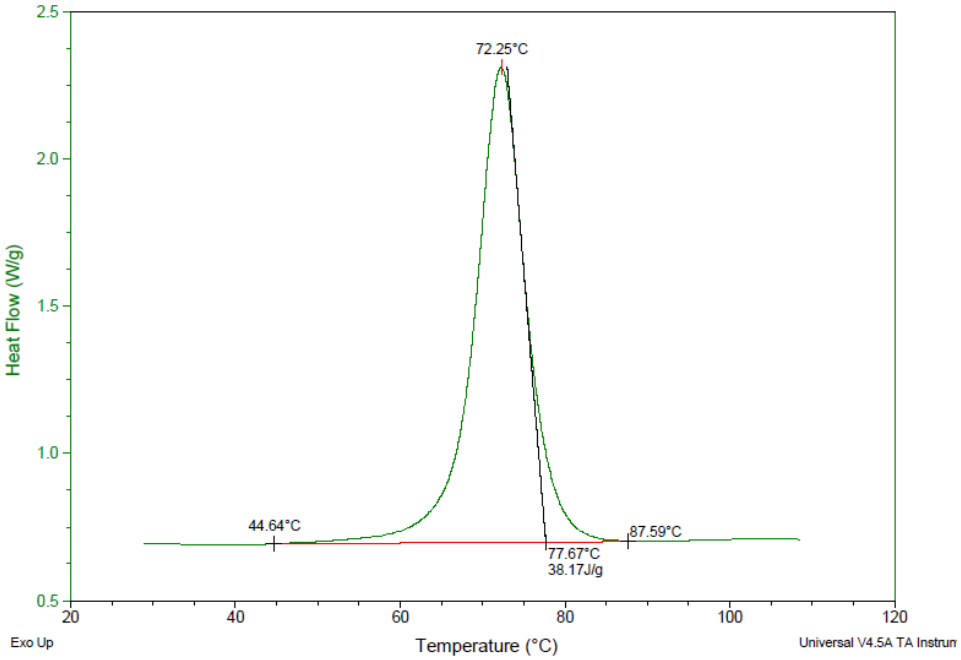

Cooling cycle

Sample 1-5

Resin 1 / 0.06 wt% peroxide

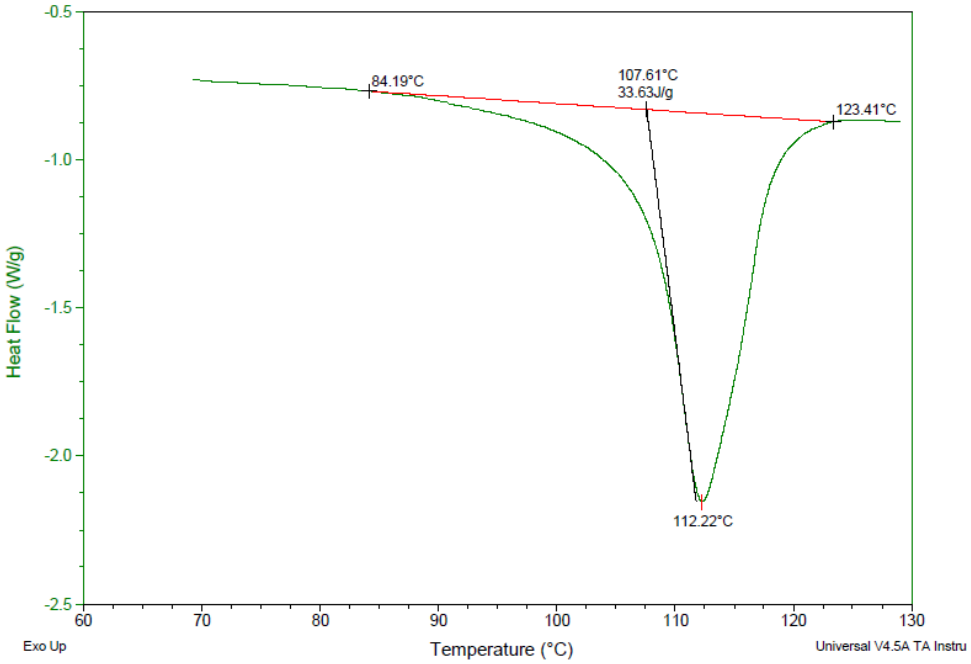

Second heating cycle

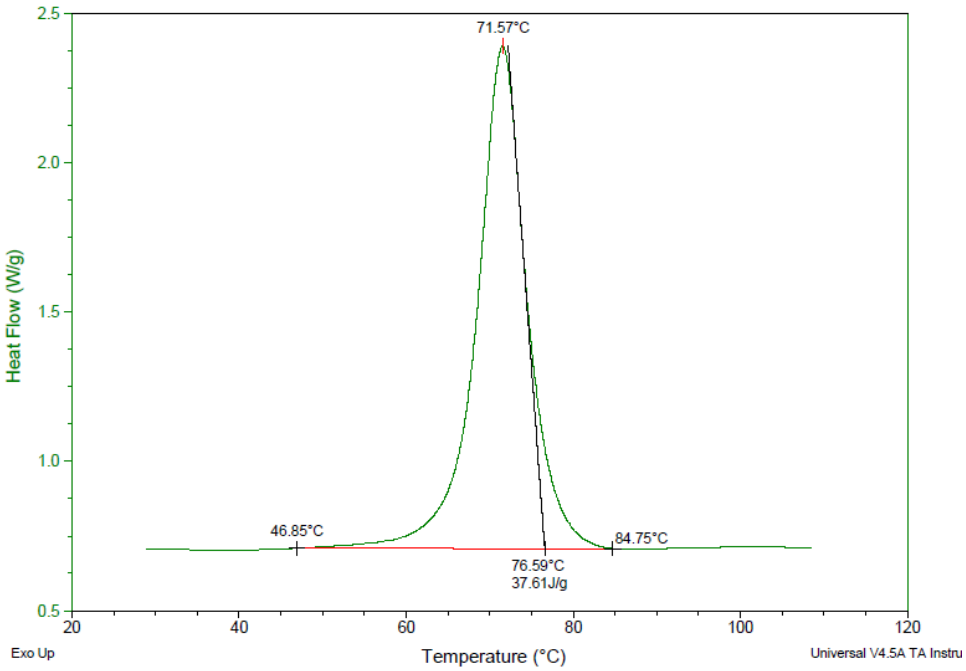

Cooling cycle

Sample 1-6

Resin 1 / 0.08 wt% peroxide

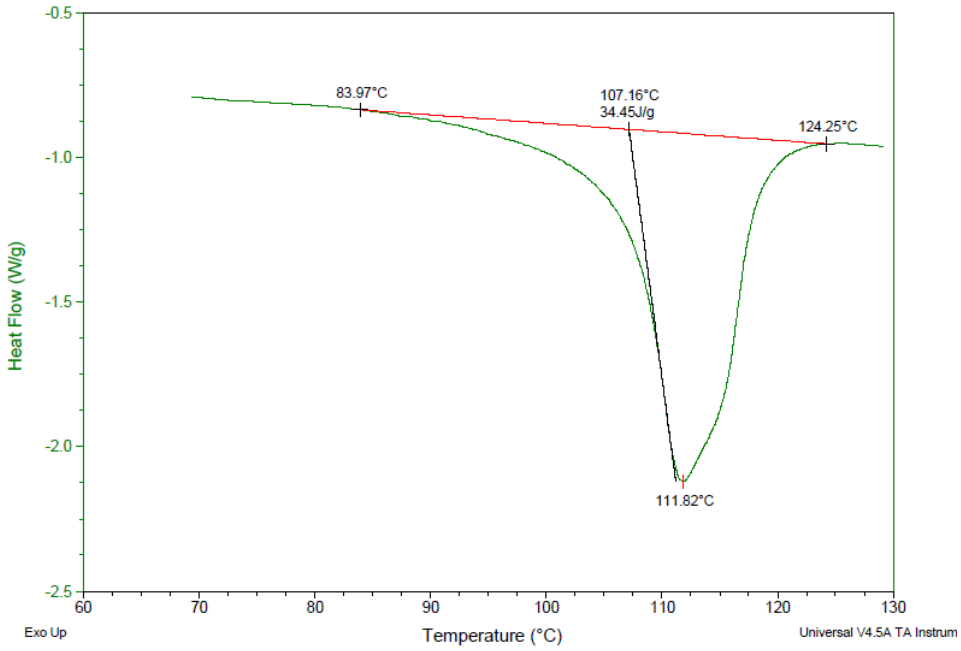

Second heating cycle

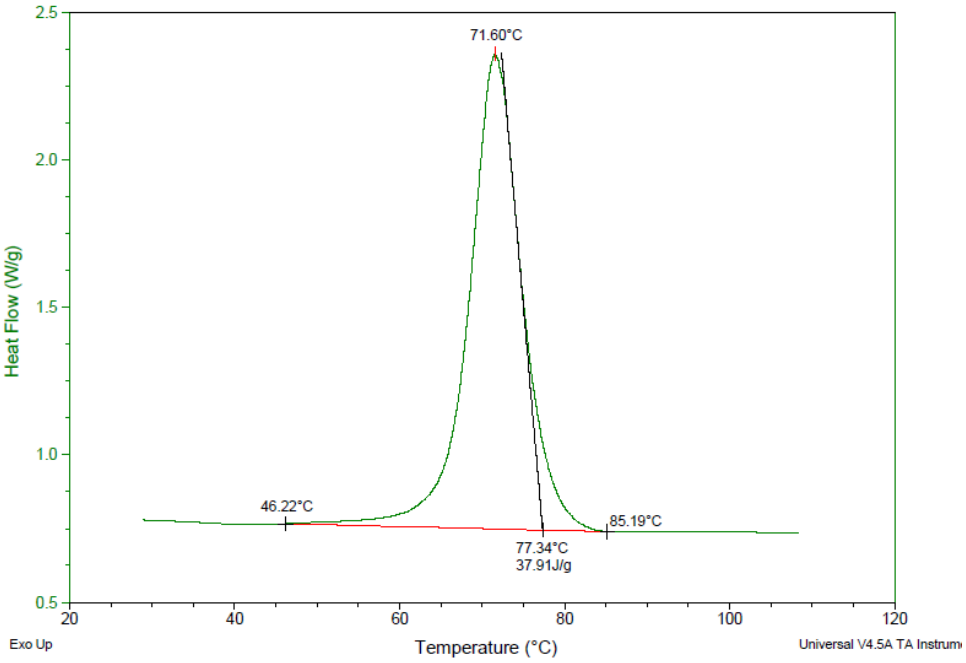

Cooling cycle

Sample 2-1

Resin 2 / 0 wt% peroxide

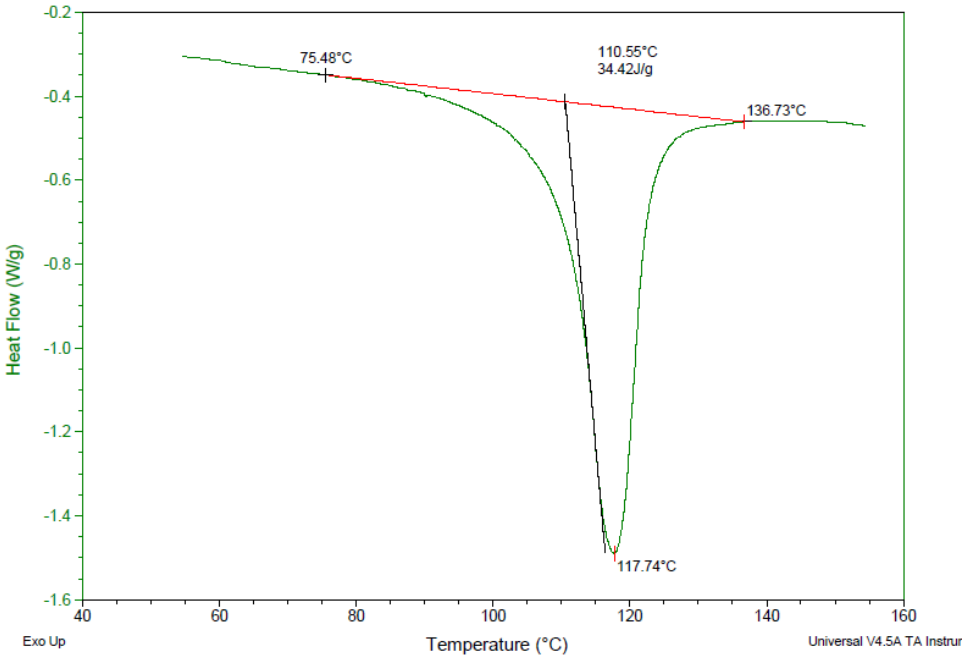

Second heating cycle

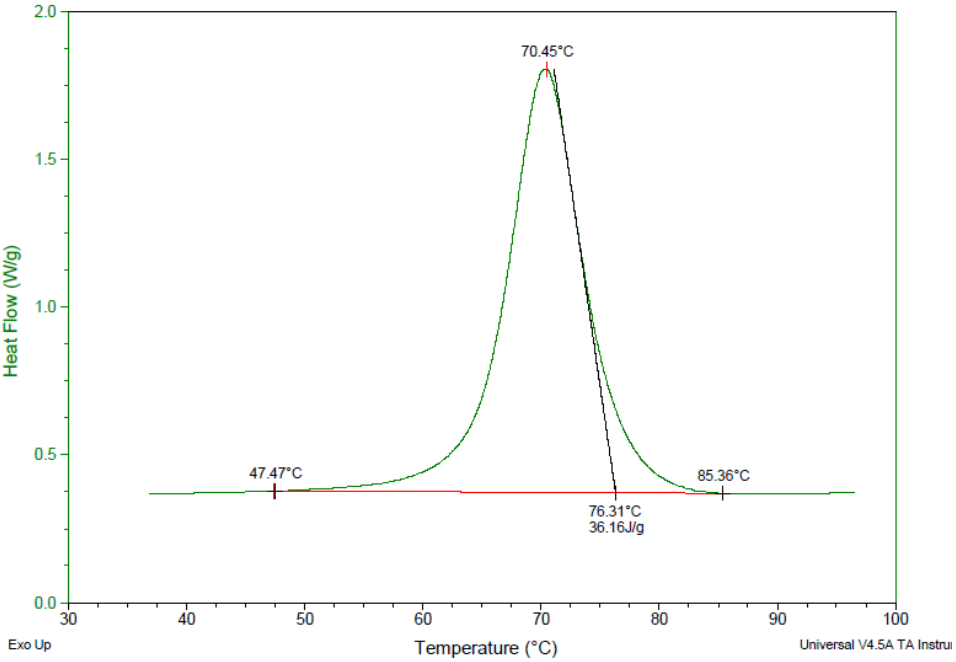

Cooling cycle

Sample 2-2

Resin 2 / 0.01 wt% peroxide

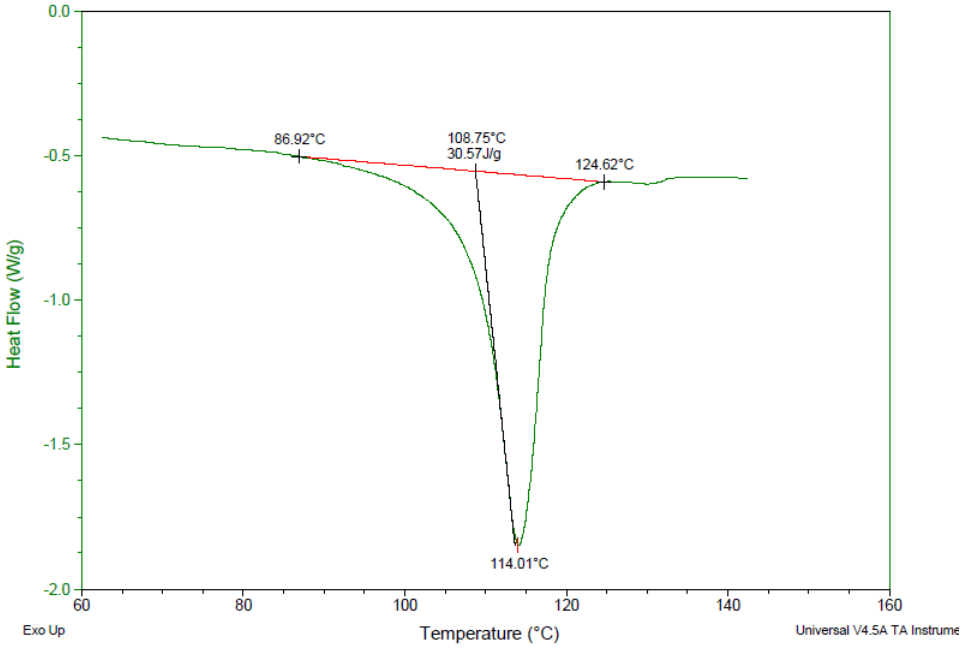

Second heating cycle

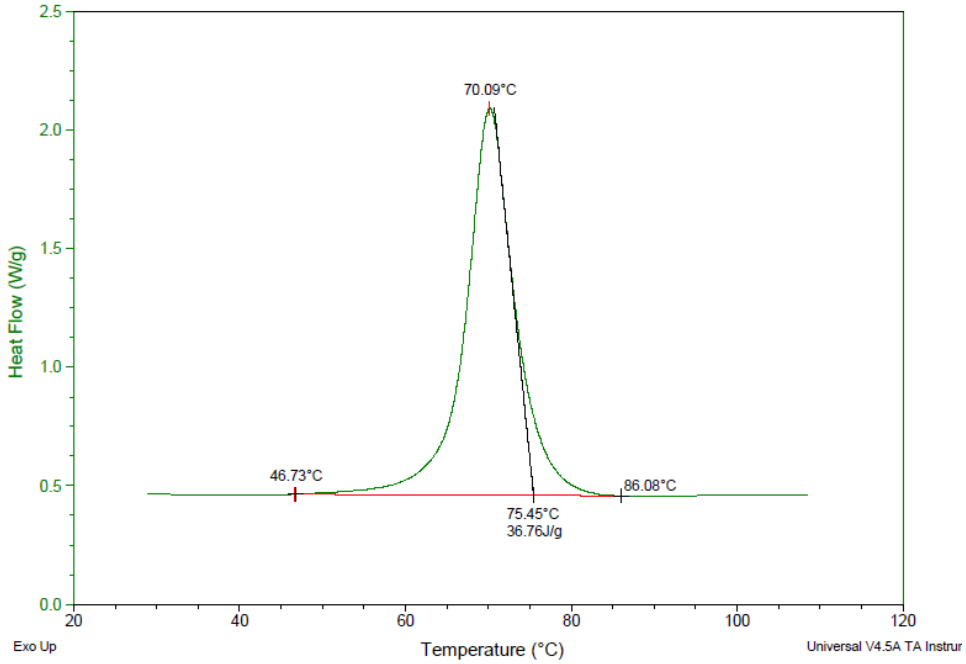

Cooling cycle

Sample 2-3

Resin 2 / 0.02 wt% peroxide

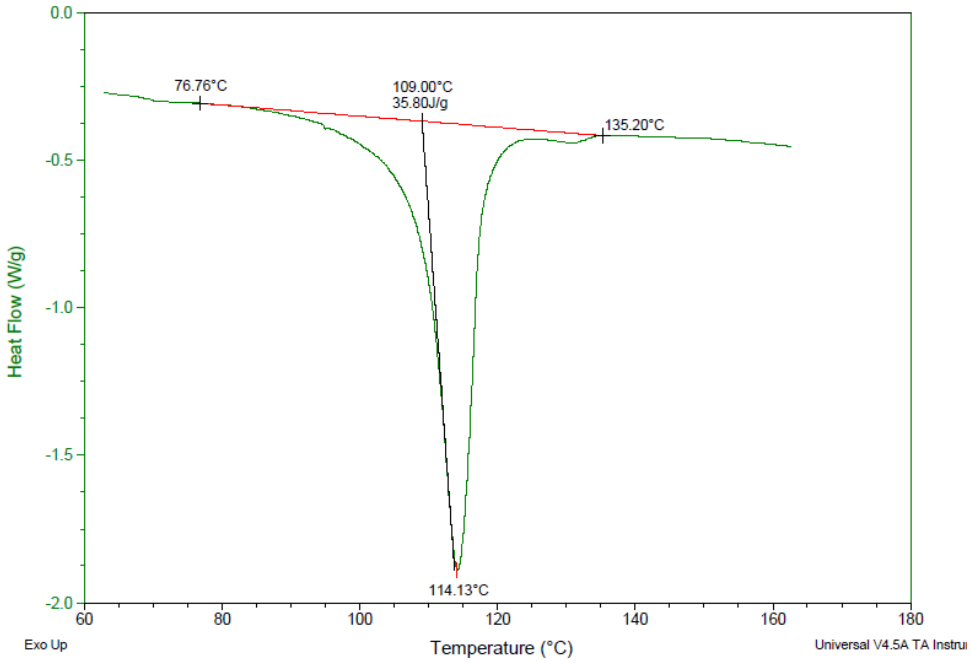

Second heating cycle

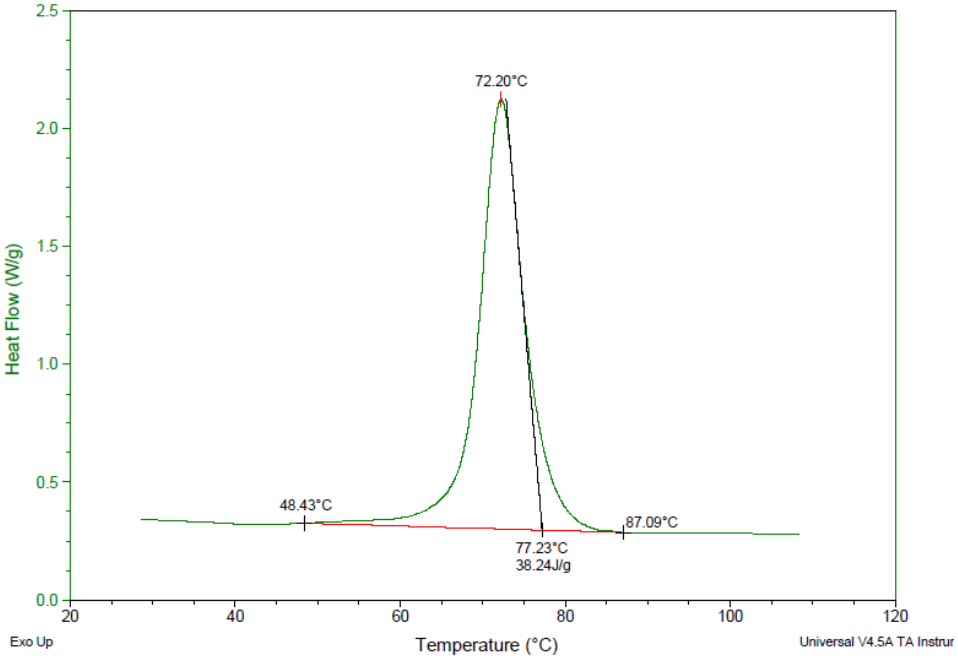

Cooling cycle

Sample 2-4

Resin 2 / 0.04 wt% peroxide

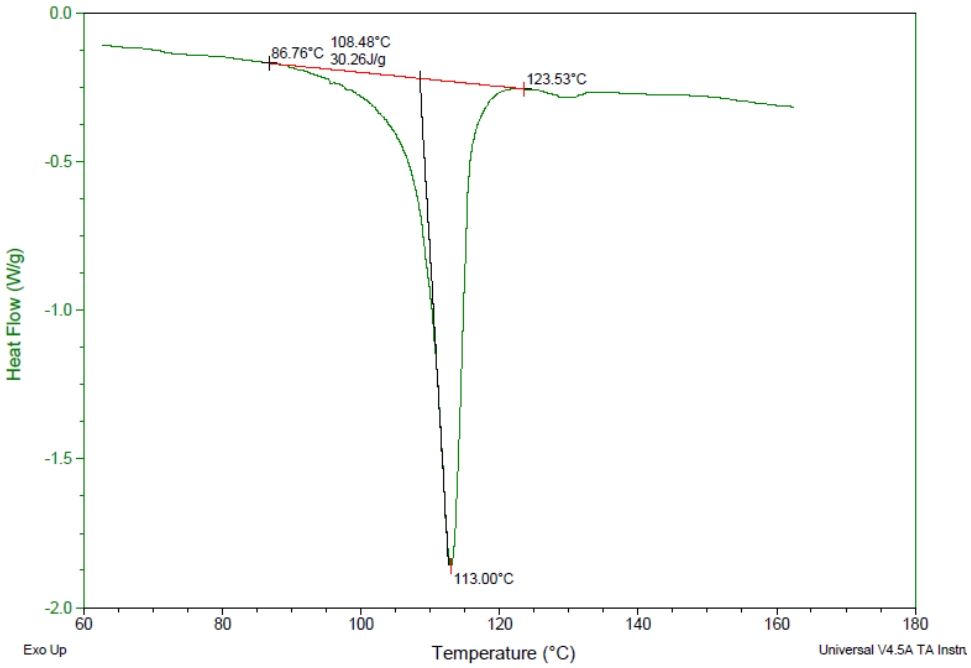

Second heating cycle

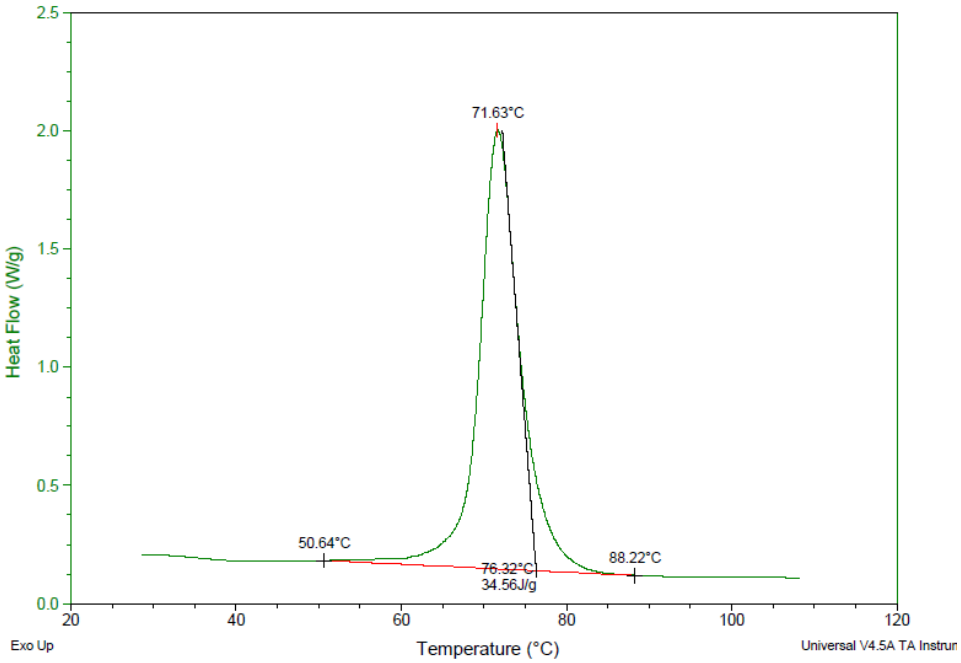

Cooling cycle

Sample 2-5

Resin 2 / 0.06 wt% peroxide

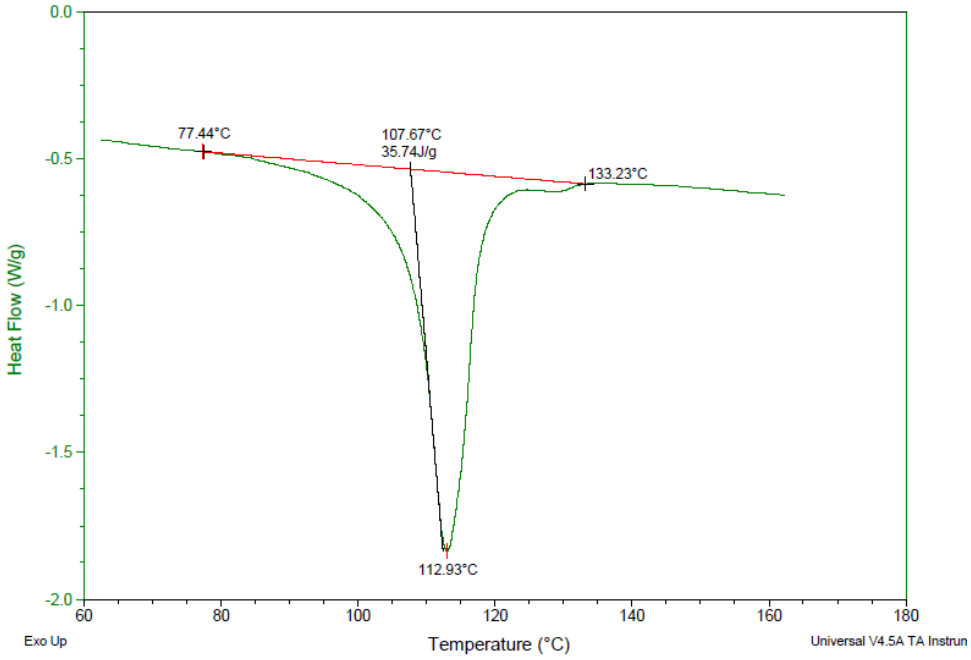

Second heating cycle

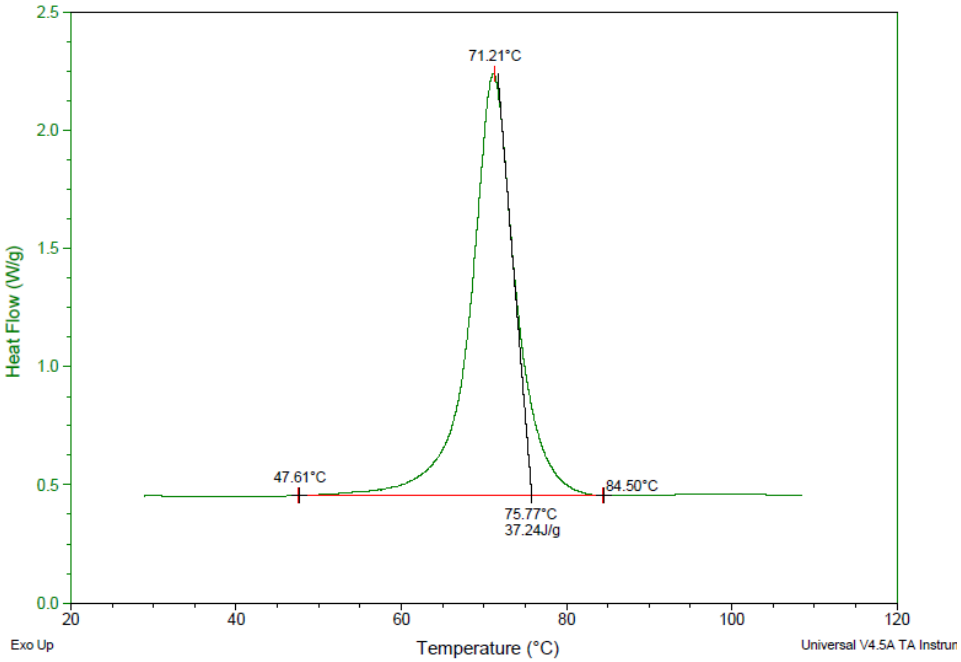

Cooling cycle

Sample 2-6

Resin 2 / 0.08 wt% peroxide

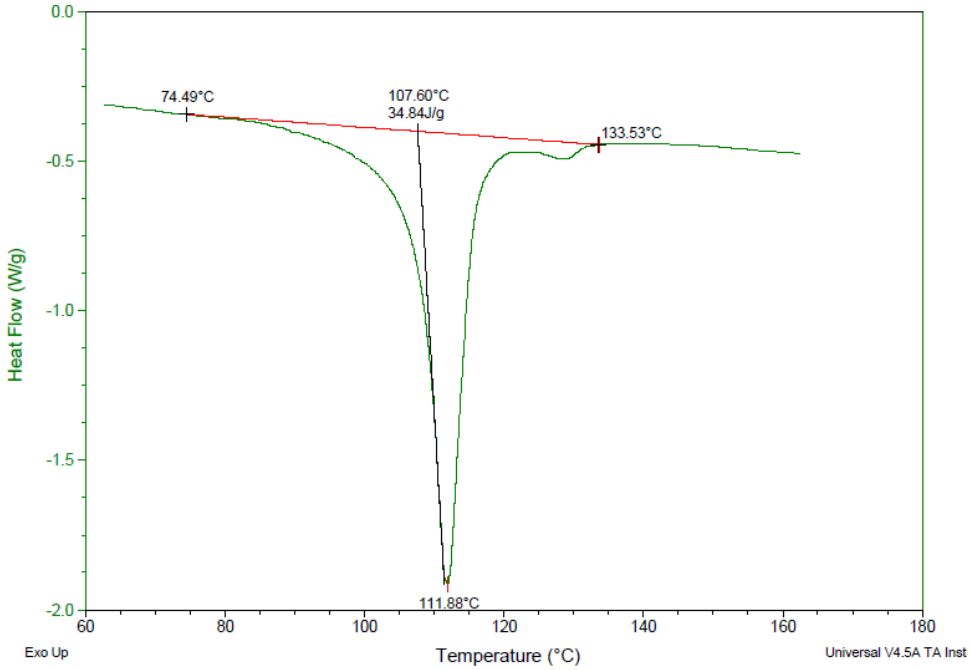

Second heating cycle

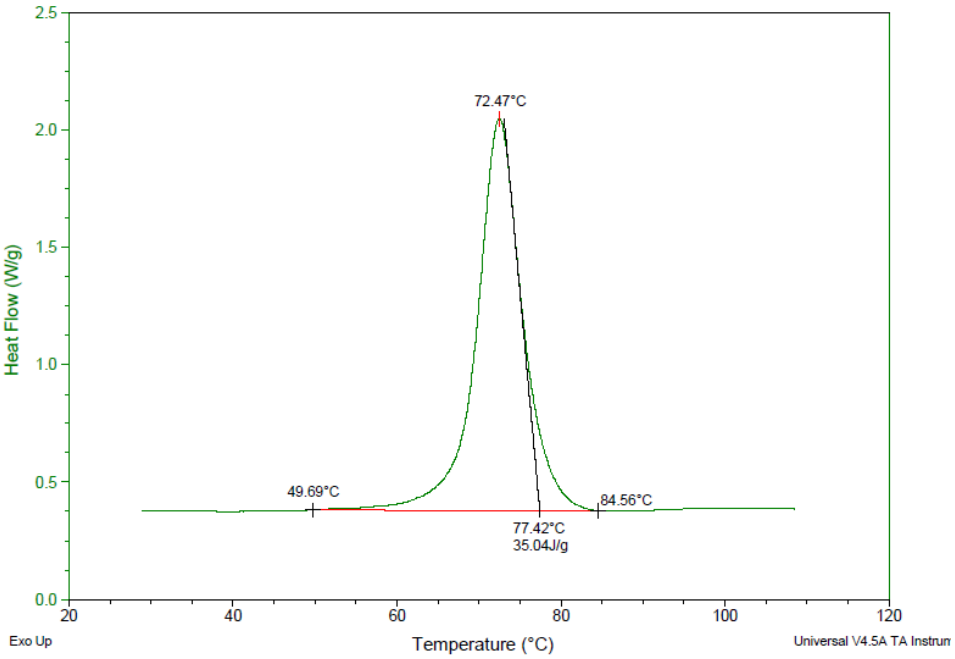

Cooling cycle

Appendix B:
Rheological raw data

Sample 1-1

Resin 1/ 0 wt% peroxide at 150 ºC

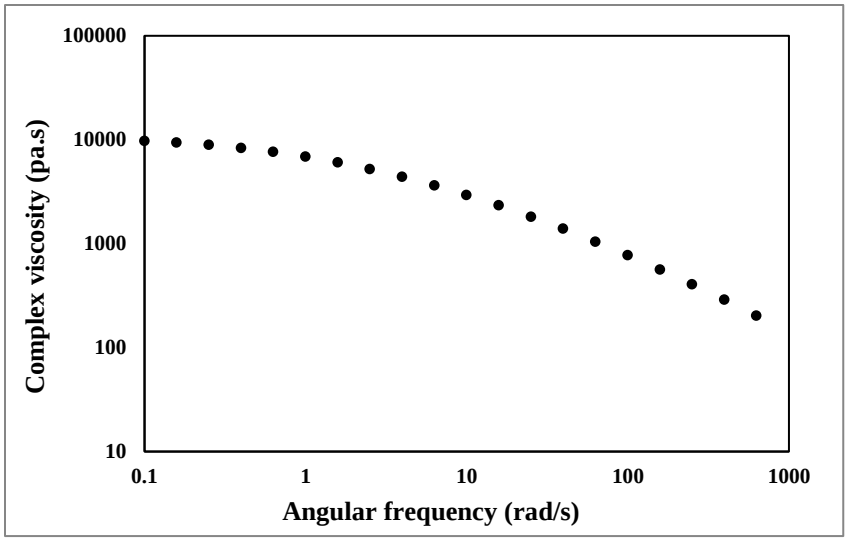

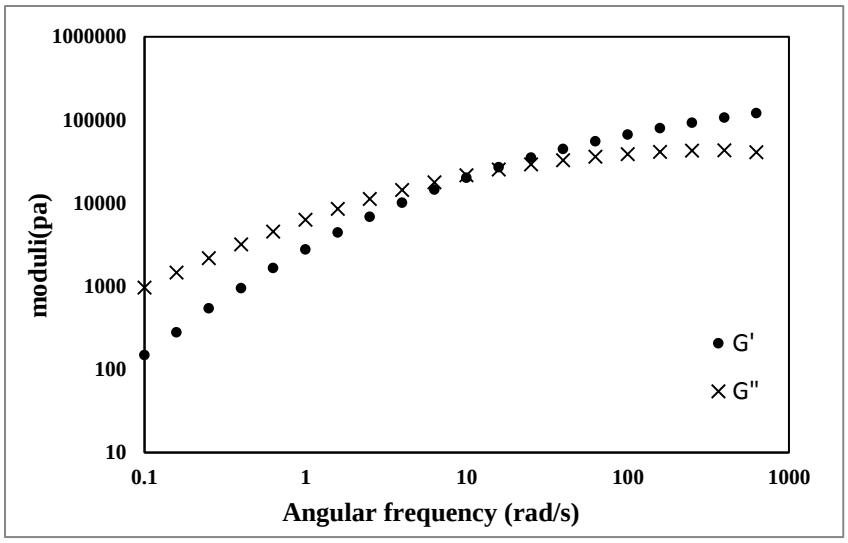

Sample 1-1

Resin 1/ 0 wt% peroxide at 170 ºC

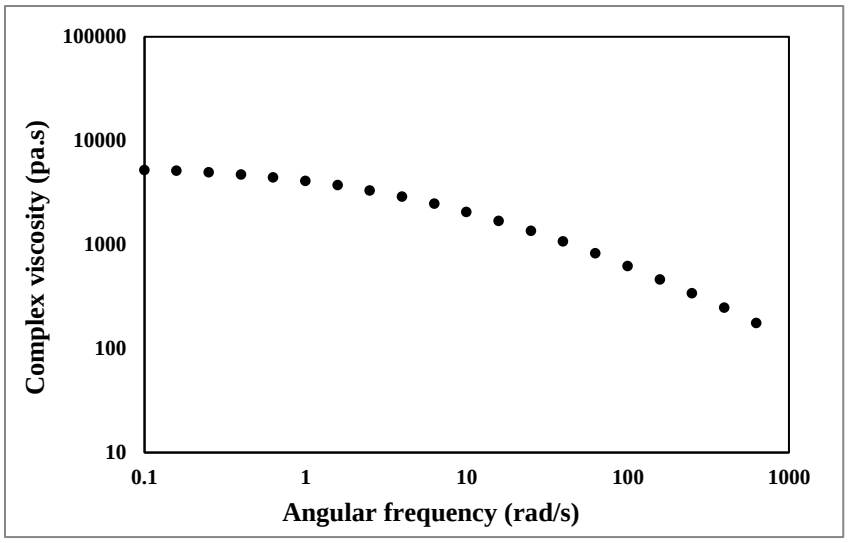

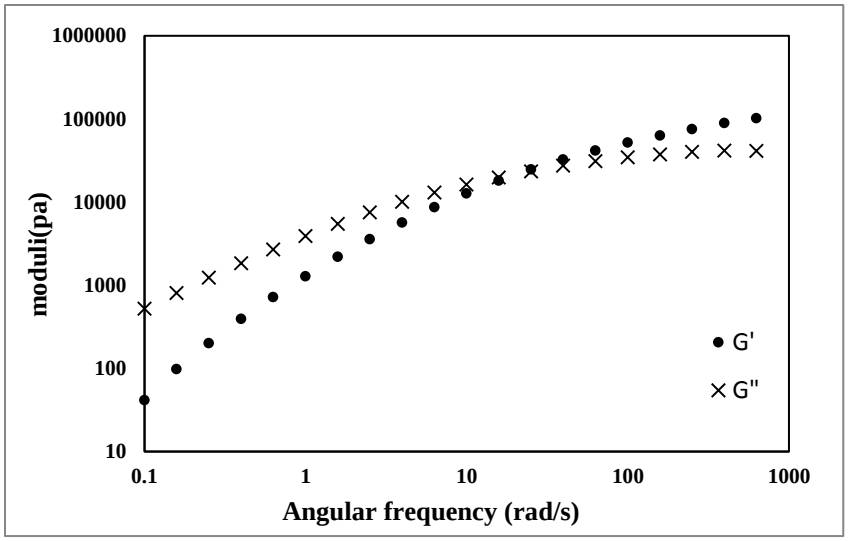

Sample 1-1

Resin 1/ 0 wt% peroxide at 190 ºC

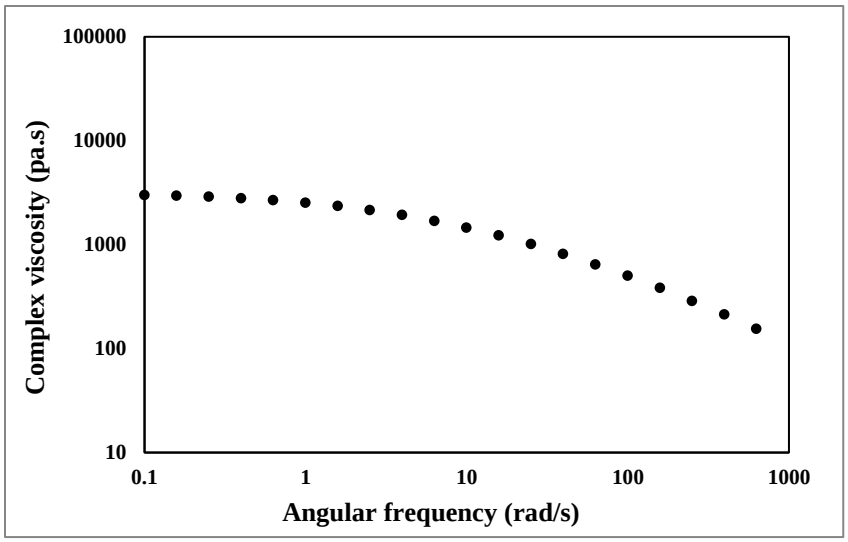

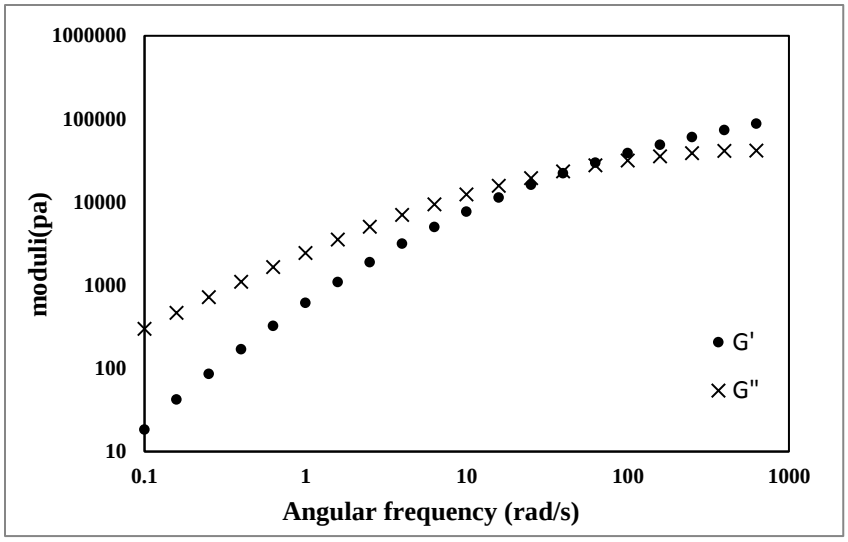

Sample 1-2

Resin 1/ 0.01 wt% peroxide at 150 ºC

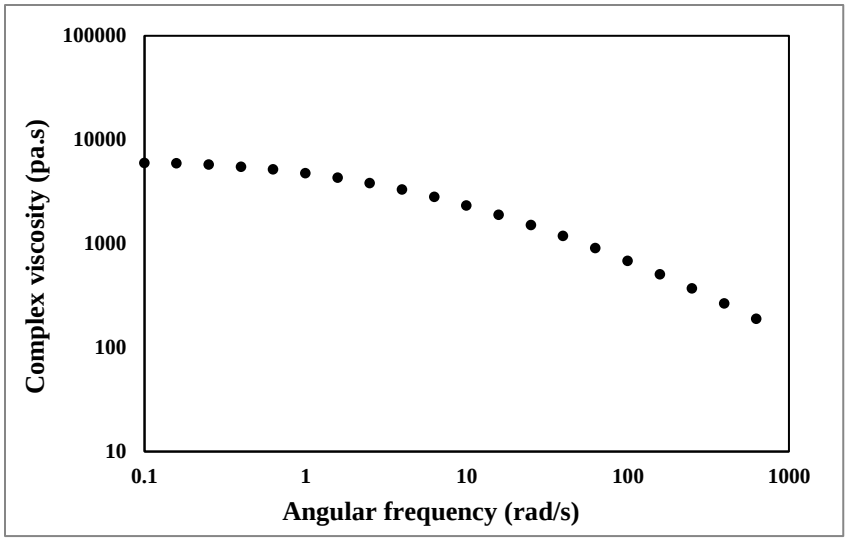

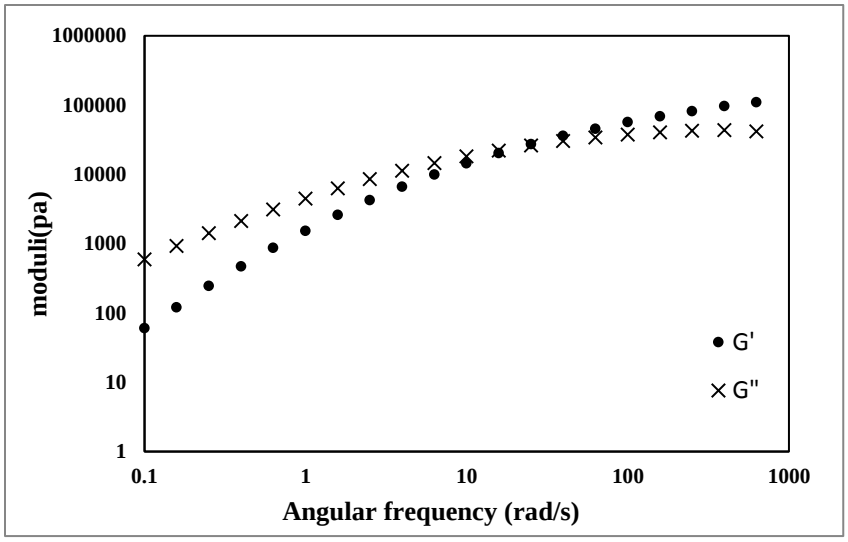

Sample 1-2

Resin 1/ 0.01 wt% peroxide at 170 ºC

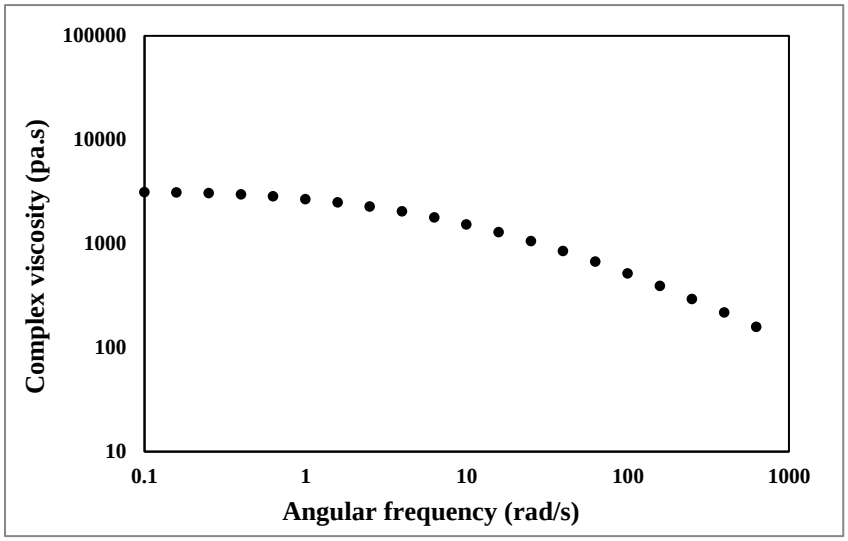

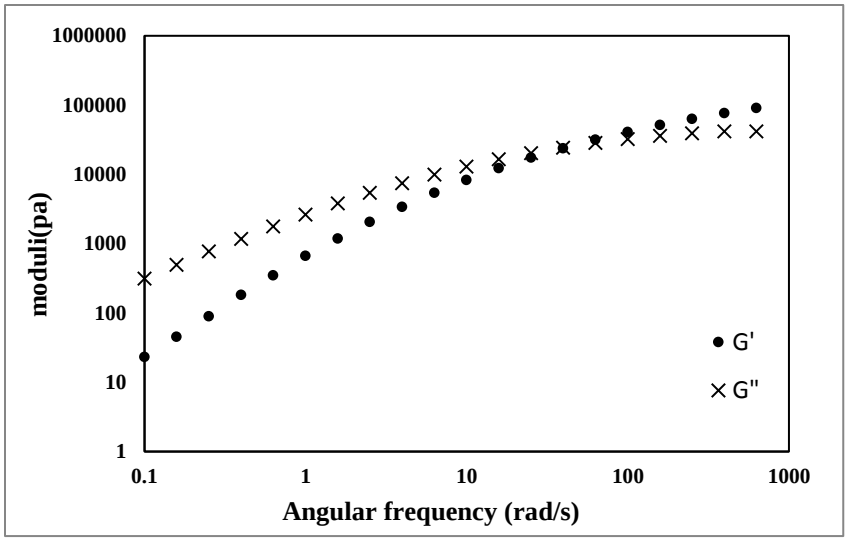

Sample 1-2

Resin 1/ 0.01 wt% peroxide at 190 ºC

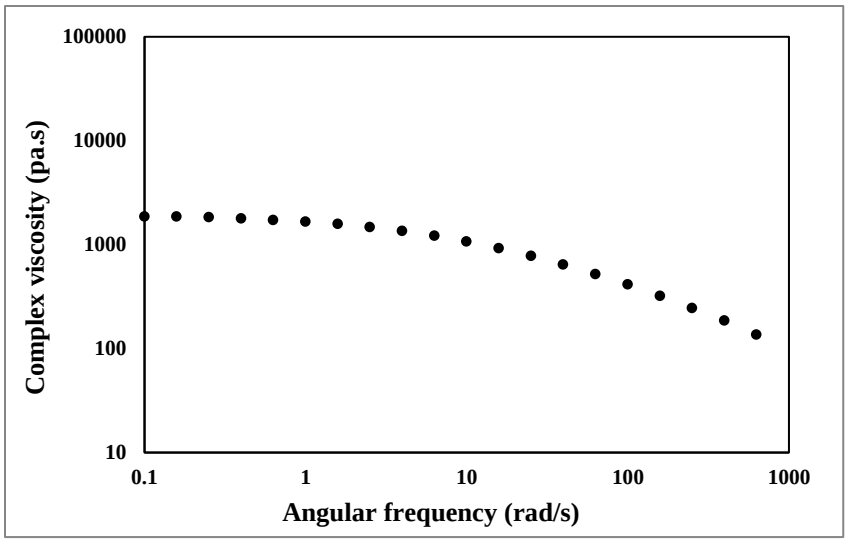

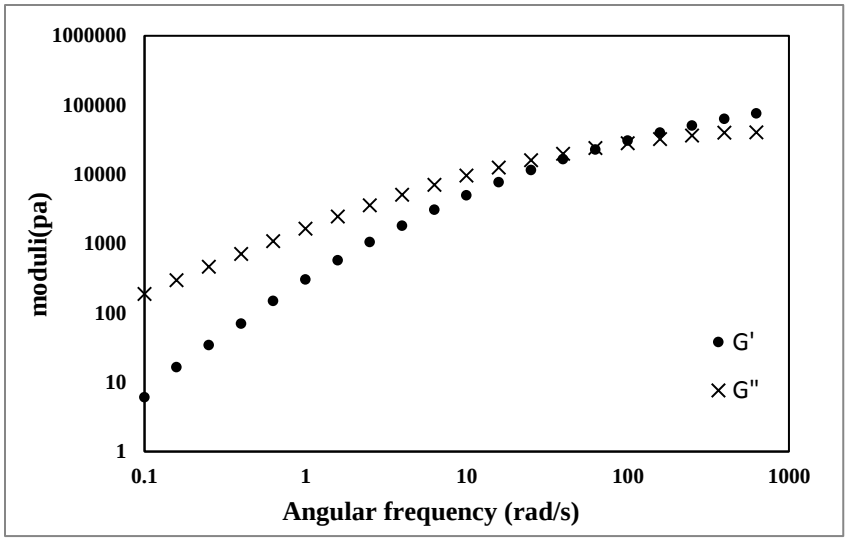

Sample 1-3

Resin 1/ 0.02 wt% peroxide at 150 ºC

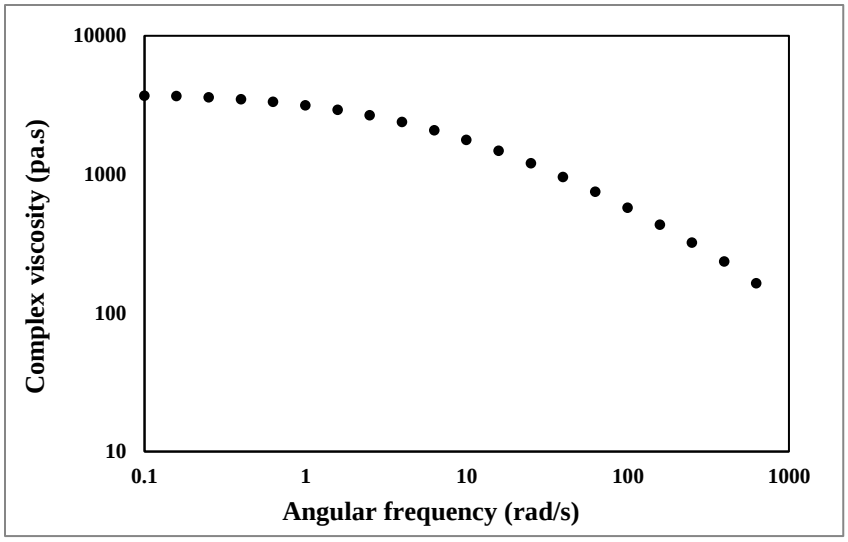

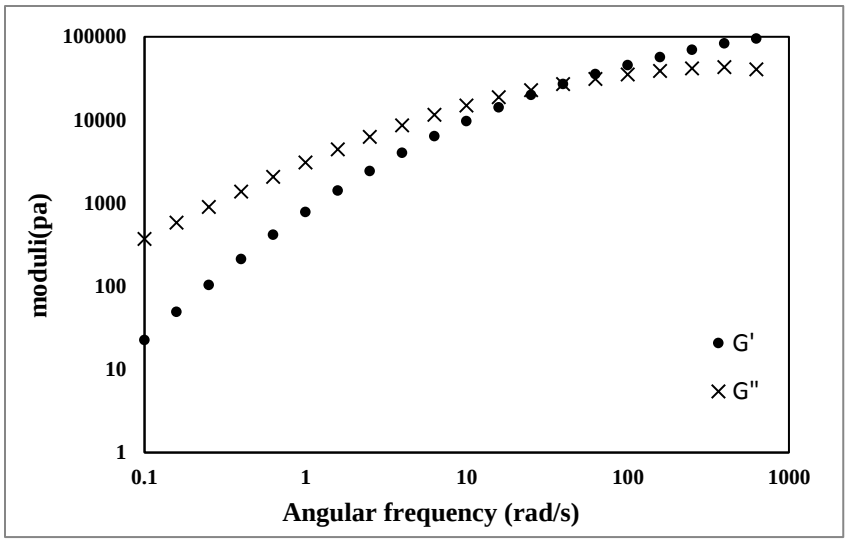

Sample 1-3

Resin 1/ 0.02 wt% peroxide at 170 ºC

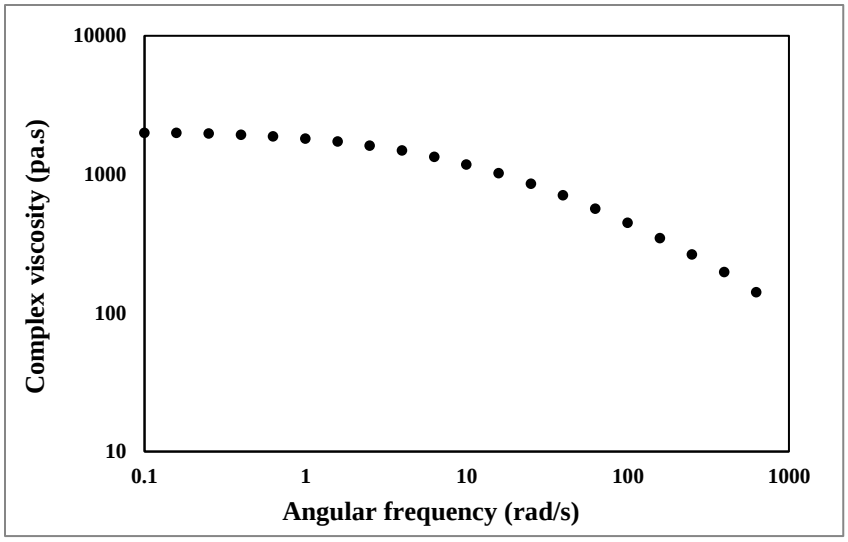

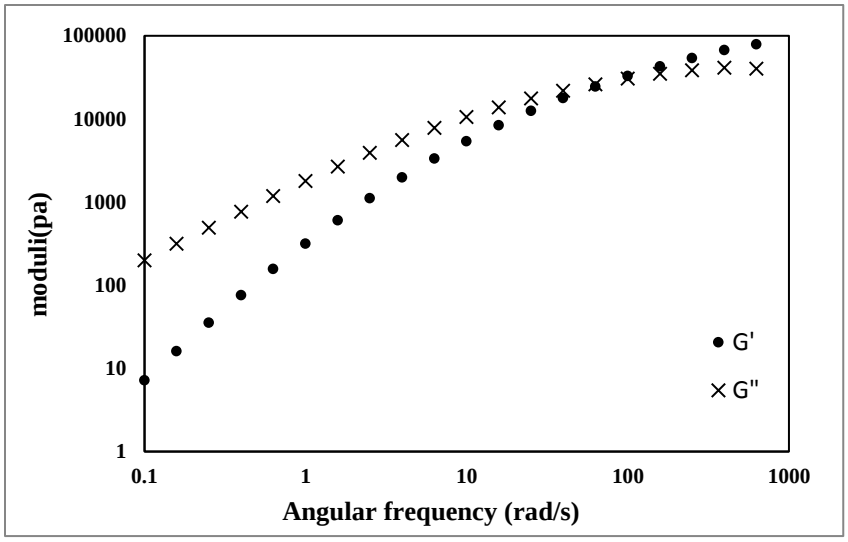

Sample 1-3

Resin 1/ 0.02 wt% peroxide at 190 ºC

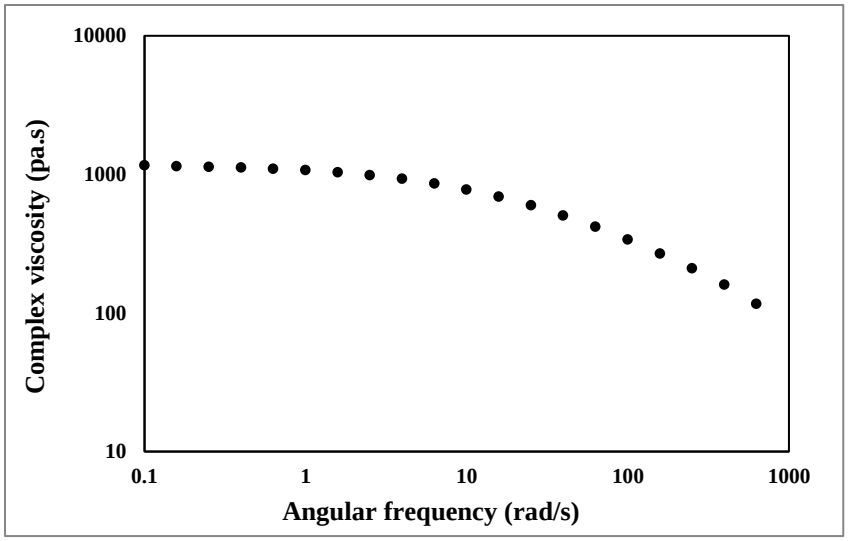

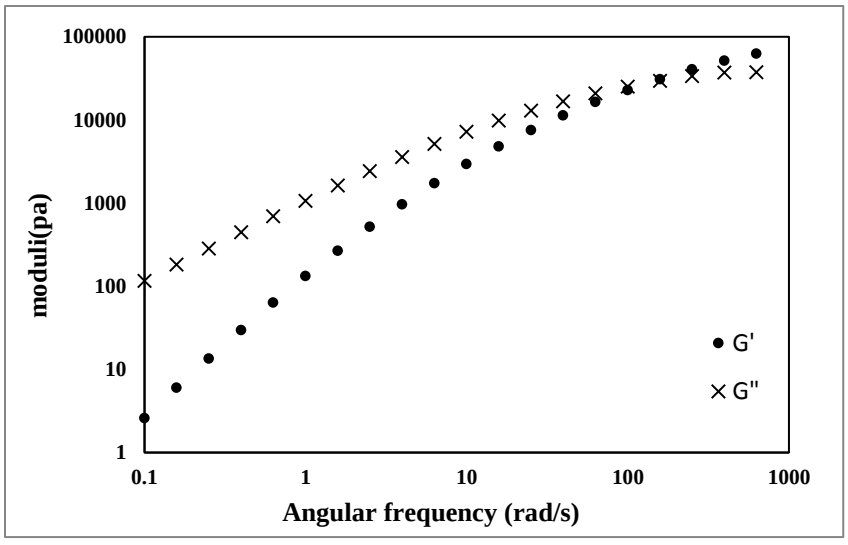

Sample 1-4

Resin 1/ 0.04 wt% peroxide at 150 ºC

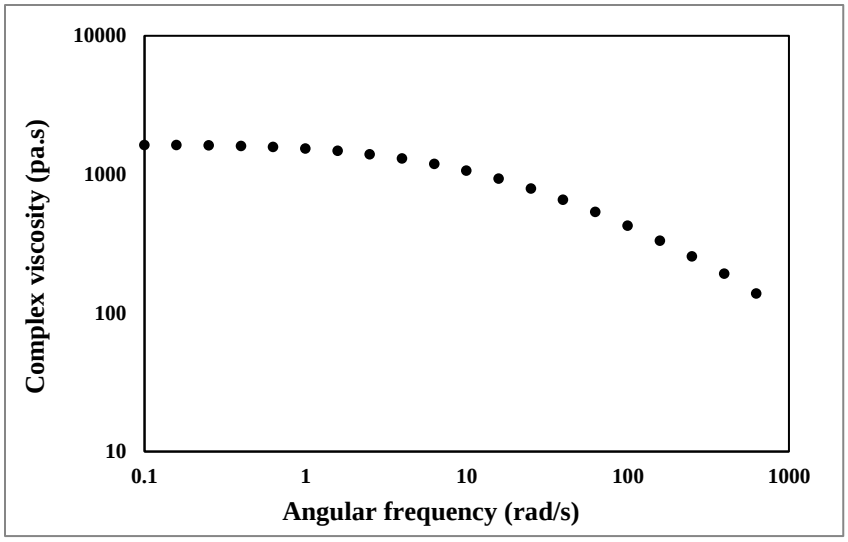

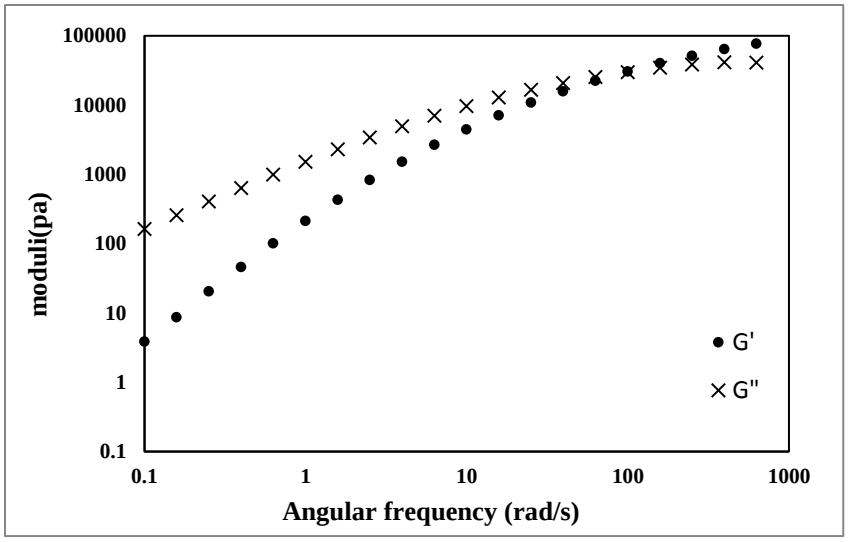

Sample 1-4

Resin 1/ 0.04 wt% peroxide at 170 ºC

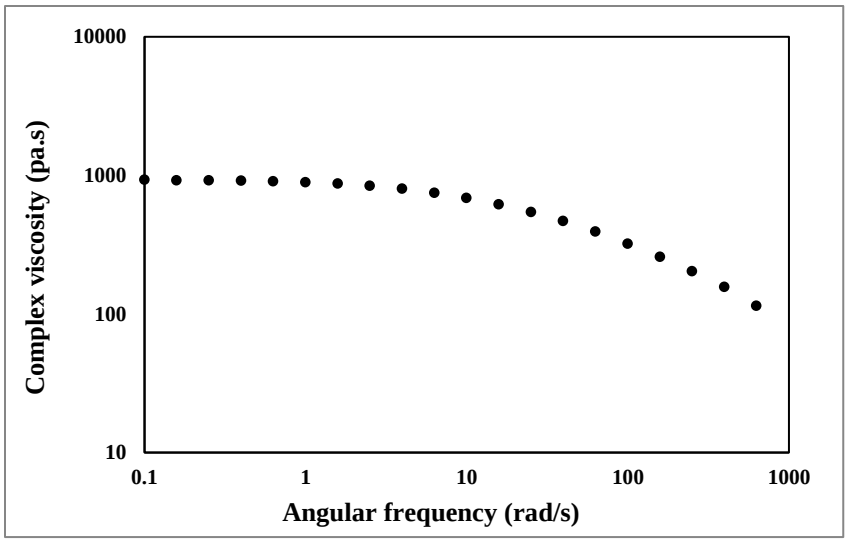

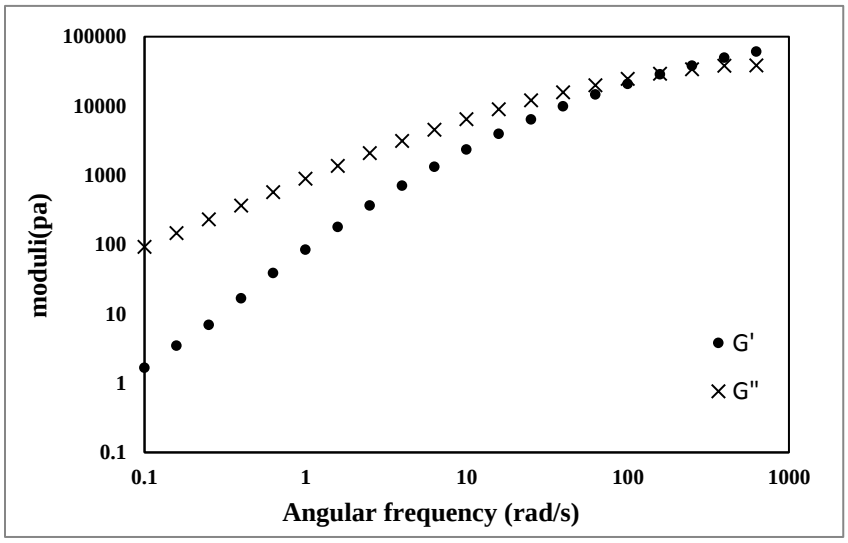

Sample 1-4

Resin 1/ 0.04 wt% peroxide at 190 ºC

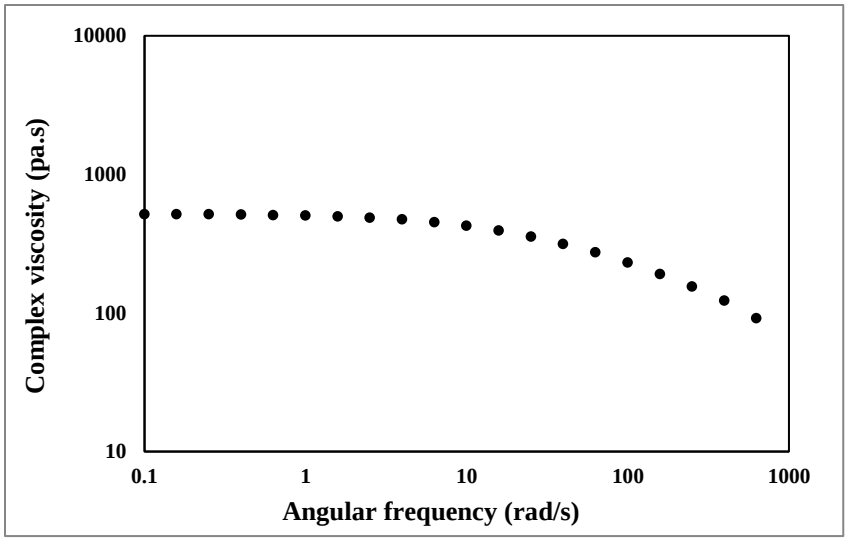

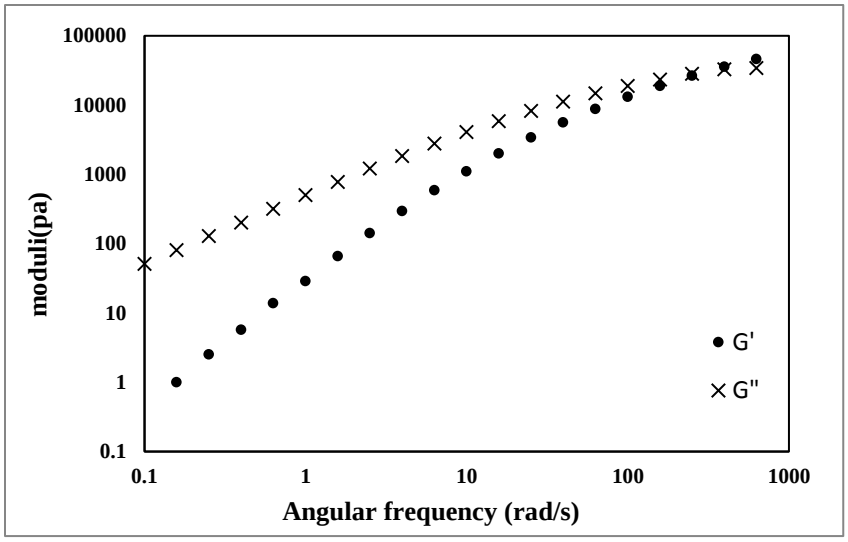

Sample 1-5

Resin 1/ 0.06 wt% peroxide at 150 ºC

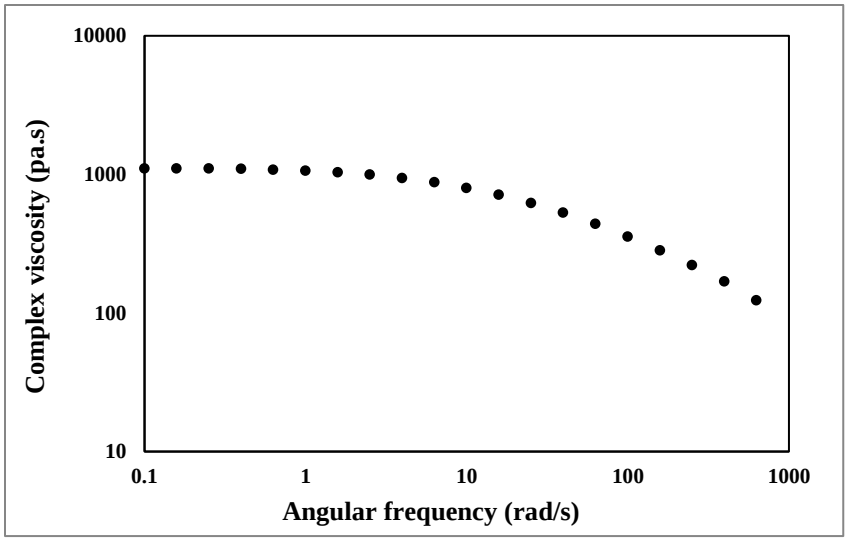

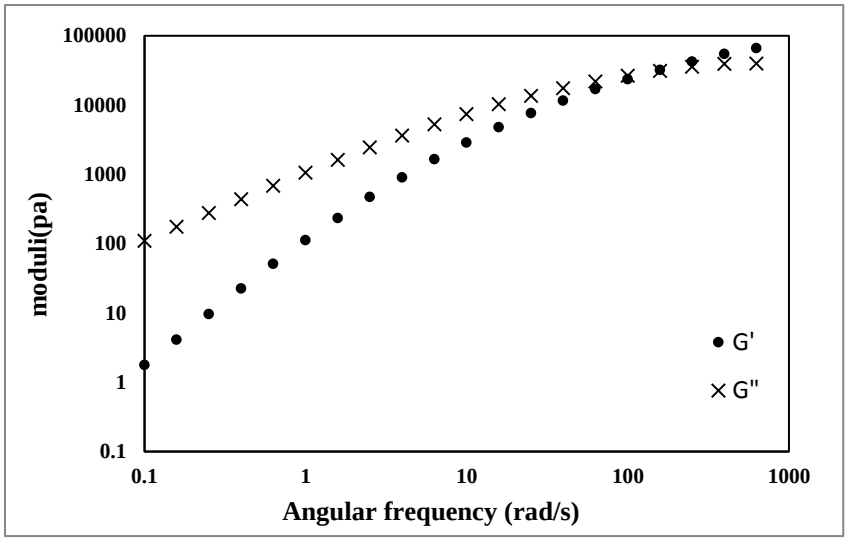

Sample 1-5

Resin 1/ 0.06 wt% peroxide at 170 ºC

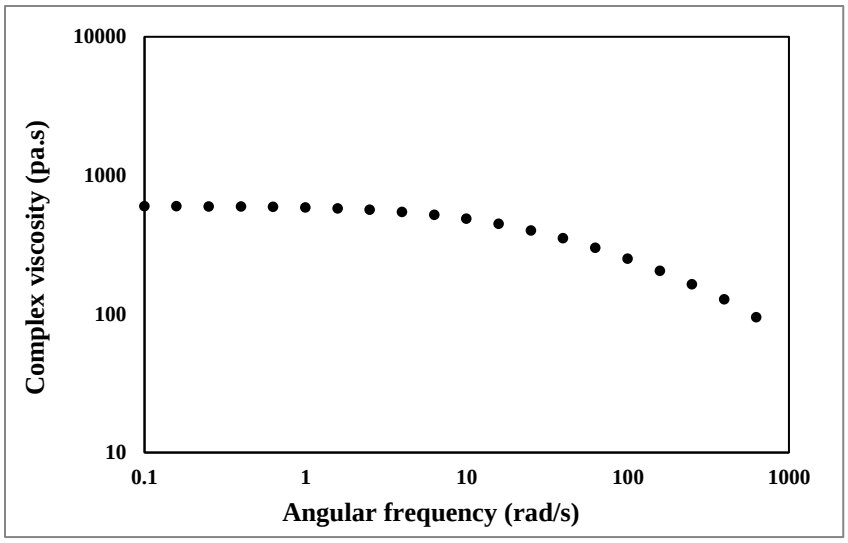

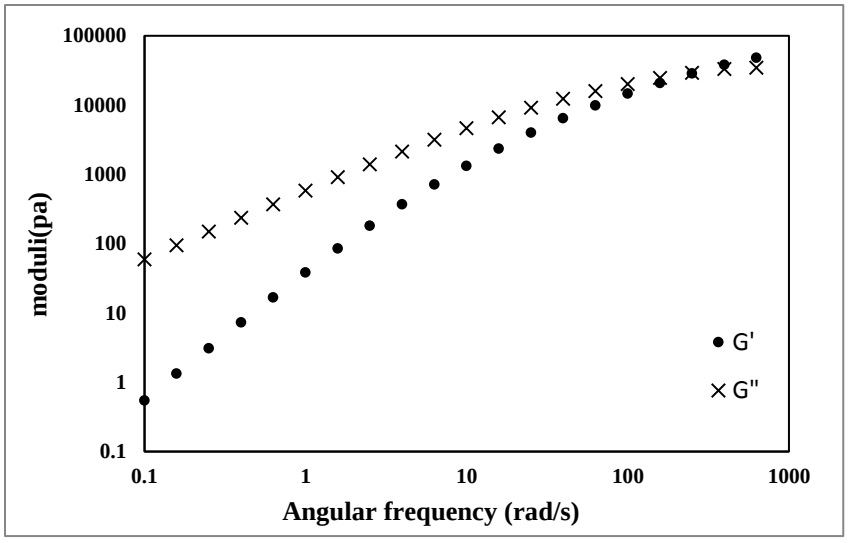

Sample 1-5

Resin 1/ 0.06 wt% peroxide at 190 ºC

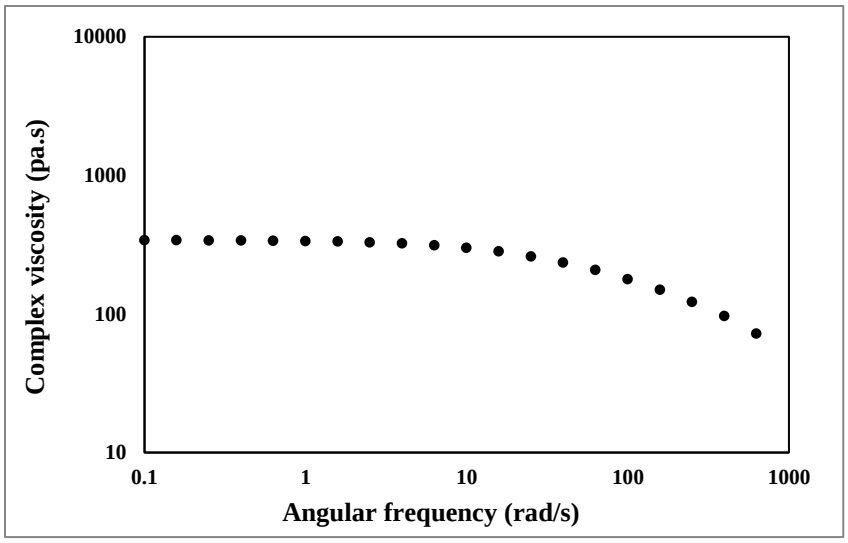

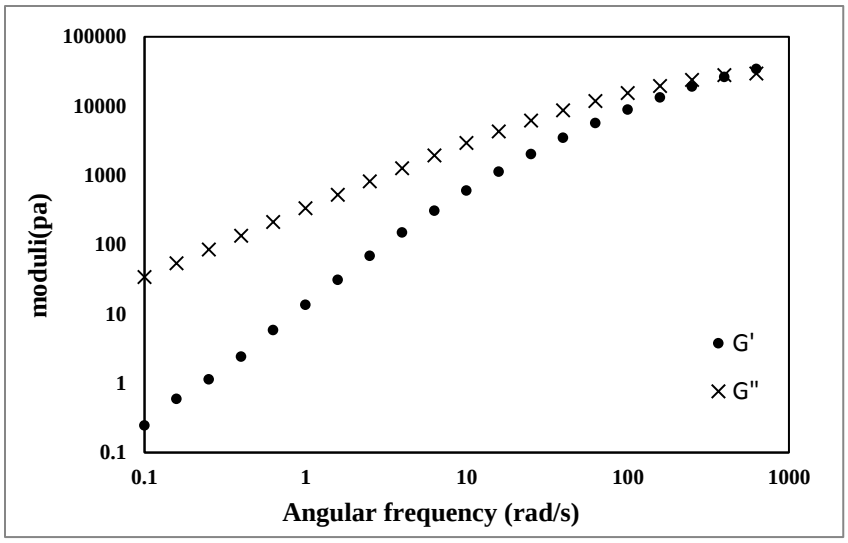

Sample 1-6

Resin 1/ 0.08 wt% peroxide at 150 ºC

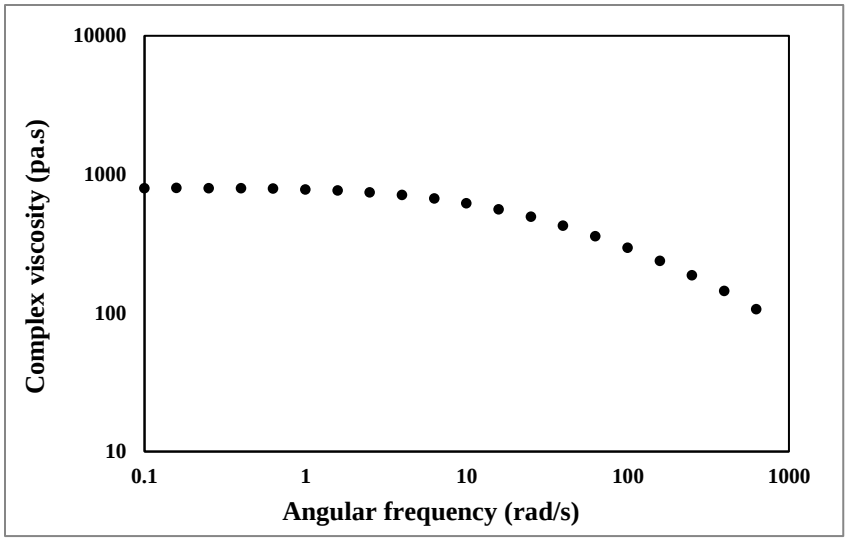

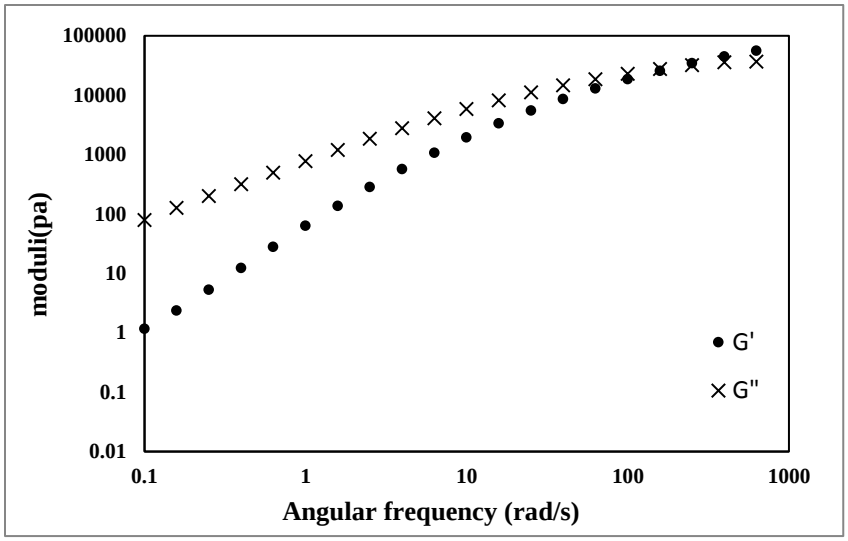

Sample 1-6

Resin 1/ 0.08 wt% peroxide at 170 ºC

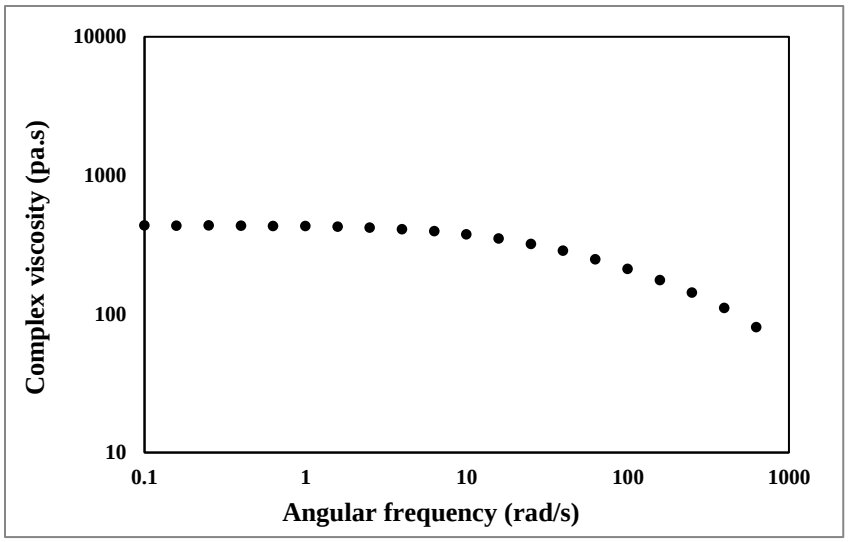

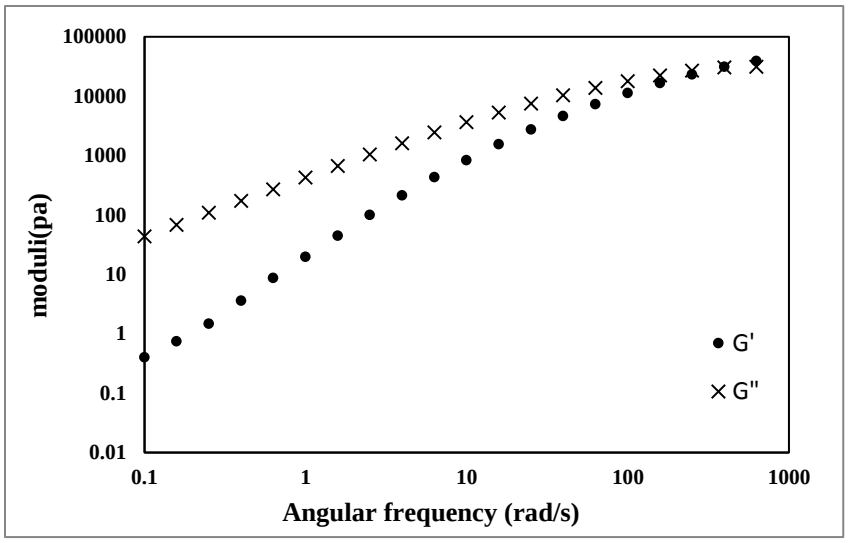

Sample 1-6

Resin 1/ 0.08 wt% peroxide at 190 ºC

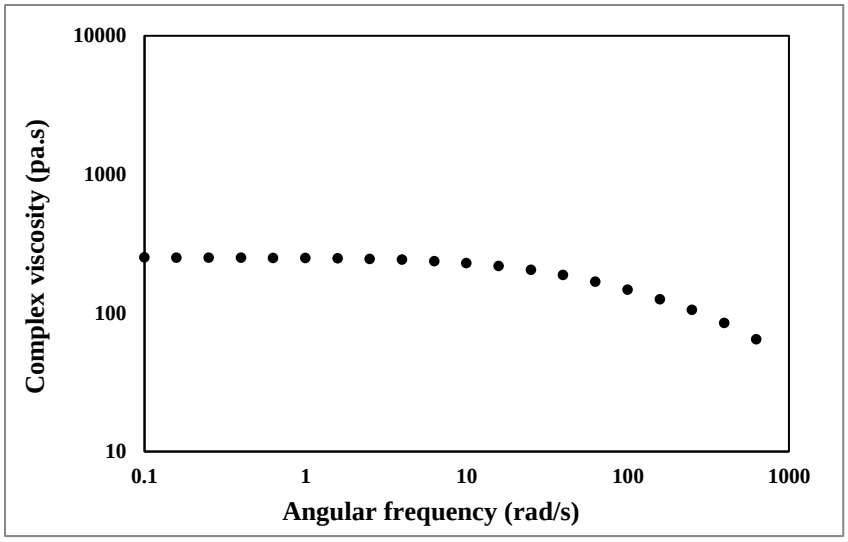

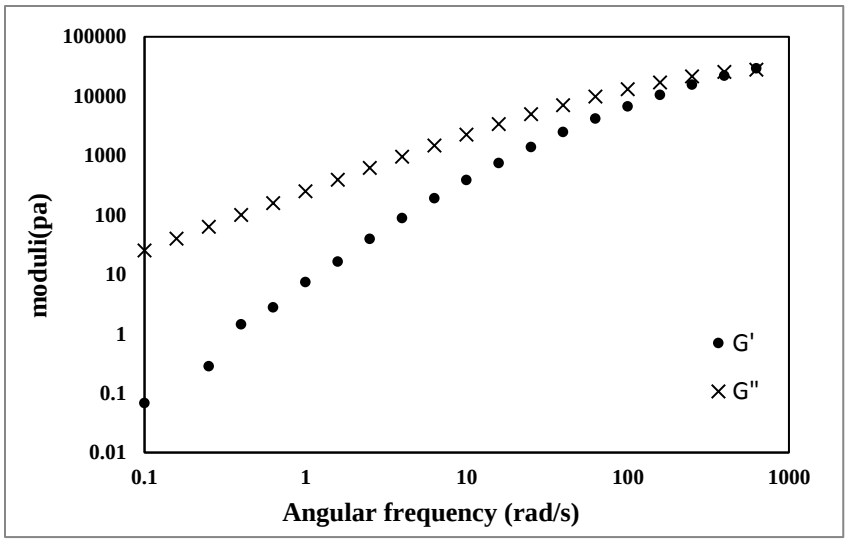

Sample 2-1

Resin 2/ 0 wt% peroxide at 150 ºC

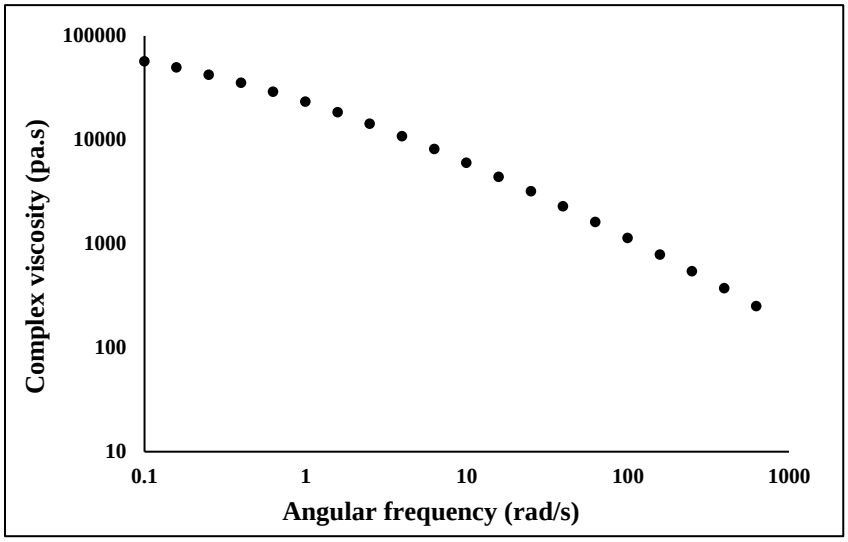

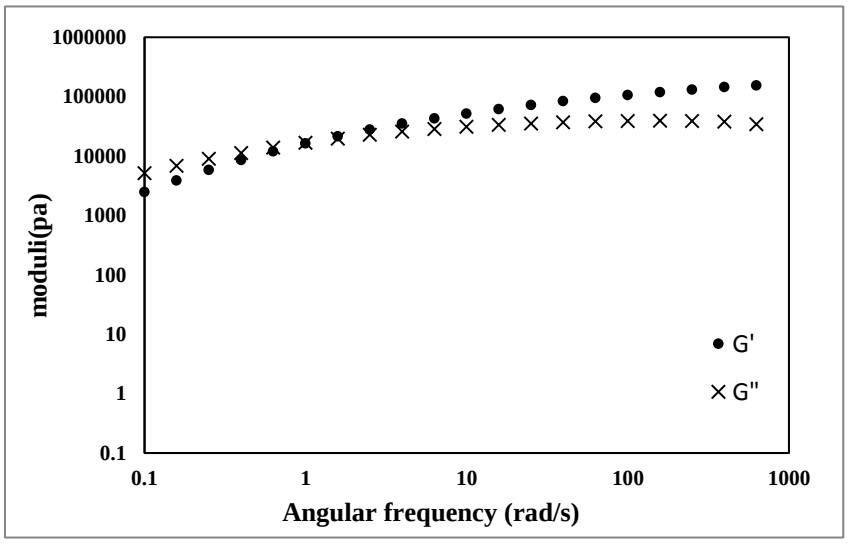

Sample 2-1

Resin 2/ 0 wt% peroxide at 170 ºC

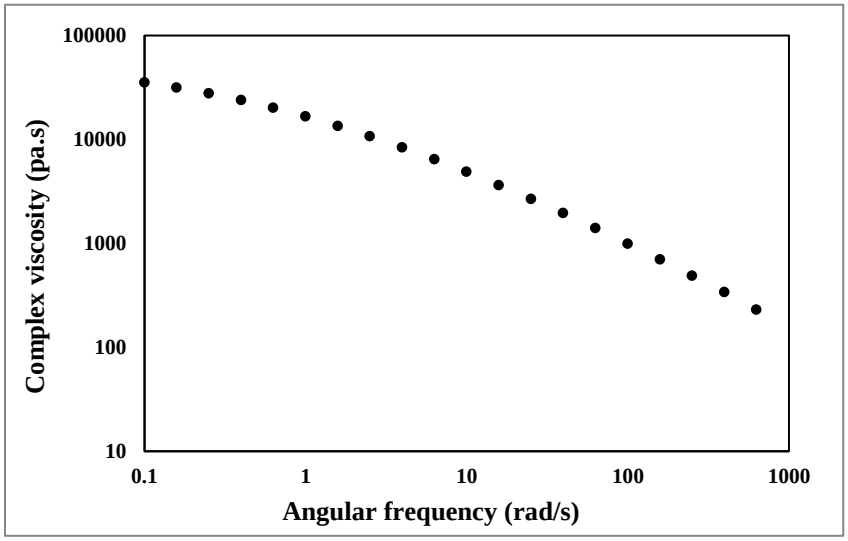

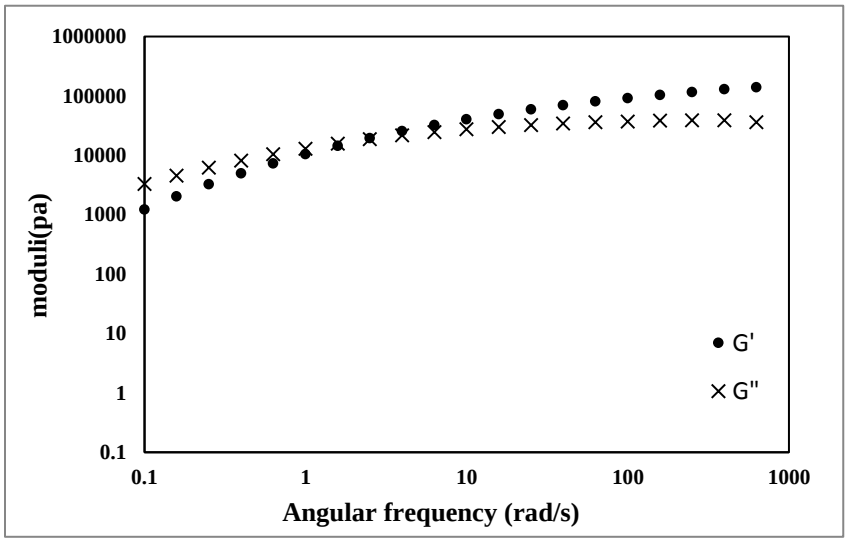

Sample 2-1

Resin 2/ 0 wt% peroxide at 190 ºC

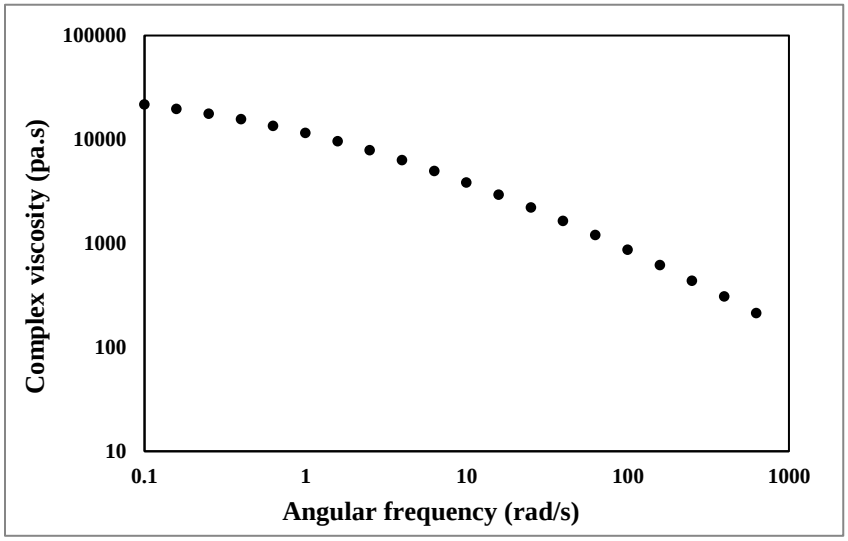

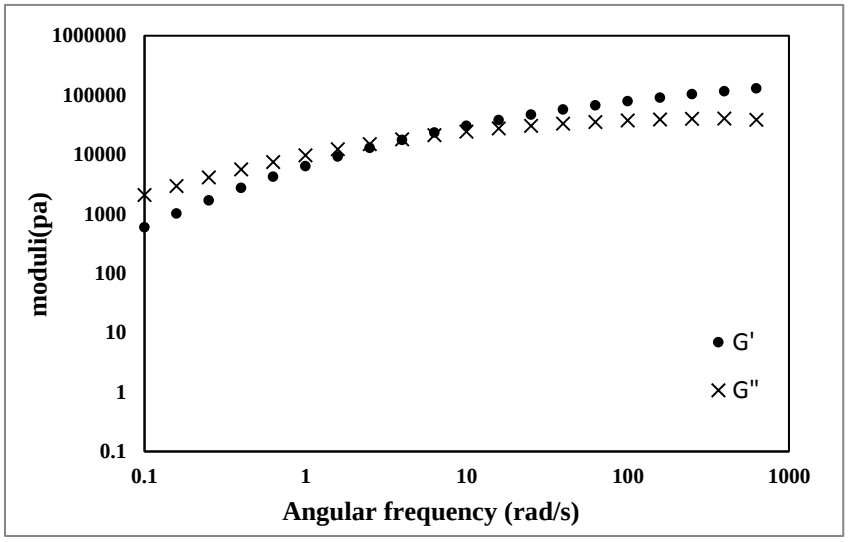

Sample 2-2

Resin 2/ 0.01 wt% peroxide at 150 ºC

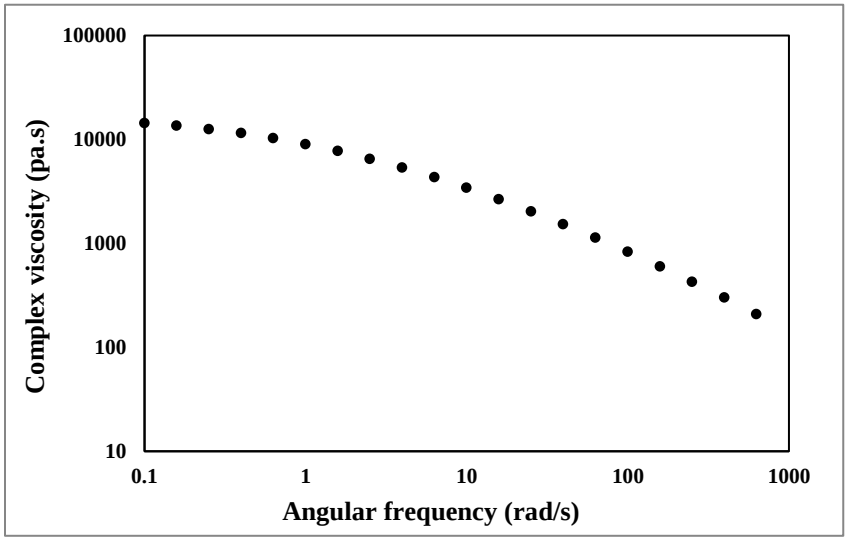

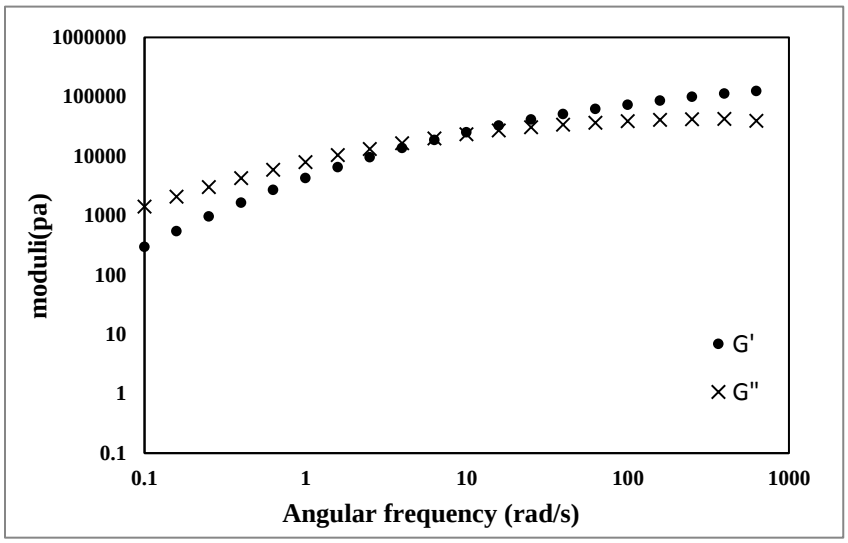

Sample 2-2

Resin 2/ 0.01 wt% peroxide at 170 ºC

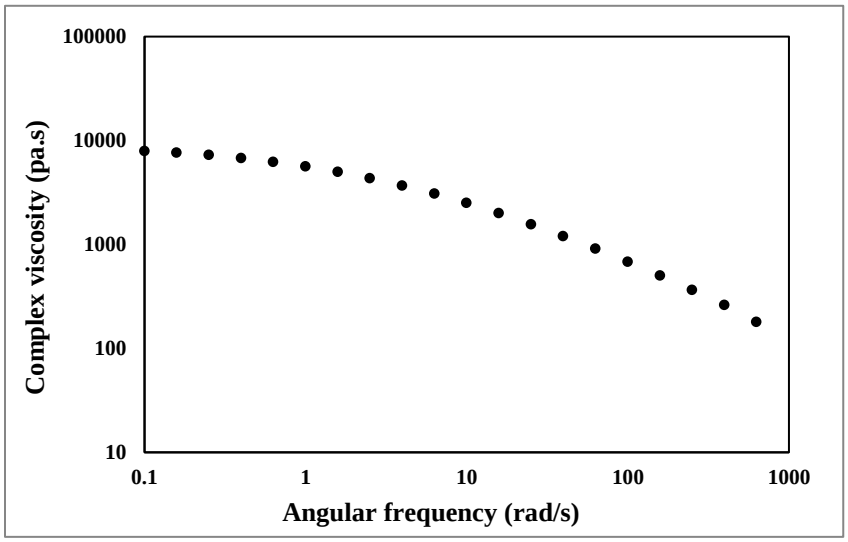

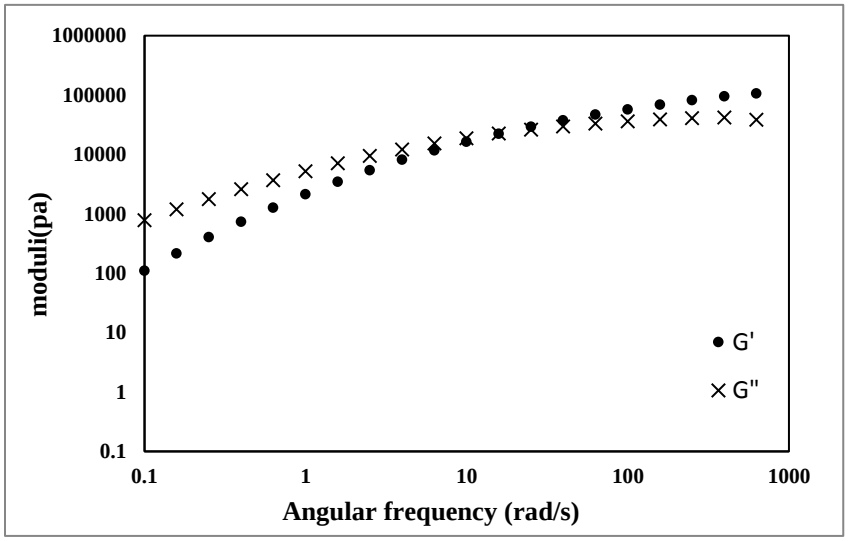

Sample 2-2

Resin 2/ 0.01 wt% peroxide at 190 ºC

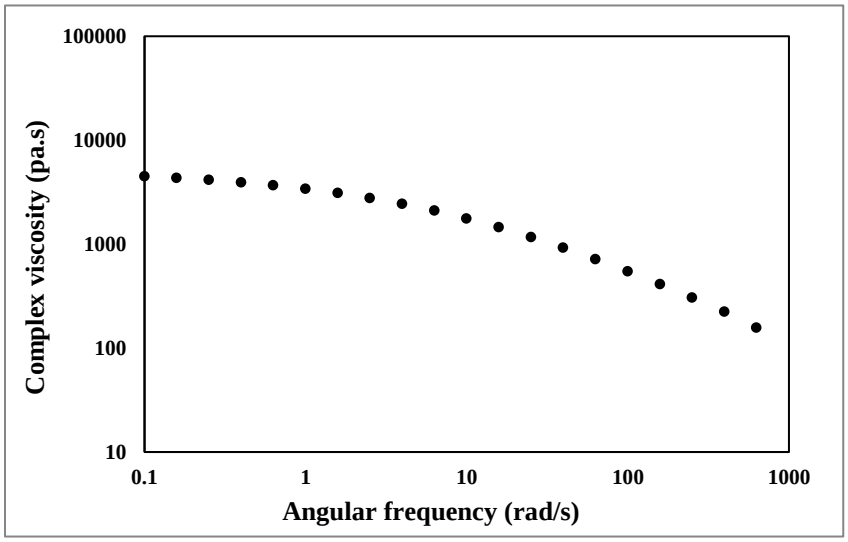

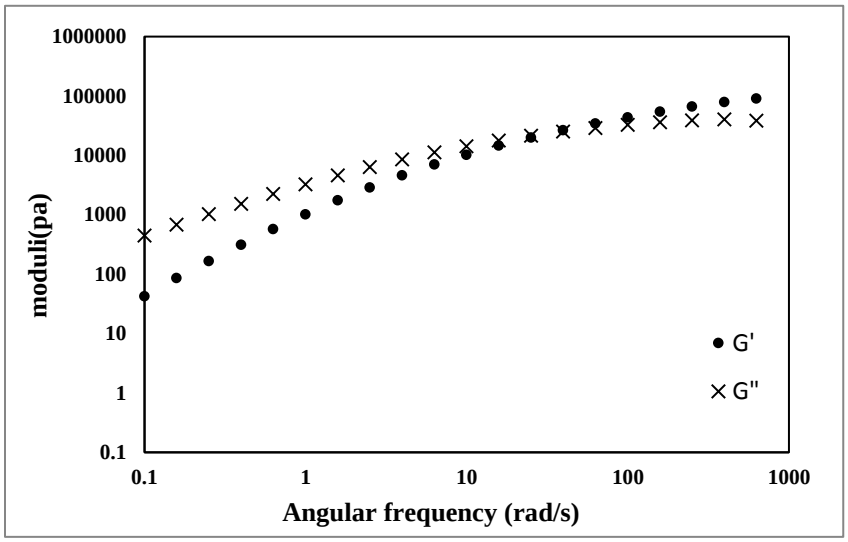

Sample 2-3

Resin 2/ 0.02 wt% peroxide at 150 ºC

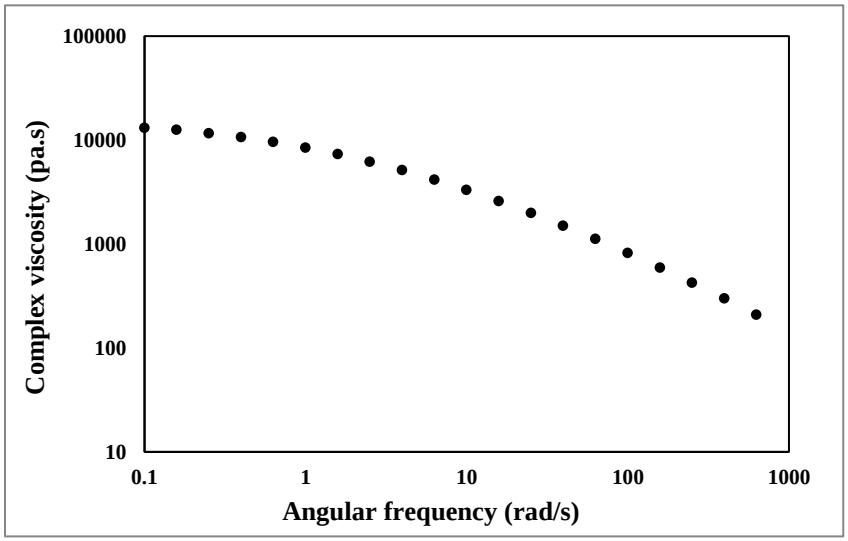

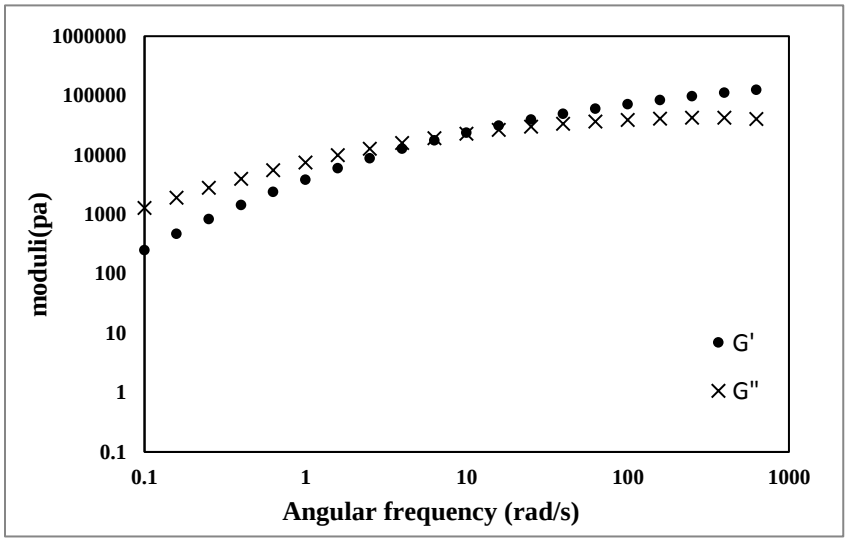

Sample 2-3

Resin 2/ 0.02 wt% peroxide at 170 ºC

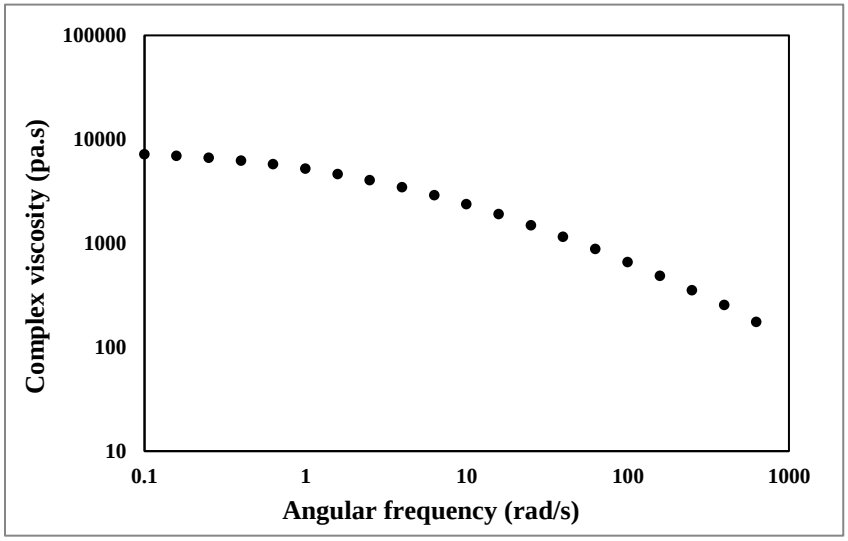

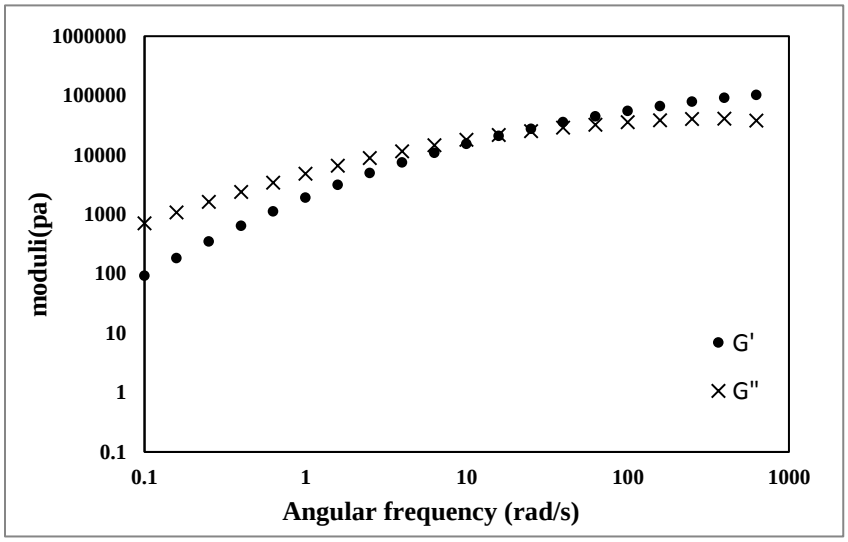

Sample 2-3

Resin 2/ 0.02 wt% peroxide at 190 ºC

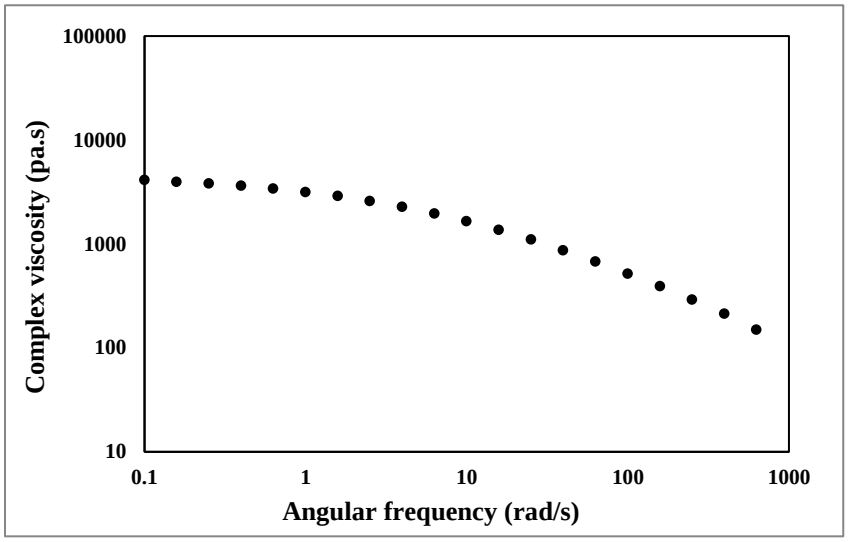

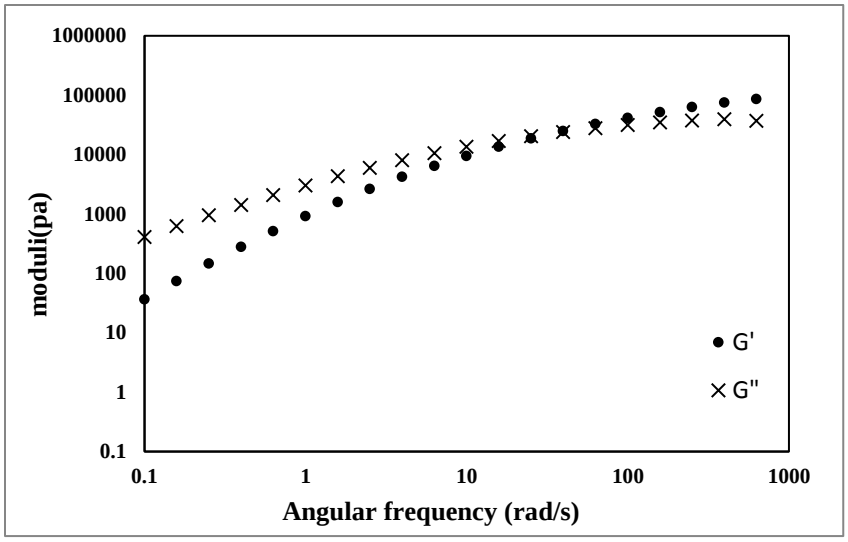

Sample 2-4

Resin 2/ 0.04 wt% peroxide at 150 ºC

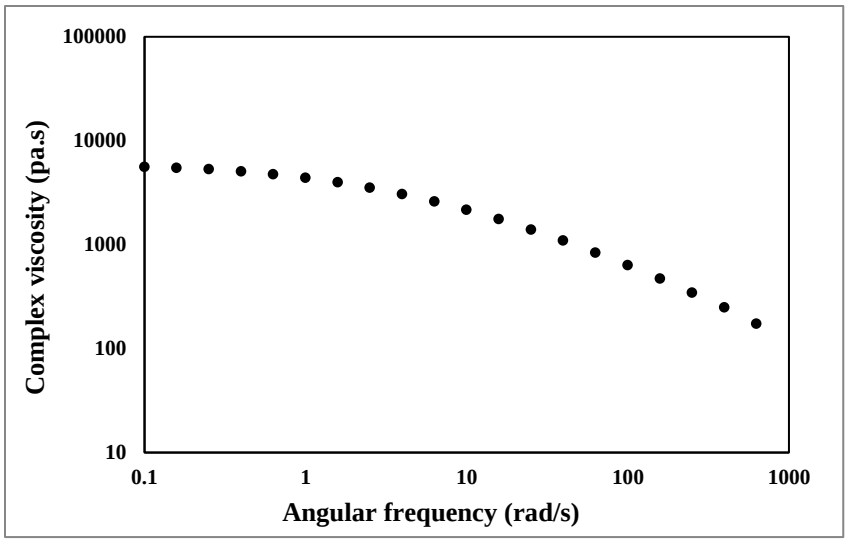

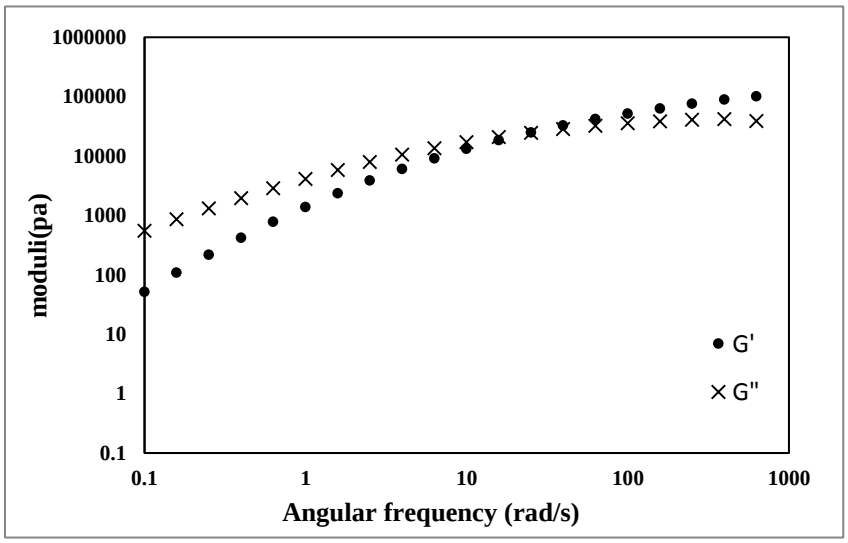

Sample 2-4

Resin 2/ 0.04 wt% peroxide at 170 ºC

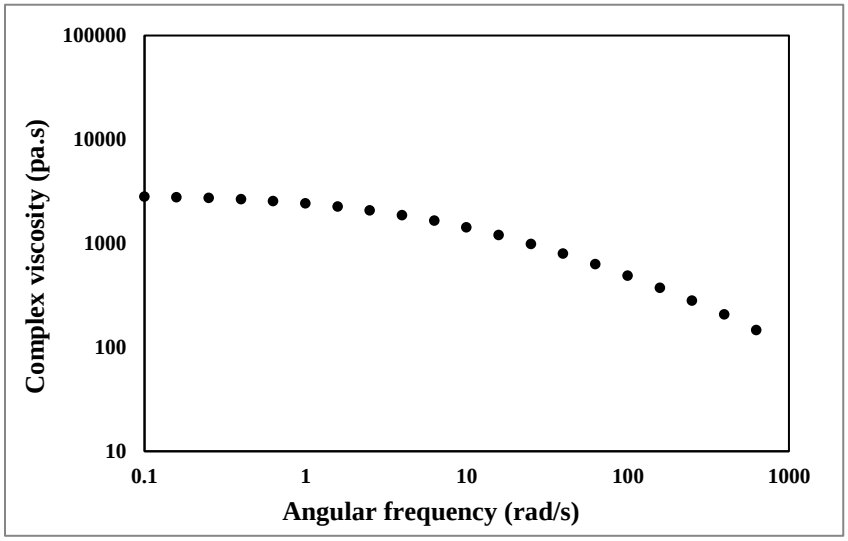

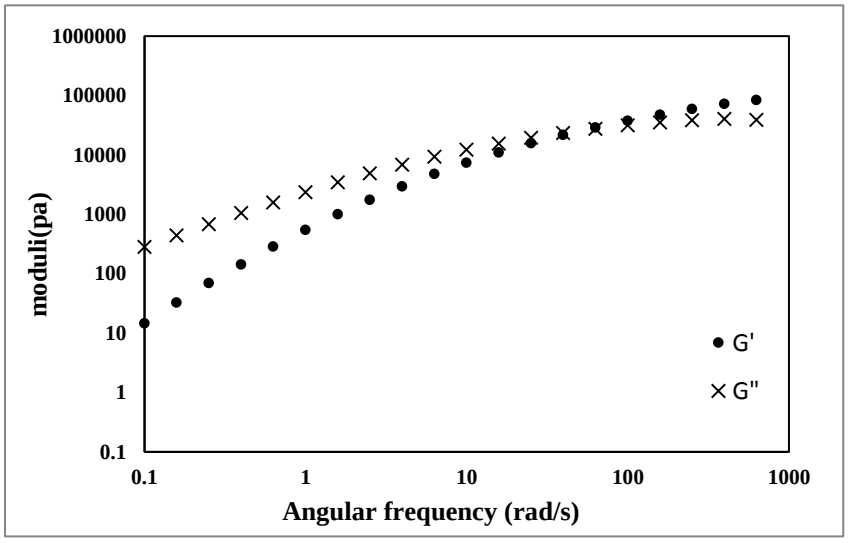

Sample 2-4

Resin 2/ 0.04 wt% peroxide at 190 ºC

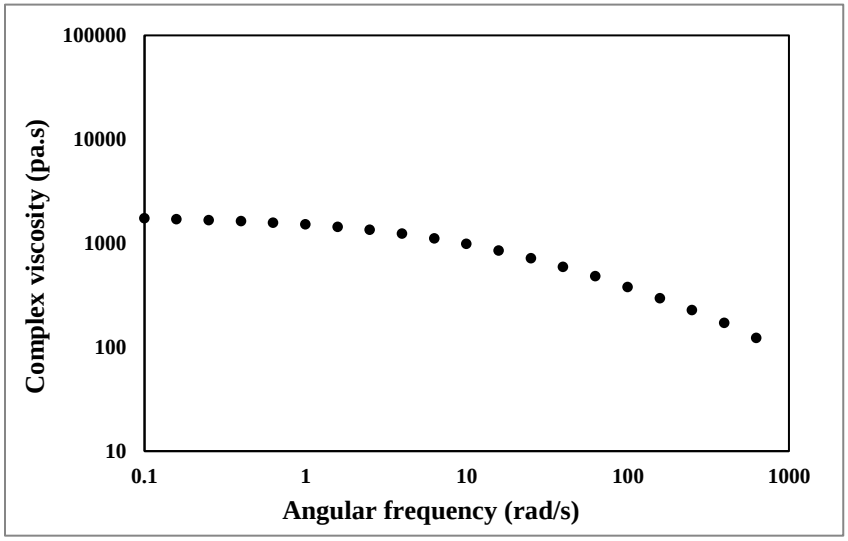

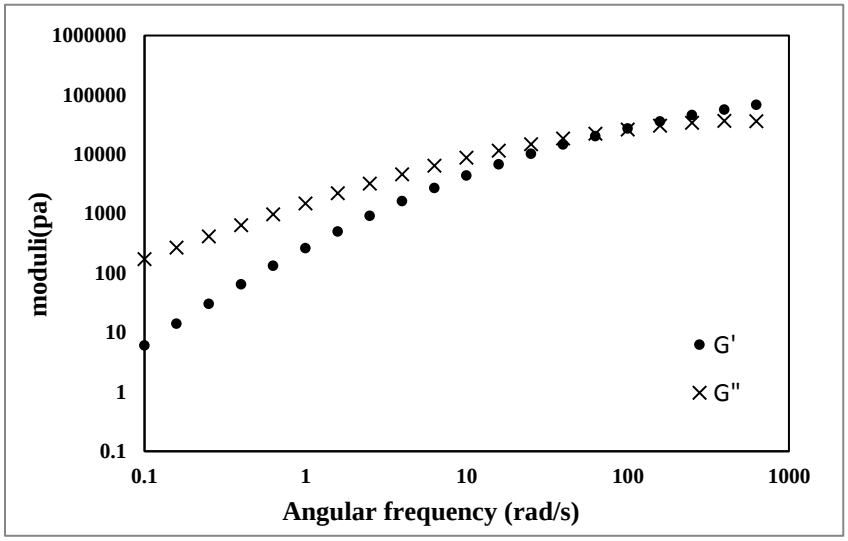

Sample 2-5

Resin 2/ 0.06 wt% peroxide at 150 ºC

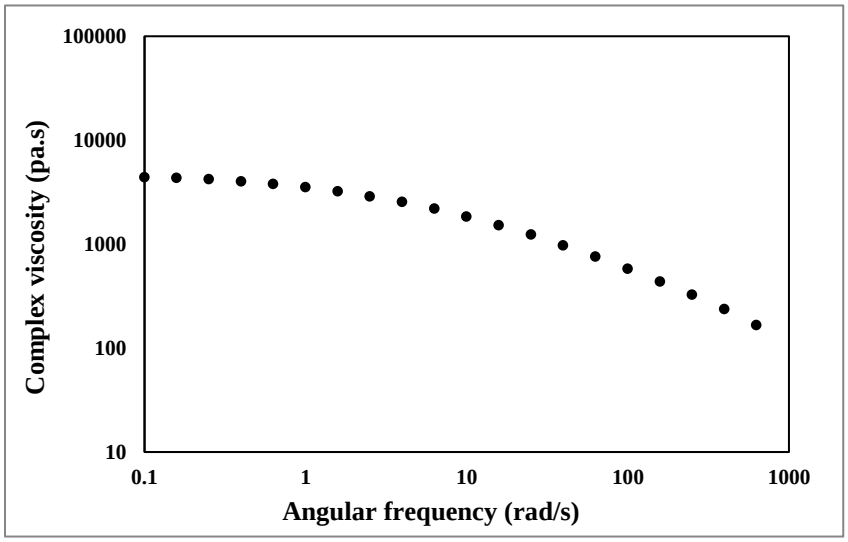

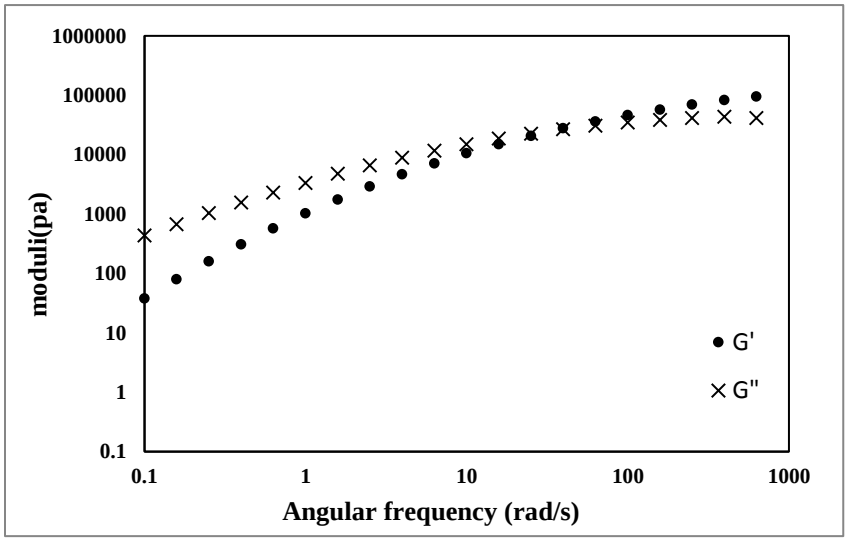

Sample 2-5

Resin 2/ 0.06 wt% peroxide at 170 ºC

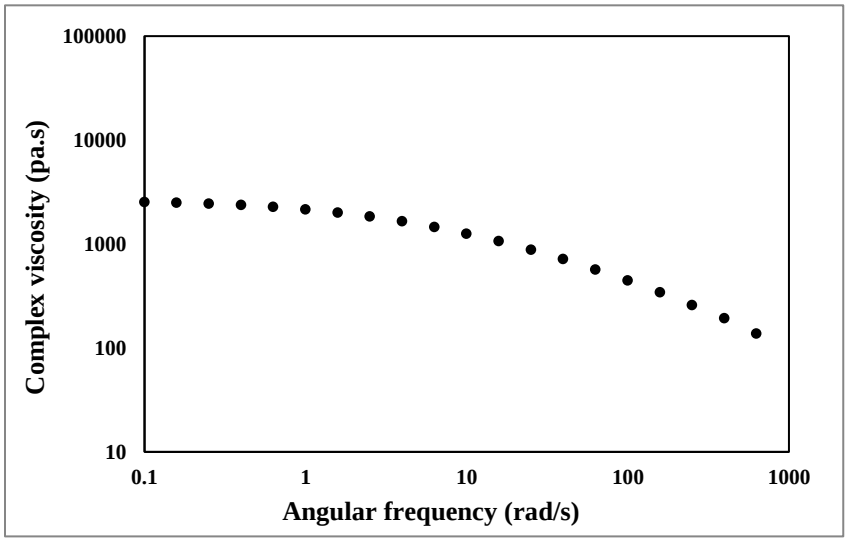

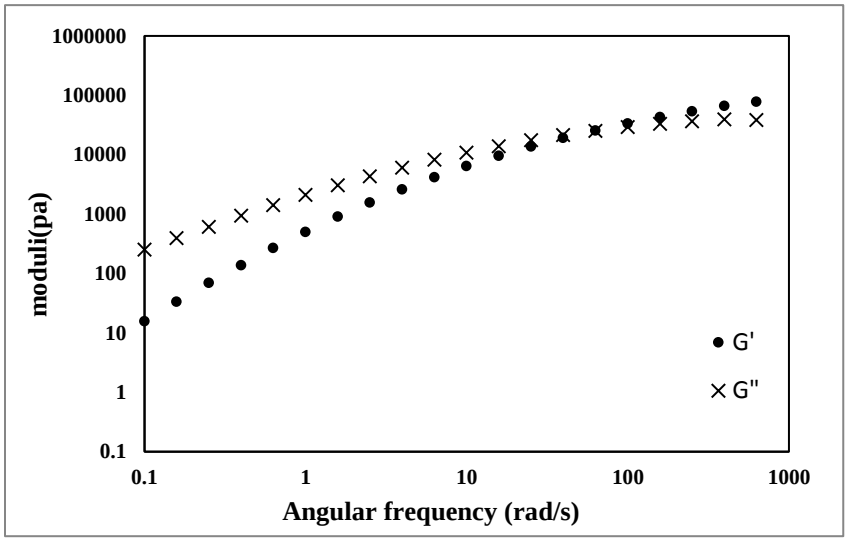

Sample 2-5

Resin 2/ 0.06 wt% peroxide at 190 ºC

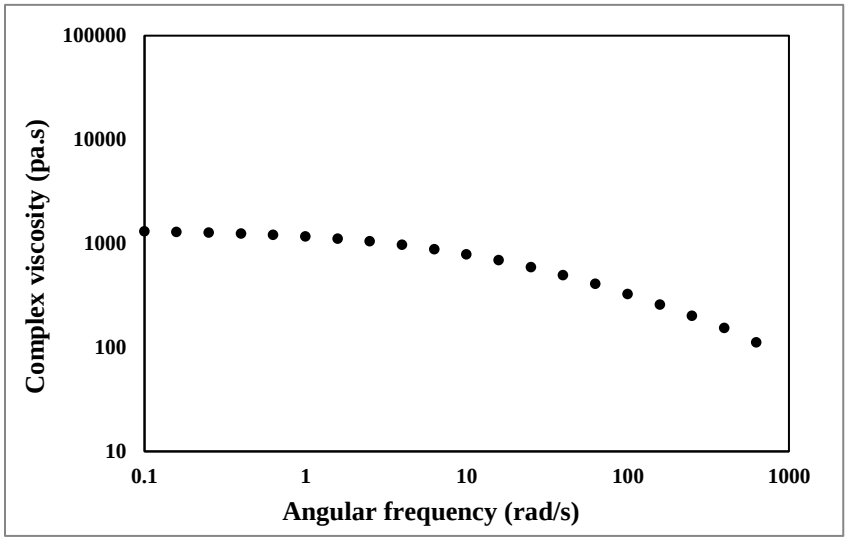

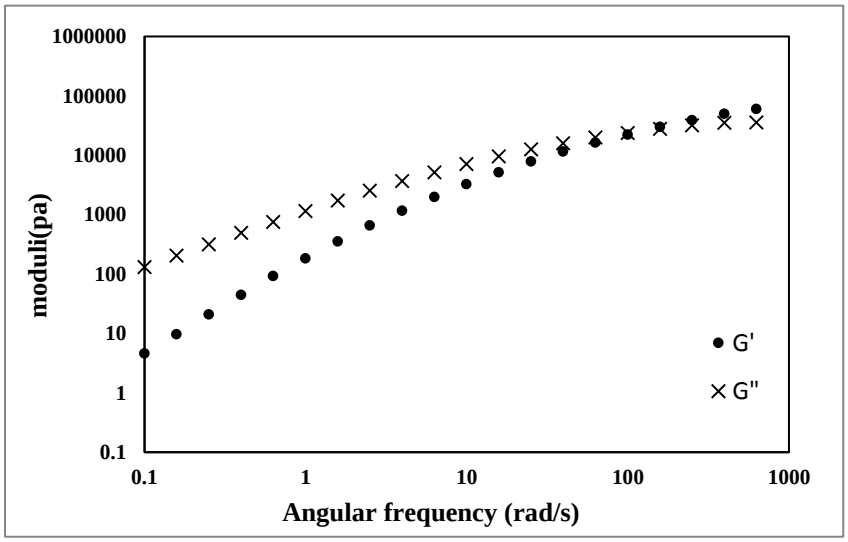

Sample 2-6

Resin 2/ 0.08 wt% peroxide at 150 ºC

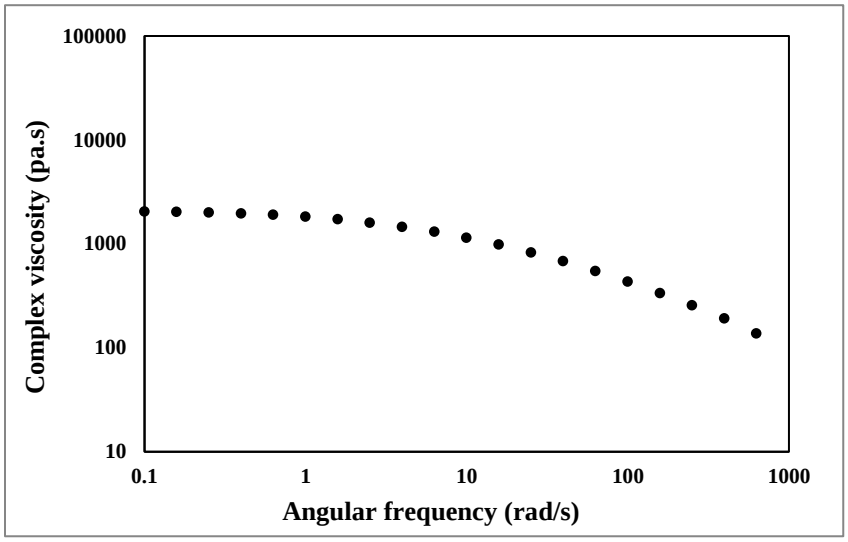

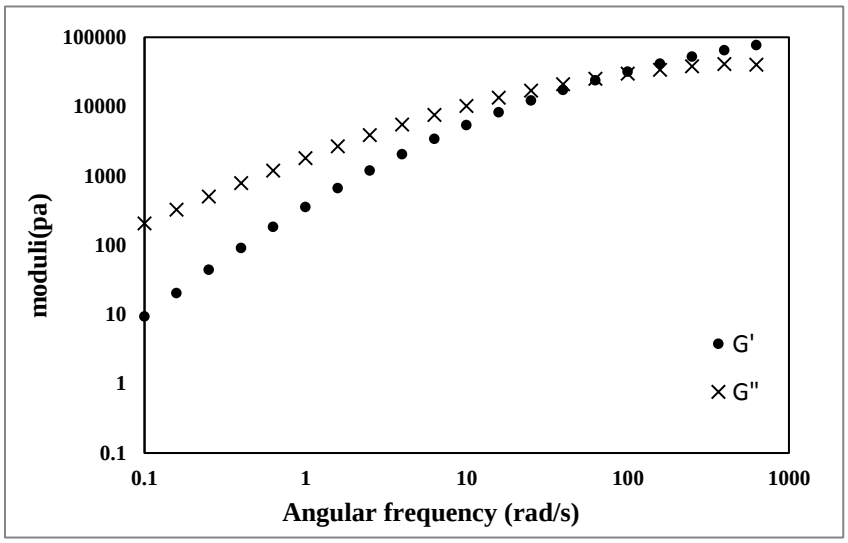

Sample 2-6

Resin 2/ 0.08 wt% peroxide at 170 ºC

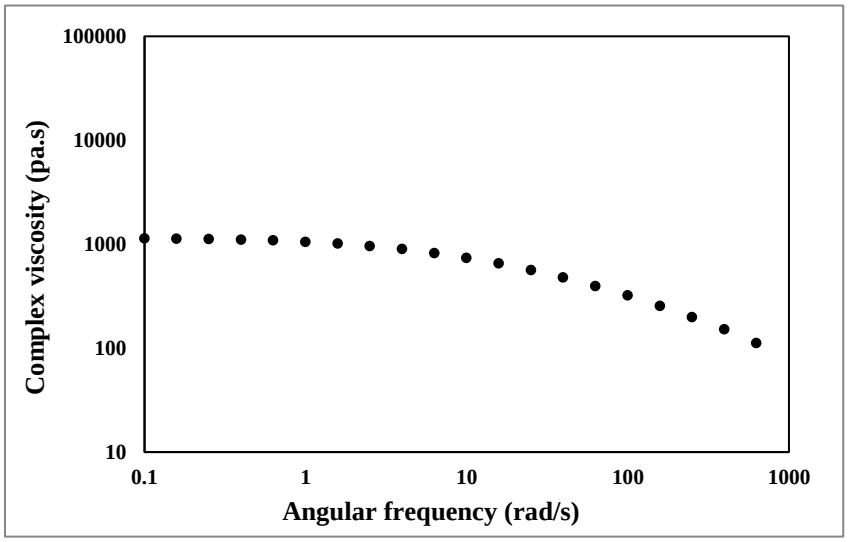

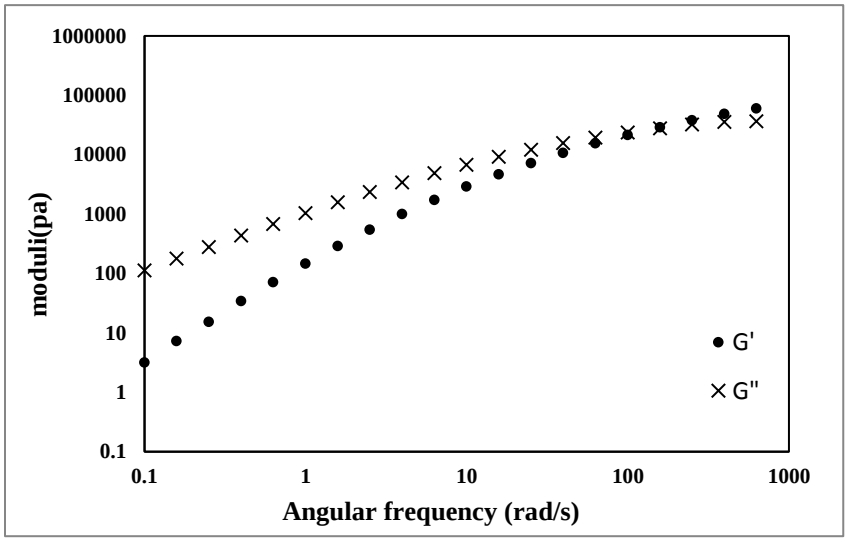

Sample 2-6

Resin 2/ 0.08 wt% peroxide at 190 ºC